A Proposed Experimental Methodology for Assessing the Effects of Biophysical Properties and Energy Content on Live Fuel Flammability

by

Oleg Melnik

A thesis submitted in partial fulfillment of the requirements for the degree of

Master of Science

in

Forest Biology and Management

Department of Renewable Resources
University of Alberta

ABSTRACT

The effectiveness of fire management tactics and safety of firefighters strongly depend on the reliability of fire behaviour predictions that is currently limited by a lack of understanding of the flammability of live fuel. Until now fire modeling has been primarily based on the flammability of dead fuel using the assumption that combustion of the live fuel has a very limited effect on fire behaviour. However, the analysis of the existing data revealed that live fuel constituted from 48% to 60% of fuel consumed during the passage of a flame-front, meaning that live fuel plays a significant role in determining frontal fire intensity and fire behaviour. Introducing a new definition of flammability and a test method for flammability assessment, this study identifies how and to what extent live fuel and its properties may affect frontal flame intensity.

By evaluating flammability directly in a flame, the proposed oxygen consumption calorimetry method better represents the high-intensity combined radiative and convective heat transfer prior to ignition as well as the conditions of oxygen deficiency and high concentrations of water vapor within the flame-front. The flammability of live fuel consumed within the flame-front was defined as energy release contribution to the frontal flame and represented the energy-generation component of the energy balance of the flame-front rather than just an energy content of separate fuel elements. The flammability was measured as the change in energy release from the flame resulting from interaction with live fuel during average flame-front residence time. Assessing the flammability of fresh shoots rather than just foliage allowed for better representation of the live plant

material consumed in the flame-front. Live fuel flammability range, factors, and seasonal trend were investigated on a tree branch scale and a new high-resolution volume measuring technique was also introduced.

The variation in live fuel flammability for white spruce was more than twice that measured using existing techniques suggesting that the actual changes in live fuel flammability have been underestimated by current fire modelling systems. Measured negative values of flammability for new shoots in the beginning of the season indicated a reduction in the energy release of the combined system of live fuel and frontal flame assumed to result from the high water content of live fuel and oxygen deficiency. Dry matter content and variables characterizing chemical composition of the fuel were replaced by a newly-introduced variable – energy content per unit of fresh mass or volume. Using the gravimetric approach, the energy content did not improve the prediction of flammability; however, when using the volumetric approach, variation in flammability was better explained by energy content than by water content. The proposed volumetric multivariable flammability model (adjusted $R^2 = 0.87$) was able to better predict flammability compared with the volumetric single-variable models (adjusted $R^2 = 0.79$). The Canadian Fire Behaviour Prediction System assumes only one seasonal maximum in flammability occurring in early-mid June, but it was instead observed one month earlier. Two additional spikes in flammability occurred in early July and mid-August, when the lowest seasonal values were expected. The mid-August spike in the flammability was caused by a second seasonal minimum in water content induced by drought.

If applied to a known amount of live and dead fuel in a vegetative canopy, the proposed approach allows for evaluation of the combined energy release contribution to the flame-

front by live and dead fuel on a vegetative canopy scale without modeling fuel consumption. This measure of the forest stand energy release response to fire conditions can further be used in the development of a numerical stand characteristics-based fuel classification and as a forest stand flammability input to fire behaviour modelling systems.

ACKNOWLEDGEMENTS

I am sincerely obliged for guidance, help, endless patience, and contribution to this project to my supervisor Mike Flannigan and to committee members Mark Ackerman, Dan Thompson, and Sara McAllister. Special thanks for great help in my work go to Stephen Paskaluk who is co-author of this project. Many thanks to Stavros Sakellariou, Cordy Tymstra, Brian Stocks, Dale Wade, Ralph Nelson, Greg Baxter, Ray Ault, Xianli Wang, Peter Murphy, Martin Alexander, Kelvin Hirsch, Richard Carr, Ted Hogg, Elisabeth Beaubien, Linda Seale, Craig and Olga d'Entremont, Dave Finn, Hugh Wallace, Dave Schroeder, Bogoljub Stancovic, Ginny Marshall, Karen Blouin, François Robinne, Brett Moore, Michael Abley, Rodrigo Campos, Luiz Fernando Drummond Salvador, and to all members of our firelab who helped me a lot in my work.

I would like to express my highest gratitude and love to my family, who understood, supported, and inspired me, helped a lot with this project, and for their patience in listening of my endless stories about fire, flammability, transpiration, and evaporation: to Katia, Amanda, Sasha, Kuzia, to my mama Tamara for giving strength and inspiration to accomplish this project and to my papa Mikhail for his advices and help in field and lab work. My deepest and most sincere gratitude goes to my friend, supporter, advisor and sponsor during this study, very best person to whom I express all my gratitude and Love – my wife Larisa.

TABLE OF CONTENTS

LIST OF TABLES

LIST OF FIGURES

LIST OF ABBREVIATIONS

ABBREVIATION	DEFINITION OF TERM	UNITS
Adjusted R^2	Coefficient of determination adjusted for the number of the predictors in the model	( )
ANHC	Actual net heat content of a vegetative canopy	$MJ\ m^{-2}$
BUI	Buildup Index	( )
CC	Calorimetric content (gross heat of combustion, dry mass basis)	$kJ\ g^{-1}$
Ch	Chemical composition	-
CFFDRS	Canadian Forest Fire Danger Rating System	-
CSF	Crown spread factor	( )
CSI	Crown spread index	( )
D	Fresh density	g cm^{-3}
DC	Drought Code	( )
$dH_{eff}60s.GRAV$	Differential effective heat of combustion per unit of the initial fresh mass of the sample (fresh mass basis)	$kJ\ g^{-1}$

$dH_{eff}60s.ML$	Differential effective heat of combustion per unit of mass loss (mass of fuel consumed)	$kJ\ g^{-1}$
$dH_{eff}60s.VOL$	Differential effective heat of combustion per unit of the initial volume of the sample	$kJ\ cm^{-3}$
dHRR	Differential heat release rate	*W*
DMC	Duff Moisture Code	( )
DM.GRAV	Dry matter content expressed gravimetrically per unit of the initial fresh mass of the sample (fresh mass basis)	( )
DM.VOL	Dry matter content expressed volumetrically per unit of the initial volume of the sample	g cm^{-3}
DSC	Differential scanning calorimetry	-
DWF	Density water-free	g cm^{-3}
DWF_0^w	Density of the oven-dry cell walls material without any voids	g cm^{-3}
EC.GRAV	Gravimetric calorimetric content per unit of fresh mass (fresh mass basis)	$kJ\ g^{-1}$
EC.VOL	Volumetric calorimetric content (per unit of the initial volume of the sample)	$kJ\ cm^{-3}$

$E.LOSS_{O_2}$	Combined reduction in energy release for live fuel element's flame and for the frontal flame due to oxygen deficiency in the flames interaction zone per unit of the fuel fresh mass or volume	$kJ\ g^{-1}$ $kJ\ cm^{-3}$
$E.LOSS_{H_2O}$	Combined reduction in energy release for live fuel element's flame and for the frontal flame due to effects of live fuel's water content in the flames interaction zone per unit of the fuel fresh mass or volume	$kJ\ g^{-1}$ $kJ\ cm^{-3}$
FBP	Fire Behaviour Prediction System (sub-model of the Canadian Forest Fire Danger Rating System)	-
FMC	Foliar moisture content (dry mass basis)	%
FWI	Fire Weather Index System (sub-model of the Canadian Forest Fire Danger Rating System)	-
H_{eff}	Effective heat of combustion (fresh mass basis)	$kJ\ g^{-1}$
H_{gross}	Gross (higher) heat of combustion (dry mass basis)	$kJ\ g^{-1}$
H_{net}	Net heat of combustion (dry mass basis)	$kJ\ g^{-1}$

HR	Heat release (total)	kJ
HRR	Heat release rate	W
$Loss_{O_2}$	Per unit of $EC.VOL$, reduction in energy release for both frontal flame and live fuel element's flame due to oxygen deficiency in the flames interaction zone (relative reduction in energy release due to oxygen deficiency, unitless)	( )
$Loss_{H_2O}$	*P*er unit of $EC.VOL$, reduction in energy release for both flames in the flames interaction zone due to effects of live fuel's water content (relative reduction in energy release due to effects of live fuel's water content, unitless)	( )
M_{cw}	Mass of container and water	g
M_{cws}	Mass of container, water, and sample	g
M_s	Fresh mass of the sample	g
M_{wr}	Mass of water replaced at 20°C	g
$M.LOSS$	Mass of fuel consumed, mass loss	g
$PNHC$	Potential net heat content of a vegetative canopy	$MJ\,m^{-2}$
PWF	Porosity water-free	( )
r	Correlation coefficient	( )

R^2	Coefficient of determination	( )
S/V	Surface area to volume ratio	$cm^2\ cm^{-3}$
SWC.GRAV	Shoot water content expressed gravimetrically (dry mass basis)	%
SWC.VOL	Shoot water content expressed volumetrically as mass of water in the unit of the initial volume of the fresh sample	g cm^{-3}
TGA	Thermal gravimetric analysis	-
V	Volume	cm^3
V_{wf}	Volume of water-free cell wall substance in 1 cm^3 of the fresh sample	cm^3
V_w	Volume of water in 1 cm^3 of the fresh sample	cm^3

1 INTRODUCTION

1.1 WILDLAND FIRE ACTIVITY AND CHANGES IN CLIMATE

Changes in climate and increased human activity have induced a substantial shift in fire regimes, growth in fire season length, fire occurrence, area burned, fire intensity, and rate of spread. Over a 30 year period the decadal average area burned increased from 6 500 km^2 in 1960s to 29 700 km^2 in the 1990s for the North American boreal forests (Kasischke & Turetsky, 2006). In Canada due to 0.8°C higher average temperatures from May to August, a significant increase in area burned has been reported from the 1970s to the 1990s (Gillett et al., 2004). By the end of the 21st century in Canada, a 75% increase in fire occurrence is predicted according to Canadian Climate Centre general circulation model (GCM) scenarios and 140% according to Hadley Centre GCM scenarios (Wotton et al., 2010). Under the Intergovernmental Panel on Climate Change Special Report on Emissions Scenarios (IPCC SRES) A2 scenario of climate change, an eightfold increase in area burned for the areas previously called the Intensive and Measured Fire Management Zones in Ontario by 2100 is expected. These changes will be caused by increased fire weather and a predicted 92% growth in the number of fires escaping initial attack (Podur & Wotton, 2010). In the boreal forest of western Canada, a rise in the number of large uncontrolled fires is predicted due to increases in Daily Severity Rating and the growth of fire intensity above levels acceptable for fire control (de Groot et al., 2013).

The predicted growth in wildland fire and the resulting increase in carbon emissions from biomass burning can provide additional positive feedback on the tropospheric warming further magnifying climate change. For example, in 1998–1999 and 2002–2003, when intense global fires occurred, growth rate anomalies in the greenhouse gases (carbon dioxide, carbon monoxide, methane, hydrogen, ozone and methyl chloride) were strongly correlated to biomass burning (Simmonds et al., 2005). The increased emission of carbon dioxide related to wildland fire is balanced by the increased biomass production and hence by a higher rate of carbon dioxide consumption by plants. However, increased emissions

of other greenhouse gases and the effects of black carbon (Ramanathan & Carmichael, 2008) on global and regional climate forcing are not compensated by the natural processes in the ecosystems as efficiently as for carbon dioxide emissions. A recent study suggested that permafrost carbon release from wildland fires could increase four-fold (Abbott et al., 2016) by 2100 due to climate change and associated water stress and disturbance.

The challenge of balancing carbon emissions caused by wildland fire, and other challenges that wildland fire management is and will be facing due to changes in climate, should be better predicted and addressed. This requires substantial advances in fire modelling, aiming to develop more accurate fire behaviour prediction systems.

1.2 ACCURACY OF PREDICTION OF FIRE BEHAVIOUR

The effectiveness of fire management in preserving ecological, economic, social and cultural values and in maintaining the security of human life strongly depends on accurate prediction of important characteristics of wildland fire – fire behaviour. Accurate predictions are also essential in planning prescribed fire of high value or importance and in fuel treatments and fire mitigation programs. Merrill and Alexander (1987) defined fire behaviour as the characteristics of fire ignition, development, and spread. Those most commonly used operationally are the forward rate of fire spread and fireline intensity. Depending on behaviour and the potential danger of the particular fire(s), mitigation may require different levels of fire management, administration, and sometimes military response at local, provincial, national, or even international scales. It is very important to predict fire behaviour in advance to allow sufficient preparedness providing necessary resources and adequate fire management response planning. With the varying levels of success, fire behaviour has been modeled in different ways in the world. In Canada, the Fire Behaviour Prediction (FBP) System has been used along with the Fire Weather Index (FWI) System as submodels of the Canadian Forest Fire Danger Rating System (CFFDRS) (Forestry Canada, Fire Danger Group, 1992). The CFFDRS is also fully implemented in

New Zealand and parts of the United States. Components of the CFFDRS have been used in Mexico, Sweden, Spain, Portugal, Argentina, Indonesia, Malaysia, and Fiji. The two different models with the same name – National Fire Danger Rating System (NFDRS) – are used in the United States (Bradshaw et al., 1984) and Australia (the components of the Australian NFDRS are Grassland Fire Danger Index (GFDI) and Forest Fire Danger Index (FFDI) (Sharples et al., 2009) based on the McArthur fire danger rating).

It is commonly expected that with modern technological advances, these fire modelling systems should be able to predict extreme and catastrophic fire events accurately, thus minimizing economic losses and risks to human life. The history of fires with multiple fatalities does not show a substantial decrease in numbers of losses, however indicates growth in the frequency of these events (see Appendix 1). Modern weather forecasting and fire modelling tools generally provide satisfactory predictions of the level of danger of wildland fire; however, they still can be improved to provide adequate fire management and administrative response sufficient to ensure safety of population in the dangerous fire events.

One of the recent examples is Black Saturday Victorian Bushfires in Australia, 2009. In one day, several wildfires in south-eastern Australia burned over 450 000 ha resulting in 173 fatalities. The largest of them, the Kilmore East fire in Victoria burned 100 000 hectares in only 12 hours, taking 121 lives. The characteristics of this fire far exceeded predictions: rates of spread of main fire front at 68-153 meters per minute (4-9 km per hour), transport of firebrands (sources of new ignitions in the form of burning plant material transported by wind and convection) and ignition of spotfires (fires ignited by firebrands) up to 33 km ahead of the fire front (which was 55 km in width), and average fireline intensities up to 88 000 kilowatts per meter of fireline length. These intensities were sufficient for development of a pyrocumulonimbus cloud that injected the combustion products into the lower stratosphere (Cruz et al., 2012). In other words, that wildfire transformed into a firestorm with flame heights measured in hundreds of meters. Despite the obvious differences in fuels and fire weather conditions compared with those for Black Saturday Victorian Bushfires in Australia, the power, characteristics, and appearance of wildland fire in temperate and northern climates can be surprisingly similar,

as for example Chisholm Fire 2001 (Alberta Sustainable Resource Development, 2001), and Flat Top Complex Fire in Slave Lake 2011 (Flat Top Complex Wildfire Review Committee, 2012).

In operational firefighting, the most common cause of wildland fire-related accidents is "misjudgment of the behaviour of the propagating fire front" (D. X. Viegas, 1993) that leads to inadequate fire attack planning and failure to ensure firefighters' safety (Campbell, 1995). Due to underestimation of fire behaviour and resulting exposure to the extreme conditions of the fire front (burnover, dozer and engine burnover, entrapment, scouting fireline, vehicle fire, burns, heat stroke, hypothermia, heat exhaustion, asphyxiation, suffocation), on average 5 wildland firefighters lose their lives in the USA annually. This resulted in 519 losses from 1910 to 2014, which makes up 48% of the total losses related to wildland fire (NIFC, 2014). According to Campbell (1995), accurate prediction of fire behaviour is the first line of defense: training, communication, technologies, and equipment cannot be fully reliable if prediction of wildland fire behaviour is incorrect. The accurate prediction of wildland fire behaviour is only possible if all of the three main groups of factors determining fire behaviour – fuel, weather, and topography – are fully taken into account.

1.3 FLAMMABILITY OF LIVE FUEL

While weather and topography are well-studied and sufficiently represented in the fire modelling systems that are currently used, fuel-related variables are only partially addressed. The main characteristic of fuel is its flammability, which can be defined as ability of fuel to ignite and sustain combustion. The flammability of a vegetative canopy that is composed of combustible live and dead plant material – live and dead fuel – is evaluated using mostly the water content of dead fuel. However, water content, other physical-chemical properties, as well as flammability of live and dead fuel are distinctively different.

1.3.1 Distinctive features of live fuel

1.3.1.1 Properties and combustion of live fuel

Live fuel burns differently from dead fuel (Finney et al., 2012). For example, the same moisture content of live and dead plant material results in different flammability. Dead fuel which has water content above 35% of dry mass typically does not sustain flaming combustion; however fresh live foliage of conifers, which normally has a water content of 85% to 120% of dry mass, easily burns in a crown fire. It was suggested that with rapid dehydration of live fuel during combustion, part of the water is released from the combustion zone in liquid form after structural failure of the cell walls, so losses of energy for water evaporation can be smaller than for dead fuel (Finney et al., 2012). Also, the rapid release of the intercellar solution into the flame might lead to a substantial increase of the energy release due to presence of the flammable sugars and starches in the solution. The differences in combustion of live and dead fuel can be also explained by dissimilarity in spatial structure (including surface-area-to-volume ratio that is much greater in live fuel), chemical composition, dry matter content, and density. These factors stay relatively constant in dead fuel, but for live fuel they vary noticeably throughout the growing season. Therefore, all of these factors should be carefully considered in modelling the flammability of live fuel.

1.3.1.2 Factors affecting flammability of live fuel

In the FBP CFFDRS, seasonal changes in flammability of live fuel are evaluated using only water content (Forestry Canada, Fire Danger Group, 1992). However, the variation in flammability of foliage through the “spring dip” (time period of the lowest water content of coniferous foliage) is caused not only by water content. The flammability of live fuel is determined also, by changes in density and chemical composition (Jolly et al., 2014) and by consequent changes in calorimetric content (the gross heat of combustion, or the theoretical limit of energy release with combustion of dry material in a pure oxygen environment). Calorimetric content depends on the total mass of substances composing the

fuel (fuel density or dry matter content), on their relative proportions in the fuel (fuel chemical composition), and on the calorimetric value of each particular substance. Therefore, variation in density and chemical composition results in changes in calorimetric content.

Seasonal changes in chemical composition and density and the resulting changes in gross heat of combustion are noticeably different among species and for different years. The gross heat of combustion increases during the vegetative season due to phenological development of species both for old and new foliage (Chrosciewicz, 1986a), (Philpot, 1971). Additionally, drought and temperature-related increases in the content of highly flammable volatiles causes further growth in the gross heat of combustion. As was shown by Blanch et al (2009), for *Pinus halepensis* and *Quercus ilex*, the increase in terpene concentration was 54% and 119% due to drought, and 597% and 280% as a result of temperature rise from 30℃ to 40℃. According to a study on flammability of leaf litter (Ormeño et al., 2009), higher terpene contents resulted in increased spread rates and shorter combustion times (burn table tests); terpene concentration was positively correlated to flame height and negatively correlated to flame residence time and time to ignition (epiradiator tests). Hence, simultaneous changes in water content, chemical composition, dry matter content, density, and therefore in the gross heat of combustion and energy content (gross heat of combustion per unit of fresh mass or volume), caused by seasonal development, drought, and other natural disturbances, can dramatically elevate the flammability of live fuel.

1.3.1.3 Seasonal changes in flammability

The flammability of live and dead fuels changes through the season in very different ways. The flammability of dead fuel is dominated by changes in water content through precipitation and the consequent drying which in turn depends on in-stand weather conditions. These changes are well explained and predicted with the current fire modelling systems. The flammability of live fuel is determined by changes in water content, dry matter content, chemical composition, and biophysical properties such as density, porosity,

and thermal conductivity of live plant tissue. These species-specific changes are determined by the physiological state of individual species composing a forest stand according to their age, phenological stage, and adaptation potential depending on given growth conditions and level of the natural disturbances. The understanding and use of these changes in fire modelling is very limited.

1.3.2 Limited use of flammability of live fuel in fire modelling

It is very difficult to find documented evidence of failure to predict fire behaviour accurately, and even more difficult to find documented explanations of the reasons for the inaccuracy of fire behaviour predictions. However, in almost every case of massive loss of structures or of human life both fire danger and fire behaviour were under-predicted or (in some countries) not predicted at all, resulting in a lack of resources and inadequate fire attack or evacuation planning. In non-drought conditions, when changes in flammability of live fuel are caused mostly by phenological development, the existing semi-empirical fire modelling systems perform relatively well because phenology-related changes are in part considered. In the extreme conditions when severe fire weather and elevated flammability of dead fuel are augmented by a substantial increase in flammability of live fuel (due to drought or other natural disturbances), the accuracy of fire behaviour predictions can be marginal because of the lack of valid input for changes in live fuel flammability.

The important reason for substantial increase in fire danger during drought (Groisman et al., 2007) is changes in the flammability of live fuel. By the definition, unlike the initial period of dry weather, drought is a shortage in precipitation over an extended period resulting in prolonged lack of soil moisture. Lack of water, reduced evapotranspiration, increased plant tissue temperatures, and resulting shift in rates of photosynthesis and respiration in favor to latter induce substantial changes to the physiological state and biophysical-chemical characteristics of live plants and therefore to their flammability, as was discussed in the section 1.3.1. Weather conditions-induced changes in flammability of dead fuel are fully accounted for in existing fire modelling systems. Changes in the

flammability of live fuel, caused by phenological development, drought, and other natural disturbances are very minimally accounted for, thus limiting accuracy and reliability of fire behaviour prediction.

1.3.2.1 Consideration of age- and phenology-related changes

Among several important variables determining changes in live fuel flammability with phenological development, only changes in water content are usually considered, and only for foliage (foliar moisture content, FMC). According to Alexander & Cruz, (2012), FMC, which shows obvious a negative effect on flammability of single needles and small conifer trees in laboratory tests, has a much less evident effect on the behaviour of a crown fire (Alexander & Cruz, 2012). Due to a lack of experimental confirmation of the effects of water content on flammability on the forest stand scale, the phenology-related species-specific changes in water content of live fuel are considered by the FBP CFFDRS System only partially. FMC is not used for deciduous stands; however, crown fires can occur in deciduous and mixedwood (predominantly deciduous) forest stands affected by drought. For instance, during May 27-29, 2001, the Chisholm fire complex (LWF-063 and LWF-073 Chisholm fires, 2001, Alberta) showed continuous crown fire behaviour in deciduous (D-1) and mixedwoods that were predominantly deciduous (mixedwood stands as low as 25% conifer) M-1 (25% conifer) fuel types characterized by extreme spread rates, spotting distances, fire intensities and fuel consumption. The predictions of crown fire for deciduous (D-1) and mixedwoods that were predominantly deciduous were stated in the daily operational fire plans for May 27 (intermittent crown fire) and for May 28 and May 29 (continuous crown fire) (Alberta Sustainable Resource Development, 2001). Averaged for all conifers, FMC is used by the FBP System mainly for prediction of the initiation of crowning by calculation of the critical surface fire intensity. FMC is partially used for rate of spread and fire intensity calculations, since it is applied for the C-6 (conifer plantation) fuel type only (Forestry Canada Fire Danger Group, 1992). In natural coniferous stands, as well as all mixedwood and deciduous stands, phenology-related changes in behaviour of crown fire that involve substantial consumption of aerial (crown) live fuel, are evaluated using weather-induced changes in the water content of surface dead fuels. Age dependent

changes in the flammability of live fuel are not accounted for by the FBP CFFDRS System. Live plants composing a forest stand are considered as an inert fuel mass that changes its water content and hence flammability only during a "spring dip" in late May – early June regardless of age, phenological stage, growth conditions, and occurrence of natural disturbances affecting plant water availability conditions (drought), forest health (insects, diseases), and stand structure (windthrow, tree mortality).

1.3.2.2 Consideration of changes in flammability of live fuel caused by drought

Neither the American NFDRS nor the FBP CFFDRS systems have a valid input for drought-induced changes in flammability of the live part of a forest stand. The most dangerous fires, however, occurs with the beginning of drought (Groisman et al., 2007). A considerable decrease in water content in live plant tissue is accompanied by a manifold increase in terpene concentrations caused by drought and high temperature induce a substantial increase in the flammability of the live fuel (see section 1.3.1). The input for the effect of drought on live fuel flammability used by the FBP System is not fully reliable, because it is based on the estimation of water content in the soil layers 7 cm and 18 cm deep represented by Duff Moisture Code (DMC) and Drought Code (DC) respectively. These indices are further used for calculations of Buildup Index (BUI, represents total fuel available for fire spread), Fire Weather Index (FWI), and then fire intensity and rate of spread (Van Wagner, 1987). However, drought level and hence the flammability of live vegetation are determined by soil water availability conditions in a much deeper root-zone horizon, measured by meters rather than by centimeters. The water status of plant species, in many cases, depends on the ability of plants to uptake water from the water table which is sometimes deeper than 18 m (Lewis & Burgy, 1964). The maximum rooting depth, which determines a plant's ability to supply water during drought, was found to be on average 2 m for boreal forest and cropland, 4 m for temperate coniferous forest, 3 m for temperate deciduous forest and grassland, 5 m for sclerophyllous shrubland and forest, and 10 m for desert, (Canadell et al., 1996).

The sensitivity of DMC, DC, and BUI to plant water stress caused by drought (and hence to water content and flammability of live fuel) diminishes with the increase in maximum

rooting depth. However, reliability of these indices is questionable even for shallow rooting depths of boreal stands. On a dry site in peatlands for example, the maximum rooting depth of black spruce *(Picea mariana)* and tamarack *(Larix laricina)* was measured approximately at 60 cm and was strongly correlated with, and limited by, *depth to water table* (the greatest depth > 90 cm) (Lieffers & Rothwell, 1987). Even with the lowest soil water content readings in the upper portion of this horizon at 7-18 centimeters deep (DMC and DC nominal fuel depth correspondingly) during prolonged dry weather conditions, plants can be fully supplied by water (because roots depth is normally limited by water table). In May and June (peak fire activity in boreal forests), the opposite situation is possible, when the top soil layer 7-18 centimeters deep is fully saturated with water due to melting snow (DMC, DC and BUI have the lowest readings), while the trees can be still affected by drought. Three things can make this possible: delayed recovery of plants from water stress, dryness of the lower soil horizon due to the water table being shifted down by prolonged drought, and delayed thawing of peat. The roots in the lower soil horizon can still be frozen (meaning no soil moisture available) in May and June, since peat thaws much slower than mineral soil. The DMC, DC and BUI are reliable indicators of fuel conditions during normal weather conditions when forest stand flammability is determined by flammability of dead fuel. However, they may misrepresent flammability of live fuel in the extreme fuel-weather conditions during drought, when reliable predictions are especially needed.

In the American NFDRS, FMC is successfully used for forecasts of the energy release component (ERC) as a broad approximation of moisture content of living herbaceous plants and small woody shrubs, according to weather and remote sensing data on their greening and curing. However FMC is not applied for forest tree species (NFDRS, 2011).

1.3.2.3 Accounting for other natural disturbances

Insect infestations cause a further increase in the flammability of live fuel (Jolly et al., 2012) by causing changes in the chemical composition and water content of live plant tissue. Drought, tree mortality, insect and disease outbreaks, and wind damage lead to a decrease in canopy cover and to changes in the mass-energy balance of the forest canopy

due to an increase in the near-ground solar radiation and reduced aerodynamic resistance of the canopy (Royer et al., 2011). This results in higher evapotranspiration, increased plant surface temperature causing a positive feedback on the level of drought. Changes in fuel distribution accompanied by drought cause considerable changes in plant physiology and chemical composition (Royer et al., 2011) and hence in flammability. Changes in flammability of live fuel due to tree mortality and insects are accounted for partially in the mountain pine beetle stands, M3 (Dead Balsam Fir Mixedwood–Leafless), and M4 (Dead Balsam Fir Mixedwood–Green) fuel types by empirical approximation of the FMC. Changes in flammability caused by disease, wind damage, and canopy cover decrease are not considered. In order to determine whether there is a need to consider changes in live fuel flammability in fire modelling separately from dead fuel, one must answer the question of whether live fuel combustion substantially contributes to the intensity and propagation of the frontal flame of wildland fire.

1.3.3 Importance of combustion of live fuel in determining fire behaviour

With given fire weather and topographic conditions, the behaviour of wildland fire is determined by the flammability of plant material consumed – of live and dead fuel. Fire behaviour can be predicted accurately only if characteristics and flammability of both live and dead fuel are fully taken into account. There are several examples where increased flammability of live fuel and thus increased fire danger were underestimated; one of them is the Lower North Fork Wildfire in Colorado, March 2012.

1.3.3.1 Example: Lower North Fork Wildfire in Colorado, 2012

Dead fuel was wet due to melting snow still present on the ground, so the estimated behaviour of this prescribed fire, predicted using conditions of dead fuel, was far from extreme. Despite low flammability of the dead fuel, the flammability of the forest stands was extremely high due to drought-induced changes in biophysical and chemical characteristics of the live fuel after a severe winter drought. The potential danger of the

prescribed fire caused by extreme flammability of the live fuel was underestimated. The escaped prescribed fire grew into a devastating fire event. The colors of the flame and smoke clearly showed the extreme intensity of an oxygen-deficient crown fire, where the frontal fire intensity and rate of spread were limited only by wind speed and atmosphere stability conditions – not by flammability of the live fuel. In one week three lives were lost, 24 structures destroyed, 4,140 acres burned and more than 900 homes in the area evacuated. This example suggests that the flammability of live fuel can be decisive in determining fire behaviour. The intensity of the effect of live or dead fuel on frontal fire characteristics, however, depends on the proportion of live and dead fuel consumed by frontal flame.

1.3.3.2 Proportion of live fuel consumption in the frontal flame

Ever since development of the first successful fire modelling systems in the 1980s, it has been considered that flammability and combustion of the live part of a vegetative canopy has a very limited effect on the behaviour of wildland fire, because the consumption of live fuel is less than the consumption of dead fuel. This assumption is used as basis of most fire behaviour models and it is seemingly supported by experimental data from the Sharpsand Creek experimental fires 1975-1981 (Stocks, 1987). These data, however, represent total crown fire consumption without separate consideration of frontal fire consumption and post-front consumption. Post-front consumption does not affect fire behaviour; it is represented mainly by dead fuel in the forest floor with smoldering shifting the measured proportion of live and dead fuel consumed towards dead fuel. To substantiate the necessity of this study on the flammability of live fuel, the additional analysis of these data was performed using an approach that estimated frontal fire fuel consumption separately from post-front fuel consumption (Call & Albini, 1997). The analysis was performed with the permission and approval of the results from the first author of the data source (Stocks, 1987).

The proportion of live fuel consumption to the total fuel consumption in the flame-front of the crown fire varied from 48% to 60% with an average of 54% according to the results of this analysis (see Table 3 in Appendix 2). Since during the Sharpsand Creek experimental

fires live fuel in the understory and overstory of the forest stand was measured only as foliage of live plants and the rest of the plant material consumed was assumed to be only dead branches less than 0.99 cm in diameter, the proportion of live fuel consumed was, probably, underestimated. It is very unlikely that only foliage was consumed without consumption of, at least the finest, live twigs. This was confirmed by Stocks et al., (2004) stating that most of live roundwood less than 1 cm in diameter was consumed by the frontal flame. This suggests that the calculated consumption of live fuel by the flame-front of the crown fire at 53.9% on average to total frontal fire consumption using data from Stocks (1987) was actually considerably higher.

Therefore, crown fire behaviour is heavily influenced by the combustion of live fuel due to the higher proportion of its consumption in the frontal flame. Crown fire, moreover, makes up the larger part of the area burned in the boreal forest (Amiro et al., 2004). Even for surface fire, in many cases, live fuel consumption can be substantial when there is a significant presence of live herbaceous on the forest floor, shrubby plants, secondary species, and new regeneration in the lower understory. Live fuel plays a very important role in determining the behaviour of crown fire due to higher proportion of live fuel consumption by the frontal flame compared with dead fuel consumption. One of the explanations is that live fuel has characteristics of mass and size distribution that are favorable for combustion: light, high surface to volume live fuel in the upper part of canopy versus larger low surface to volume dead fuels in the lower part of canopy close to forest floor surface. These indicate the essential importance of a better understanding of the flammability of live fuel and the criteria of flammability: characteristics of the ignition, consumption and energy release.

1.3.3.3 Increase in live fuel consumption with growth in fire intensities

The predicted growth in fire weather conditions and fire intensities resulting from climate change (de Groot et al., 2013) suggests that the proportion of live fuel consumption will also increase. Theoretically, with the increase in fire weather conditions and fire intensity

and the transition from surface fire (mostly dead fuel consumption) to active crown fire (mixed live and dead fuel consumption) and then to (very rare) independent crown fire (mostly live fuel consumption), the proportion of live fuel consumed to total frontal fire consumption grows due to higher involvement of crown fuel which is represented mainly by live plant material. This was in part confirmed by the results of the analysis of the experimental data from the Sharpsand Creek experimental fires 1975-1981 (Stocks, 1987) already discussed in the previous sub-section ("Proportion of live fuel consumption in the frontal flame"). Consumption of live fuel by flame-front increased with growth in Fire Weather Index (FWI) and fire intensity (see Fig. 3 and Fig. 4 in Appendix 2). The data showed, however, only slight increase in the proportion of live fuel consumption to total frontal fire consumption (%) with growth in fire intensity (Fig. 5 in Appendix 2).

1.3.3.4 Growth in live fuel consumption with increase in natural disturbances

As a consequence of changes in climate, the increase in drought and other natural disturbances predicted for many regions will cause additional growth in the proportion of live fuel consumption in the total frontal fire consumption. Theoretically, in drought conditions, the proportion of live fuel consumed increases due to the growth in live fuel flammability caused by drought-related changes in physiological state and physical-chemical properties. The analysis of the experimental data from the Sharpsand Creek experimental fires supported this assumption showing an increase in live fuel consumption with an increase in DC and BUI indices (Fig. 1 and Fig. 2 in Appendix 2). Other natural disturbances such as insects, diseases (changes in water content and chemical composition), as well as consequent tree mortality and windthrow (changes in spatial structure resulting in increase in drought) cause further growth in flammability of live fuel and in its consumption by fire.

Actual changes in future fire regimes may be even more substantial than that predicted using the existing long-term weather-forecasting and fire behaviour models. The FBP CFFDRS model that is often used to predict future fire activity, for example, accounts for the expected changes in weather conditions and for corresponding changes in flammability

mostly of dead fuel. Hence the rise in flammability of live fuel, due to physiological changes in water, dry matter, and chemical contents of live plant tissue with growth in natural disturbances (Allen et al., 2010), (Williams & Liebhold, 2002) is not accounted in the predictions of future fire regimes.

1.3.3.5 Increase in spatial variation of flammability of forest stands

Changes in climate can alter the frequency, intensity, duration, and timing of natural disturbances (Dale et al., 2001) causing growth in the spatial heterogeneity of the forest stands depending on the level and type of natural disturbance (Turner, 2010) and related changes in flammability of live fuel. Spatial variation in species composition may lead to large spatial variation in forest stands flammability due to species-specific response of live plants to different levels of natural disturbance and due to differences in the phenological development of the species. While predicted to be the same for all forest stands within a given fuel type and under the same weather conditions, fire behaviour in the particular forest stand can be dramatically different depending on the disturbance level (especially drought), species composition, and resulting level of live fuel flammability.

Fatal and near-fatal incidents usually take place under moderate fuel and weather conditions when the potential danger of change in fire behaviour was unexpected (Wilson, 1977). The most common and most important reason for these incidents is failure to predict sudden shift of fire behaviour from apparently harmless to devastating when moderate simultaneous changes in factors determining fire behaviour become “aligned” (Campbell, 1995). This can happen when even small, favorable for fire growth, changes in weather and terrain conditions coincide with changes in live fuel conditions as the fire front propagates through different forest stands. This sudden shift in fire behaviour, caused by changes in live fuel flammability, can neither be expected nor predicted because flammability of live fuel is not included in the fire modelling process. Due to the unique biophysical and chemical properties and characteristics of combustion of live plant tissue, the existing definition, measure, and methods designed for dead fuel flammability assessment may not properly represent live fuel or combinations of live and dead fuel.

1.4 ASSESSMENT OF FLAMMABILITY OF LIVE FUEL

1.4.1 Definition of flammability

Issues associated with the combustion and flammability of live fuels are among the most important factors limiting the use of physically-based fire modelling (Finney et al, 2012). There is no commonly accepted definition or measure of live fuel flammability which leads to a large variety of methods and variability in results. In this study, flammability of fuel is defined as its effect on the flame-front: change in energy release from the frontal flame resulting from the interaction with this fuel consumed during the passage of the flame-front. Introduction of this definition of flammability is an attempt to address issues associated with live fuel flammability defining and measuring. Currently, fresh plant material composing live fuel, fire conditions for adequate flammability assessment, and criteria for evaluation of flammability are misrepresented, not clearly specified or defined.

1.4.1.1 Live plant material composing live fuel

The type and size of live plant material defined as live fuel has not yet been clearly specified. It is still unclear what live fuel is: foliage only, twigs with attached foliage (shoots), branches, or whole plants? Live fuel is usually represented in tests by foliage alone; though according to Stocks et al (2004), most of the live plant material less than 1.0 cm in diameter in the understory and overstory was consumed by crown fire. The fire behaviour response of foliage alone, shoots, or whole branches to the test conditions can be quite different due to differences in their water content, physical-chemical properties, and substantial differences in their spatial structure. When evaluating and predicting the behaviour of a fire front, it is necessary to consider live plant material which is actually consumed by the frontal flame: whole herbaceous plants as well as branches of shrubs and trees. Each separate branch or all live plant material of the vegetative canopy consumed by frontal flame can be presented as a spatially arranged system of fuel elements composed of shoots: twigs thinner than 1.0 cm in diameter with attached foliage.

The fire response of live plant material is often evaluated regardless of age, and new growth is typically excluded from analysis (Weise et al., 2005). Plant material of different ages, however, is likely to have quite different flammability due to substantial dissimilarity in water content. Water content is substantially higher for new foliage (current season foliage) in the beginning of summer compared with older foliage (Chrosciewicz, 1986b). In the beginning of the vegetative season, new growth (current season growth, foliage and twigs) of forest species has substantially different fire properties and burns differently from old growth (1-year and older growth). The proportion of the new growth in the plant composition increases during the season: from 0% (leaf emergence) to 25% by the end of the season and to 50% for some fully sun-exposed branches. The properties of new plant material change substantially with a seasonal transition of new growth to old growth.

1.4.1.2 Fire conditions of flammability evaluation

The flammability of live fuel can be defined as a potential (maximum) fire behaviour response of live plant material to fire environment conditions. Considering that fire behaviour response varies depending on fire conditions and that the targeted object of interest is behaviour of the fire front, flammability can be defined as a potential fire behaviour response of live fuel to the maximal expected fire conditions of the fire front (frontal flame). Fire conditions that are required to represent frontal flame (type, intensity, duration, and direction of the ignition heat transfer, as well as low oxygen availability and high concentrations of carbon dioxide and water vapor) are usually not specified in the current definitions of flammability. Fire conditions are usually determined in the tests by the equipment used rather than by the requirement to represent conditions of the frontal flame. The test conditions are substantially different from those for frontal flame and may misrepresent live fuel flammability.

1.4.1.3 Processes of fuel combustion and criteria of evaluation of flammability

Flammability is currently evaluated using ignition delay time, or time-to-to ignition (ignitibility), combustion duration (sustainability) and rate (combustibility)(Anderson, 1970), rate of fuel consumption (consumability) (Martin, 1994), flame size, height, and flame temperature (as proxy to energy release rate, or intensity), calorimetric content, energy release rate and content, et cetera. Among them, fuel water content (or moisture content) – as a proxy to flammability – and time-to-ignition are most commonly used. However, characterization of the mass-energy exchange processes of fuel consumption and evaluation of the effect of these processes on propagation of the frontal flame requires consideration of energy-based criteria of flammability, that is, energy release rate and total energy release.

The behaviour of wildland fire is determined by the extent of its frontal flame growth – from initial ignition (depending on the ignition source) to full crown fire. With given weather conditions and spatial structure in the vegetative canopy, this growth depends on the rate and amount of energy release from each already burning fuel element. The higher the energy release rate and total release during passage of the fire front (frontal fire residence time, 40-70 seconds on average), the larger the number of the next adjacent fuel elements that will be preheated and ignited, and hence (depending on weather conditions) the larger extent of fire growth. The amount of the energy released by wildland fuel after the passage of the flame front does not affect characteristics of the frontal flame and, therefore, should not be included in the assessment of such characteristics of potential fire behaviour as fire intensity and forward rate of spread. The existing definitions consider rate and total energy release regardless of actual flame-front residence time. However, depending on the spatial structure and physical-chemical properties of live fuel, energy release during 40-70 seconds of combustion within the frontal flame can be quite different compared with energy release during several minutes of combustion in the open air measured using traditional methods.

The assumption that the energy release rate (intensity) of the flame front is the sum of the energy release of the fuel elements involved in combustion if measured separately may be inaccurate. This can be caused by the possible negative effect of burning live fuel flame on

the energy release and resulting intensity of the frontal flame. This reduction in energy release for the frontal flame, caused by the high water content of live fuel and by oxygen deficiency in the flames interaction zone (live fuel flame and frontal flame), can be substantial. Therefore, flammability traditionally defined and measured on a separate fuel element scale may misrepresent the actual fire behaviour response of live fuel on the flame propagation scale.

1.4.2 Measures of the flammability of live fuel

Physical and chemical properties of live fuel are traditionally measured using a gravimetric approach (per unit of dry or fresh mass) which does not properly represent the physical-chemical properties of live fuel and the spatial three-dimensional nature of the combustion process. Traditional gravimetric measurements of water content as a proportion of the mass of water to dry mass cannot be used for live fuel. Dry mass notably varies during the vegetative season due to phenological changes in chemical composition and density of live plant tissue, so foliar moisture content measured as percent of dry mass misrepresents the actual quantity of water. Variation in foliar moisture content is explained by seasonal changes in density (and thus in dry matter content) and in the chemical composition rather than by actual changes in water content (Jolly et al., 2014), and by combined changes in both water and dry matter contents (Little, 1970).

Characteristics of combustion are determined not only by mass-to-mass proportions of different substances in the fuel, but also by their spatial distribution (concentration) in the volume that makes up the fuel. One of the most obvious reasons for the necessity of using a volumetric approach (measured characteristics are expressed per unit of volume) is the importance for combustion of such characteristics as thermal conductivity and specific heat content because these characteristics of live fuel are strongly determined by volumetric variables: density, porosity, and concentration of water in the fuel volume. Another very important characteristic of fuel, which is also volumetric, is surface area to volume ratio. The higher the ratio, the higher is surface area for a given mass to interact

with the incoming energy and hence a higher energy transfer per unit of fuel mass resulting in higher heating rates as well as reaction and energy release rates. The higher ratio also provides the higher amount of oxygen and products of the pyrolysis involved in the reaction for a given mass of the fuel.

1.4.3 Existing test methods of assessment of flammability

Due to high water content and difficulties in igniting live fuel, its flammability is widely evaluated as energy content using oxygen bomb calorimetry: the heat of combustion of oven-dry plant material in a pure oxygen environment (gross heat of combustion). These test conditions, which are quite different from the conditions of fresh live fuel combustion in the atmospheric air or in the oxygen-deficient gaseous mixture of the frontal flame (Babrauskas, 2006), are used for estimation of energy content: gross heat of combustion, H_{gross} (higher heat of combustion) (Chrosciewicz, 1986a; Van Wagdendonk et al., 1998), lower heat of combustion (H_{gross} minus energy absorption with evaporation of reaction water) (Rivera, Davies, & Jahn, 2012), and net heat of combustion H_{net} (H_{gross} minus energy absorption with evaporation of reaction water and water contained in the fuel) (Byram, 1959; Van Wagner, 1977). In the FBP CFFDRS System, the intensity of simultaneous combustion of live and dead fuel is calculated using the averaged net heat of combustion of dry, dead fuel alone at 18 kJ g^{-1} in the Byram's formula of fireline intensity (Byram, 1959). The most detailed consideration of important characteristics of live fuel combustion is provided by differential scanning calorimetry (DSC) and thermal gravimetric analysis (TGA) (Leroy et al, 2006). These techniques, however, consider thermal degradation at a very small scale and are typically performed in pure nitrogen environment representing phase of thermal degradation (pyrolysis) rather than of flaming combustion. The small sample size (usually 5-100 milligrams) used in these analytical methods due to technical limitations of the equipment, along with efficient removal of pyrolysis and combustion products, slow heating rates, and greater rate of water

evaporation due to large proportion of cut surface area of the sample can lead to a misrepresentation of fuel properties and the conditions within the frontal flame.

1.4.4 Oxygen consumption calorimetry as a base method for the study

Oxygen consumption calorimetry (Babrauskas, 1984) allows detailed evaluation of live fuel combustion in the open air burning conditions at a much more representative scale from foliage and shoots to separate trees. Heat release rate *(HRR)* from the chemical reaction of fuel with the atmospheric oxygen is the key derived variable characterizing the flammability (Babrauskas & Peacock, 1992). An integral of *HRR* during the time of combustion per unit of mass of fuel consumed, expressed as effective heat of combustion (H_{eff}) (Babrauskas, 2006), is widely used for the estimation of live plant flammability (Weise et al., 2005; Babrauskas, 2006; White & Zipperer, 2010).

The conditions of the frontal flame are only partially represented in the oxygen consumption calorimetry method. Radiative-only heat flux from a radiant heater of a cone calorimeter has much lower intensity than that of a flame. Also, in the real fire, in the upper part of the vegetative canopy (composed mostly of live fuel), the direction of the ignition heat transfer (forward or up) and the direction of the flame propagation usually coincide or are close. In the traditional tests, the direction of heat transfer and flame propagation through the tested plant material is opposite to the flow of air and of products of combustion since the ignition heat flux is applied from above and received by the upper portion of the tested fuel sample. This causes almost complete absence of convective heat transfer with the flame propagation through the sample. Together with insufficiency of the ignition heat transfer discussed above, this results in slower heating rates, delayed and inconsistent ignition and substantially longer flame residence time. An additional source of the variability and inconsistency in the ignition of live fuel is the variability in the spatial structure of tree branches. This can be substantial for live fuel.

The common opinion that radiative heat transfer is the dominant form of heat transfer with flame propagation (Albini, 1985) has been questioned by many authors (Anderson, 1969;

Van Wagner, 1977; Beer, 1991). According to the results of recent study (Frankman et al., 2013), it was concluded that depending on fuel and weather conditions, convective heating might be more important than radiative heating. They reported combined peak radiative and convective flux of the flame front measured in the field conditions of 342 and 221 kW m^{-2} for two separate crown fires. Residence time was reported 50 seconds (Frankman et al., 2013), and 74 seconds (37 seconds for the main flaming front of tall flames and another 37 seconds for the secondary flaming front of continuous short flames) (Wotton et al., 2012). Flame temperature increase was approximately 1060℃ during the first 30 sec of residence time resulting in 35 °C sec^{-1} heating rates and less than 10-20 seconds ignition delay time (Wotton et al., 2012). The radiant ignition flux of 25-50 kW m^{-2} of the cone calorimeter usually used is totally insufficient to provide the conditions of the flaming front reported (over 300 kW m^{-2} combined radiative and convective ignition flux, over 30°C sec^{-1} heating rates, 5-15 seconds ignition delay time, and 40-70 seconds flaming front residence time, and) (Frankman et al., 2013; Wotton et al., 2012).

Consequently in many cases the tested green samples exposed to the 25 kW m^{-2} radiant ignition flux did not sustain ignition and if ignition occurred, ignition delay time ranged from 52 sec to 555 sec with average approximately 120-150 sec (Weise et al., 2005), which is longer than flaming front residence time reported (Wotton et al., 2012). Delayed and inconsistent ignition lead to variability and inaccuracy of the test results where heat release represents mostly characteristics of water evaporation and pyrolysis rather than combustion behaviour. Substantially lower heating rates and much longer ignition delay time may cause increased losses of pyrolizates without ignition; therefore, energy release of the tested live fuel measured using cone calorimetry may underestimate live fuel energy release in the frontal fire conditions. Also, after 2-5 minutes of exposure to the radiant heater without ignition, the water content of the live fuel being tested can be substantially less when the fuel finally ignites. An additional source of uncertainty in respect of combustion of live fuel is the high water content of live fuel and its possible effects on the reaction rate and energy release of the incoming frontal flame.

1.4.5 Incomplete combustion in the flames interaction zone

Highly variable water content is one of the most important features of live plants. For example, for white spruce water content can vary from 75 to 480% of dry mass depending on plant growth (material) age and phenophase (season) (Chrosciewicz, 1986b). Combustion of live fuel cannot be considered as an oxidation of dry plant material after all water contained in live fuel is evaporated. It has been suggested that combustion of live fuel occurs simultaneously with water evaporation (Finney et al, 2010). The endothermic process of water evaporation and the presence of considerable concentrations of water vapor in the resulting gaseous mixture strongly affect all stages of live fuel combustion. Direct absorption of energy for water evaporation, vapor and fuel temperature increase (including increased heat transfer to the unburned part of the fuel due to an increase in thermal conductivity and specific heat content caused by high water content) can be substantial. The consequent drop in reaction temperature and hence reduction in the reaction and energy release rates, as well as dilution of gaseous products of pyrolysis and oxygen by water vapor (Ferguson et al, 2013), and oxygen deficiency due to interaction of flames of separate fuel elements (Pickett et al., 2009) cause incomplete combustion, which can result in substantial release of unburned hydrocarbons in large, high-intensity fires (Byram, 1959).

The reduction in energy release for the live fuel burning within a frontal flame due to incomplete combustion is partially estimated by oxygen consumption calorimetry. In these tests, where the fuel sample is surrounded by atmospheric air and there is no limitation in oxygen supply, incomplete combustion is caused mostly by water content due to drop in reaction temperature and rate and due to reagents dilution by water vapor. Actual energy release from live fuel burning within a frontal flame can be considerably lower than measured in the oxygen consumption calorimetry tests due to very limited oxygen supply in the flames interaction zone where flame of the burning live plant material is mixing and interacting with the incoming frontal flame (Fig. 1.1).

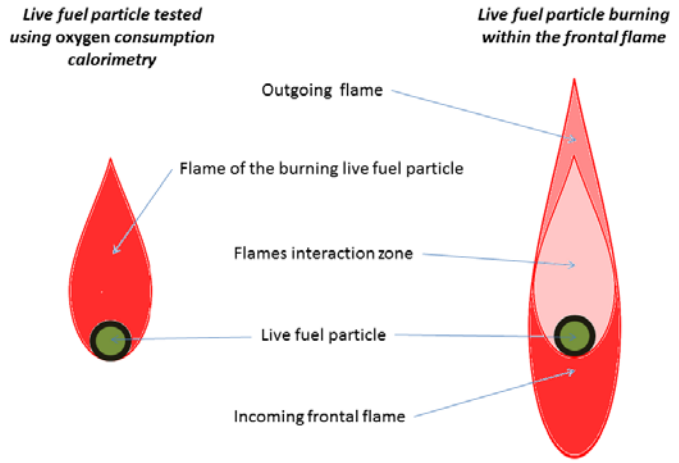

Figure 1.1 Live fuel element tested using oxygen consumption calorimetry and burning within the frontal flame. Reduction in energy release to the flame of the burning sample and incoming frontal flame in the flames interaction zone due incomplete combustion can be substantial

There is little information on the possible effect of high water content of burning live fuel on the incoming frontal flame. Reduction in energy release due to incomplete combustion can be significant not only for the outgoing flame from the recently ignited live fuel element, but also for incoming frontal flame (Fig. 1.1) causing reduction to the intensity of the outgoing flame (incoming frontal flame intensity after involving live fuel element). Due to this hypothetical energy release drop for the incoming frontal flame in the flames interaction zone, the resulting energy release growth for the frontal flame caused by the introduction into the frontal flame of the new live fuel element can be less than energy release of this burning element if measured separately. If for instance, total energy release (when burned separately) of each separate fresh needle is equal and known (= X), the total energy release of these 10 needles burning together (depending on their spatial distribution), may be less than 10*X due to reduced oxygen concentration and dilution of reactants with water vapor. Also, due to the same reasons, the increase in the total energy release of the combined flame of these 10 needles burning together caused by adding into the flame one more (11^{th}) needle will be probably less than X. Thus traditional oxygen

consumption calorimetry methods likely overestimate the *energy release contribution of the burning live fuel to frontal flame intensity* and propagation.

1.4.6 Flammability as energy release contribution to the frontal flame intensity

Energy release contribution of the burning fuel to the frontal flame intensity defines characteristics of flame growth, propagation, or decline. It represents the energy source (energy generation) component of the energy balance of the frontal flame. The state of the system of the frontal flame depends on its energy balance: the flame is stable if energy generation is equal to energy losses and it declines or grows if the sum of energy generation and losses is negative or positive, respectively. The flame front emits a large amount of energy into the environment (depending on weather, fuel, and flame characteristics) in the form of convection, radiation and heat conduction to the unburned fuel and upper soil layer (energy losses, or negative components of the energy balance of the frontal flame). Therefore, for the frontal flame to *propagate* (to sustain slow decline, equilibrium or growth state), it requires a positive energy release contribution (change in energy release to the frontal flame) at or above a threshold value from each burning fuel element (this is true on average for several elements; some elements may in fact not continue to burn but the overall front will still progress as long as there is sufficient release at the frontal flame scale). Hence, low-positive and negative values of the energy release contribution (with water content of live fuel above a certain value) will mean a decrease in intensity of the frontal flame, and eventually, extinguishing of the frontal flame. To estimate this very important threshold of live fuel flammability, and then to use it in fire growth modelling, flammability as an energy release contribution of the burning live fuel to the frontal flame intensity (energy generation component of the energy balance of the frontal flame) needs first to be defined, measured, explained and predicted on the flame propagation scale.

To date, there is no such method and empirical data properly representing live fuel flammability: live plant material consumed by frontal flame, the conditions of the fire

front, and the effect of burning live fuel on the energy release and resulting intensity of the frontal flame. Therefore, the range of variation, factors affecting live fuel flammability, and seasonal changes in flammability are unknown. By addressing these issues, the present study is an attempt to develop an experimental methodology for live fuel flammability testing and quantifying where flammability is defined and measured as an effect of the burning fuel on the energy release of the frontal flame. Better understanding of live fuel flammability and the development of practical tools for physics-based live fuel flammability modelling, which is an additional goal of this study, will be essential to the improvement of the accuracy and reliability of wildland fire behaviour prediction.

1.5 RESEARCH QUESTIONS

1. Does the proposed method represent the conditions and characteristics of live fuel combustion in the frontal flame?

2. What is the range of variation of live fuel flammability? How different is the flammability of plant material of different ages?

3. Can there be any substantial negative effect of the burning live fuel on the energy release of the frontal flame?

4. How can the flammability of live fuel be modelled? What approach and model best describes the observations?

5. How does flammability of live fuel change throughout the season and how can these changes be predicted?

2 DATA AND METHODS

2.1 FIELD SAMPLING

2.1.1 Site location and description

Shoot samples were taken at a site in central Alberta within the Central Parkland Natural Subregion, Parkland Natural Region, Eastern Alberta Plains Physiographic Region (Downing & Pettapiece, 2006). A research site was established in the ecological reserve of the Devonian Botanic Garden, ten kilometers southwest of Edmonton, Alberta (Fig. 2.1), 1.5 km south of Devonian Botanical Garden. Coordinates for the center of the site are: (53.395 ° N, 113.758 ° W). Vegetation is represented by a 50 to 70-year-old mixed stand of white spruce *(Picea glauca)* and trembling aspen *(Populus tremuloides)* with a small percentage of black spruce *(Picea mariana).* The Central Parkland Natural Subregion is the most densely populated in Alberta; densities and distribution of forest stands in the area are typical of the wildland-urban interface due to their proximity to the city of Edmonton. The average elevation is 750 meters above sea level. Soils are Black Chernozems, Dark Gray Chernozems and Gleysols. Continental climate is transitional between the Grassland and Boreal ecoclimatic provinces and is characterized by long cold winters and short warm or hot summers. Mean annual temperature is +2.3°C, the mean temperature of the coldest month being -14.7°C, and of the warmest month +16.5°C. Mean daily minimum values (December, January, February) and maximum values (June, July, August) are -20°C and +23°C respectively. The growing season spans from May to September. Mean annual precipitation is 447mm. Evapotranspiration is high due to high insolation and westerly winds; moisture availability in the growing season is generally limiting to growth after June.

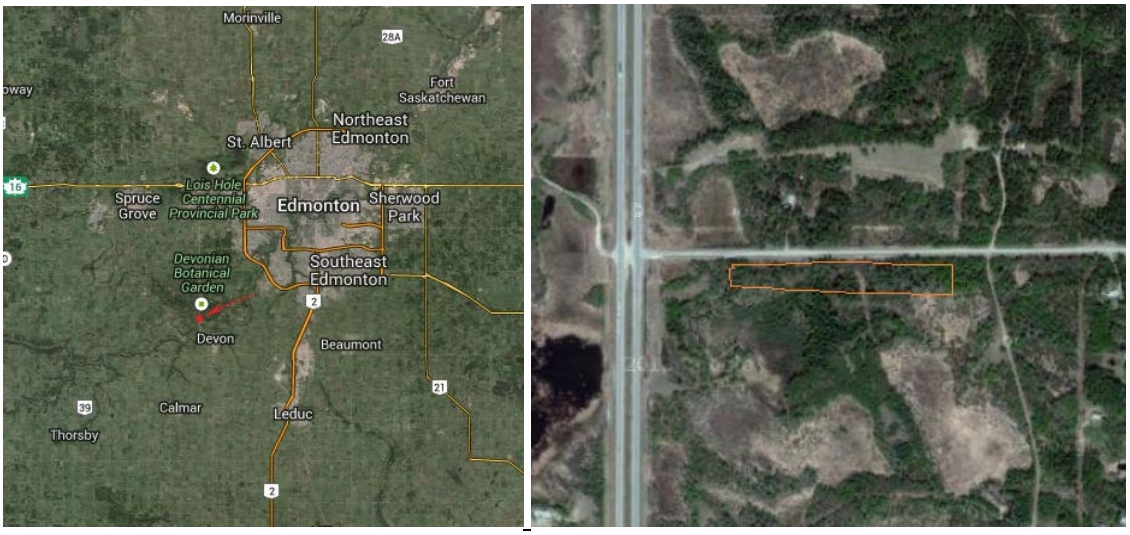

Figure 2.1 Site location map, Highway 60, southwest of Edmonton, North of Devon (left image). Solid orange line indicates boundaries of the study site. Study site is situated within Eco-Reserve area of the Devonian Botanical Garden (right image).

2.1.2 Species and trees selection

Considering that variation in the flammability of live fuel is species-specific, and that a large amount of field and laboratory work was anticipated, experimental work on the flammability of live fuel was designed to be species-specific, dealing only with one species. Since flammability is strongly affected by water content (Van Wagner, 1963), (Jolly et al., 2012), white spruce was selected for the testing due to its exceptionally high variation in foliar water content, from 78% to 480% of dry mass (Chrosciewicz, 1986b), (Keyes, 2006). In order to represent differing availability of soil water in the forest stand, six mature white spruce trees were selected for each of three slope positions: a low-lying area bordering on wetland, the middle of a hill slope, and the top of the hill, for a total of 18 trees. Trees were sequentially numbered using paint marker. All selected trees were in normal physiological conditions with slight variation in crown development and without visible signs of insects or diseases. For most of the trees, the south-oriented part of the crown was exposed to more than 50% insolation.

2.1.3 Sampling procedure

In order to represent variation in the flammability of live fuel related to phenological changes and growth conditions, all 18 selected trees of white spruce were sampled on the test site on each of 11 field trips, starting in early May until the end of October 2014**.** Sampling was performed every one to four weeks depending on the rate of changes in phenological development and on weather conditions. Samples were collected between 12:00 and 16:00 local time on days without precipitation or visible moisture on the plant surface. Using a pole pruner, one small branch was taken in the outer part of the crown within the lower one-third of the crown height on the south side of each tree, mostly in full sun exposure (Fig. 2.2).

Figure 2.2 Field sampling. Sampled tree branches were taken within lower one-third of the crown height on the south side of the crown between 12:00 and 16:00 local time on days without precipitation.

To avoid a diurnal variation in the properties of shoots, sample collection was performed using the shortest route from tree to tree within the test site. The samples were stored in large re-sealable plastic bags during sample collection and placed in a cooler during transportation. During time before flammability tests, measurements of volume and biophysical characteristics of plant material, as well as calorimetric content tests were performed. The samples were stored in a refrigerator at 4℃. Storage time varied depending on the availability of the oxygen consumption calorimetry equipment used for flammability tests. For most of the samples, storage time was one week on average; however, storage time was longer than four weeks for part of the samples taken in May and early June due to absence of the calorimetric equipment at the beginning of the field season. In the May and June samples, therefore, the actual water content of shoots was likely underestimated due to losses of water from the plant tissue into the inner space of the sealed plastic bags during prolonged storage time in the refrigerator.

2.2 LABORATORY METHODS

2.2.1 Tests and samples preparation sequence

Each set of tests included: flammability tests (measurements of differential effective heat of combustion using oxygen consumption calorimetry); tests on evaluation of volume and biophysical characteristics (dry matter content, water content, fresh density and porosity); calorimetric content tests (measurements of gross heat of combustion using oxygen bomb calorimetry), and calculations of the energy content (calorimetric content per unit of fresh mass or volume).

To represent variations in flammability related to age, new shoots (if present, depending on the time of the season), 1-year, and 2+year shoots were tested separately. To prepare fuel samples for the flammability test, the tree branch was removed from the refrigerator

and separated into shoots of different ages. All plant material with twigs 10 mm in diameter and larger, as well as fruiting and flowering parts, was removed. The shoots were left exposed to the open air, out of the plastic bag, for 15-20 minutes (including the time taken for separation of shoots) to allow evaporation of visible surface moisture on the surface of the shoots which resulted from refrigerated storage. The proportion by mass of shoots of different ages in the composition of each branch, was then estimated by weighing new, 1-year, and 2+year shoots separately, to the nearest 10 mg. During the flammability tests, the shoots that had been separated by age were kept temporarily in the plastic bags to prevent further drying.

Flammability tests for each separate tree branch were performed for the following fuel samples types: mixed shoots, new, 1-year, and 2+year shoots. Each mixed shoot sample represented a whole tree branch. Since sample size was limited (could not include entire branch), a representative sample was made up from each branch as a mixture of each age class (new, 1-year, and 2+year shoots) added in proportion to its mass on the branch. After the flammability tests for all fuel samples types (mixed shoots, new, 1-year, and 2+year shoots) from the given branch were performed, the next branch was processed and tested in the same order.

Each fuel sample was prepared in the same way. A sample holder was set on the top of a zeroed precision balance. The appropriate quantity of new, 1-year, or 2+year shoots (or each of them in the case of the mixed shoot sample) was taken out of the plastic bag (for a total of 10-15 g per fuel sample), placed in one layer in a sample holder, and weighed to the nearest 10 mg. The spatial density of the shoots in the sample holder was kept approximately constant from test to test and close to that in the given tree branch before it was separated by shoots. Immediately after each fuel sample was prepared a flammability test was performed using an oxygen consumption calorimeter.

Simultaneously with the preparation of each fuel sample of the given age, the remaining branch material of the same age was used for the preparation of a sub-sample for evaluation of volume, biophysical characteristics, and calorimetric content (oxygen bomb calorimetry). Shoots were placed in an air-tight, pre-weighed, numbered container (50ml

plastic test tube with screw cap). During the flammability tests described above, these sub-samples were stored in the cooler and then in the refrigerator before the volume and other biophysical measurements were made. Storage time was from 12 to 24 hours.

The tests on the evaluation of the biophysical characteristics were normally performed the next day after flammability tests. The mass of the air-tight, pre-weighed, numbered containers with the sub-sample inside was measured followed by measurement of the volume of the sub-samples. The sub-samples were dried in a forced-convection oven and the dry mass was measured to the nearest 10 mg using a precision balance. Biophysical characteristics (dry matter content, water content, fresh density, and porosity) were calculated, using the measured fresh and dry mass as well as the volume of new, 1-year, and 2+year old shoots. The biophysical characteristics of the mixed shoot sample from each tree branch were estimated as a weighted average of the corresponding variables measured earlier for new, 1-year, and 2+year shoots from the same branch, according to their proportions in the branch composition.

After drying in the oven, the dried plant material of the sub-samples was stored in marked paper envelopes. Calorimetric content tests using oxygen bomb calorimetry were performed from February to May 2015. Similar to the biophysical characteristics, the calorimetric content of the mixed shoot samples was estimated as a weighted average of the corresponding variables measured for new, 1-year, and 2+year shoots from the same branch, according to their proportions in the branch composition. Using the results of the calorimetric content tests as well as results of the tests on evaluation of volume and biophysical characteristics performed earlier, the energy content (calorimetric content per unit of fresh mass or volume) of live plant material was calculated.

2.2.2 Flammability testing – differential effective heat of combustion

2.2.2.1 Thin fuel sample

Since combustion is a process largely determined by spatial characteristics of fuel, it can differ depending on the scale of combustion process: leaf, shoot, branch, tree, vegetative canopy, or part of the landscape. In this study, investigation of the flammability of live fuel was performed on a tree branch scale. Unlike testing at foliage scale (of foliage only), this allows for better representation of biophysical, chemical and calorimetric properties, as well as morphological (spatial) structure of live fuel on a tree branch scale. First, not only foliage, but twigs as well were tested; the biophysical and chemical properties of twigs can be different compared with foliage. Second, the spatial characteristics of several layers of loose foliage as is tested by traditional techniques are quite different from those for the real tree branch composed of twigs with the attached foliage (shoots).

Testing on a tree branch scale, however, introduces a substantial variation in the results due to the irregularity in spatial distribution of shoots in a tree branch and hence variability in the distance to the ignition heat source, in the area of the fuel surface exposed to the heat transfer from the frontal flame, and in the aerodynamic properties affecting flame flow and propagation through the sample. Even if using a flame instead of radiative heater, the latter two sources of variation are still present. To resolve this issue, a tree branch was considered as a combination of fuel elements where their spatial arrangement within a tree branch depends on species, age, and growth conditions (especially insolation). Each fuel element was considered as a cluster of uniformly spatially distributed shoots of a given age, where the distribution of shoots within the cluster corresponds more or less to the distribution in the real tree branch.

To represent fuel element in the tests, each fuel sample was prepared by placing one layer of the shoots into a 10x10cm wire-mesh sample holder providing uniform and relative constant spatial distribution and density of plant material from test to test that is close to the spatial distribution and density in the real tree branch (Fig 2.5). Unlike the real branch, this also allowed for small sample thickness and for relatively uniform vertical spatial

structure and properties of plant material tested – the sample is “thin” (meaning that fuel properties are approximately uniform vertically and horizontally). A sample holder design that provided a constant distance from shoots to the ignition source and spatial uniformity of the fuel sample was used (Melnik et al., 2015; Paskaluk, Ackerman, & Melnik, 2015) (Fig 2.6). The distance from middle of the shoots’ layer to the base of the calibrated methane flame (top edge of the burner) was 50 mm.

Figure 2.3 Fuel sample number 132, new shoots, fresh mass 12.09 g., sampled on September 15, 2014. The shoots were placed into a 10x10cm wire-mesh sample holder and weighed using a precision balance.

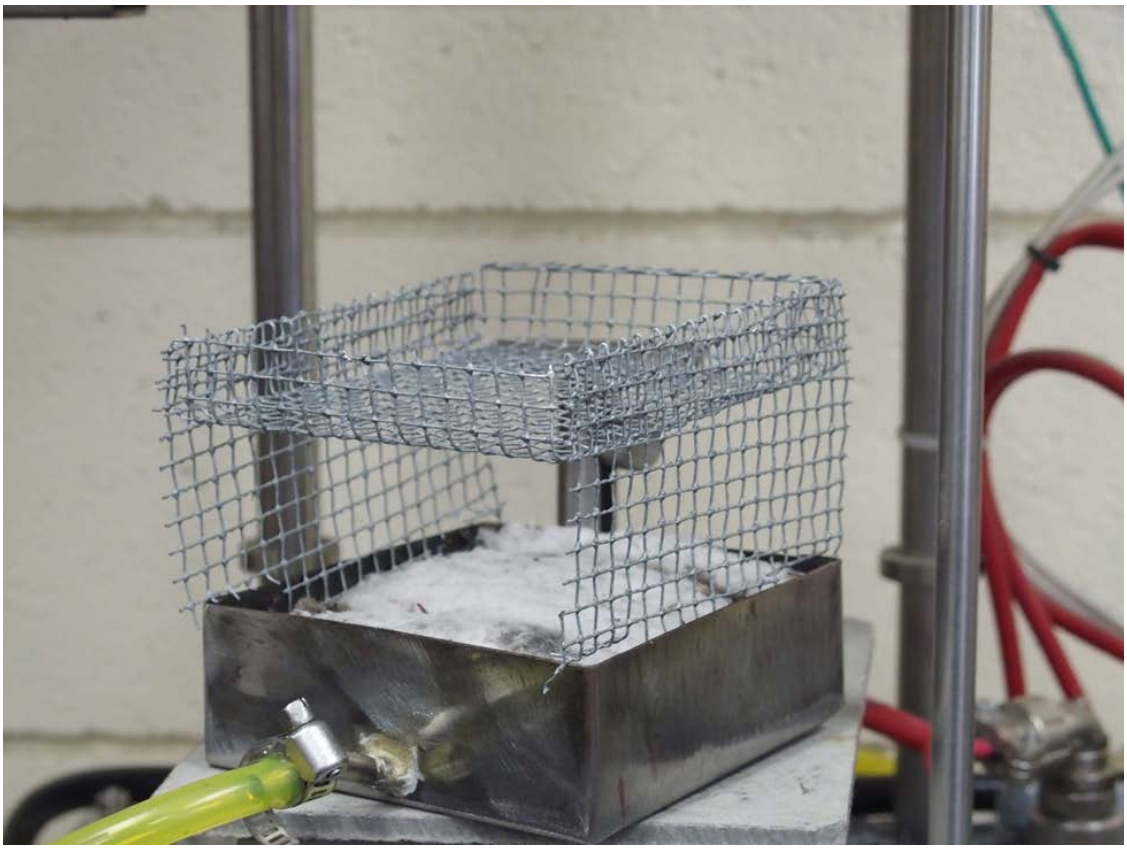

Figure 2.4 Sample holder. The design of the sample holder provides a constant distance from the shoots to the ignition source.

2.2.2.2 Linear flame propagation model

Flammability was defined and measured as an energy release contribution of the burning live fuel to the energy release of the frontal flame during the first 60 seconds of combustion (average frontal flame residence time). Flammability therefore was examined on the flame propagation scale and was evaluated using a linear frontal flame propagation model proposed in the study. Linear propagation of the frontal flame can be presented as the consequent gradual transition of the system of the interacting flames of the currently burning fuel elements (for example P1, P2, and P3 in Fig.2.6) to the unburned part of the fuel (a recently ignited live fuel element, such as P4 in Fig.2.6).

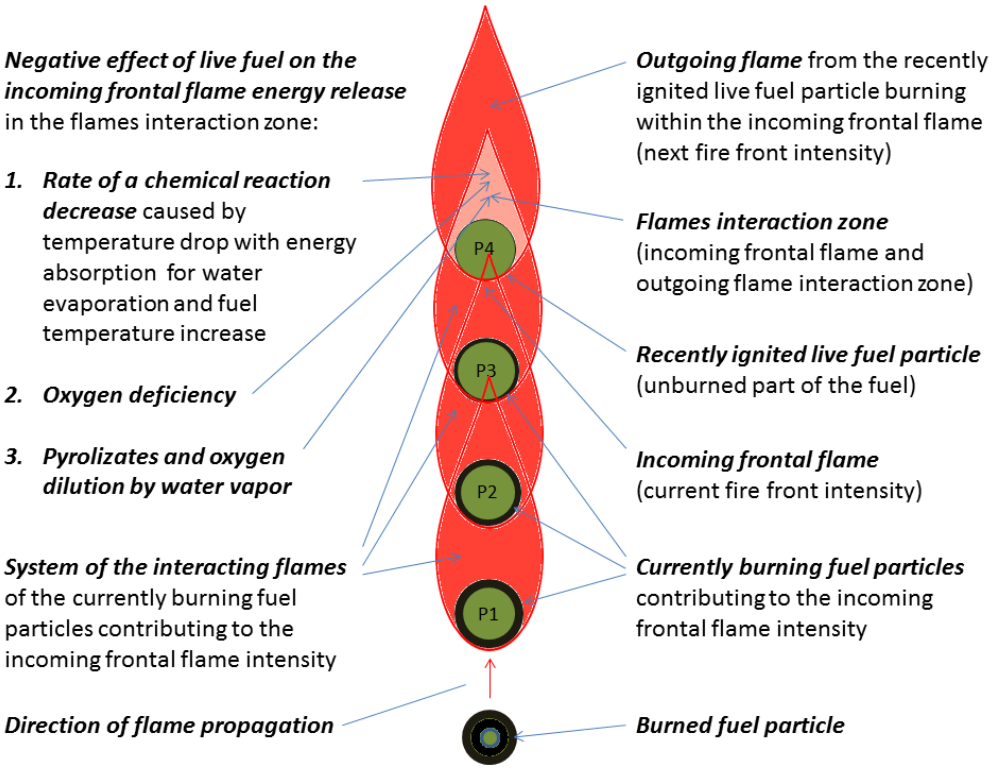

Figure 2.5 Hypothetical reduction in energy release for the incoming frontal flame due to incomplete combustion caused by high water content of live fuel and oxygen deficiency in the incoming and outgoing flames interaction zone. Vertical orientation of the fuel elements represents the experimental setup and the apparatus.

The recently ignited live fuel element is involved in the two simultaneous interactions: (1) It is exposed to the radiative and convective heating of the incoming frontal flame created by the currently burning elements, while it simultaneously causes a negative effect (due to oxygen deficiency and high water content of live fuel) on the incoming frontal flame energy release in the flames interaction zone; (2) It produces its own outgoing flame and energy release in the flames interaction zone. Energy release of the resulting gaseous mixture of the incoming frontal flame and live fuel's flame (resulting outgoing flame) will be further used for the ignition of the next fuel elements and, if the net energy release is sufficient, flame propagation. In this study, the flammability of live fuel, defined as its energy release contribution to the frontal flame intensity and propagation, was evaluated using a paired linear flame propagation model which considers both interactions (1) and (2) presented above:

$$\begin{bmatrix} Incoming\ frontal\ flame \\ (current\ fire\ front\ intensity) \end{bmatrix} \rightleftarrows \begin{bmatrix} \boldsymbol{Recently\ ignited} \\ \boldsymbol{live\ fuel\ element} \end{bmatrix} \rightarrow \begin{bmatrix} Resulting\ outgoing\ flame \\ (next\ fire\ front\ intensity) \end{bmatrix}$$

[2.1]

The resulting change in energy release (positive or negative, depending on fuel properties) for the incoming frontal flame caused by combustion of a given recently ignited live fuel element within the frontal flame can be evaluated by consideration of the interactions [2.1]. Flammability of a live fuel element, therefore, can be defined as an effect on the frontal flame – hence at a frontal flame propagation scale instead of a separate fuel element scale. Theoretically, to fully account for the reduction in energy release with incomplete combustion (Fig. 2.6), the resulting change in energy release for the incoming frontal flame caused by live fuel element combustion within the frontal flame in [2.1] can be evaluated in three steps by calculating (or measuring) all the following:

1. *Energy release* of the live fuel element in the conditions of the flames interaction zone (expected to be less than if measured by the existing oxygen consumption calorimetry method due to lower oxygen concentrations in the flames interaction zone – even if fuel is completely dry; also it can be higher due to reduction in heat losses with re-radiation to the environment)
2. *The change in energy release* for the incoming frontal flame in the flames interaction zone (expected to be negative due to lower oxygen concentrations and additional water content-associated reduction in energy release in the flames interaction zone, or positive due to heat feedback to the incoming flame)
3. *The resulting change in energy release* for the frontal flame as a difference between the incoming and the outgoing frontal flame energy release (Fig. 2.6) that can be calculated as a sum of 1 and 2 (expected to be either positive or negative depending on live fuel element properties, in particular water content)

2.2.2.3 Differential Effective Heat of Combustion

In this study, the complex calculations (or measurements) presented above (steps 1, 2, and 3) were replaced by direct evaluation of the step 3 only, skipping steps 1 and 2: the frontal flame's change in energy release caused by the interaction with the burning live fuel. It was measured as the difference in energy release between outgoing flame (the methane flame with the fuel sample in it) and incoming flame (the methane flame alone) in the model [2.1]. The flammability of live fuel was defined as the energy release contribution of the burning live fuel element into frontal flame during the first 60 seconds of combustion (average frontal fire residence time) and was directly measured as a *Differential Effective Heat of Combustion* ($dH_{eff}60s$) in the conditions representing those for frontal flame (Melnik et al., 2015, Paskaluk, Ackerman, & Melnik, 2015).

These conditions were experimentally simulated using the flame from a 100×100-mm calibrated open methane burner placed underneath a 100×100-mm sample of new, 1-year, 2+ year old shoots, and a mixed shoot sample representing a single tree branch of white spruce (Fig.2.7). The heat release rate *(HRR)* and the effective heat of combustion (H_{eff}) were measured using an oxygen-consumption calorimetry method developed for the study that provided the test conditions which were more representative of a frontal flame than either bomb calorimetry or radiant heating from a cone calorimeter. High-intensity combined convective and radiative external ignition flux (the nominal energy release of 500 kW m^{-2} of the calibrated methane burner) was used for the flammability testing. The experimental setup also provided the direction of the combined radiative and convective ignition heat transfer that coincide with the direction of the flame propagation through the fuel sample providing better representation of live fuel ignition and combustion in the real fire (see Section 1.4.4).

Figure 2.6 Experimental setup (from bottom to top): load cell, methane burner, incoming methane flame, wire-mesh sample holder, burning live fuel sample, outgoing flame (methane flame with the burning sample within the flame).

HRR of the incoming flame (open methane burner) was measured with two separate calibration runs with an empty sample holder, one before and one after each test set. The incoming flame *HRR* baseline was calculated as the average of these two test runs. This measured baseline heat release rate was compared to the measured mass flow rate of methane to confirm the result. According to model [2.1], Differential Heat Release Rate *(dHRR)* was calculated as the difference between *resulting outgoing flame* intensity *(HRR* of the methane flame with the burning sample within the flame) and *incoming frontal flame* intensity (baseline *HRR* of the methane flames alone):

$$dHRR = HRR_{(flame\ +\ sample)} - HRR_{(flame)} \qquad [2.2]$$

The flammability of the fuel sample was defined as its energy release contribution to the incoming methane flame and calculated as *Differential Effective Heat of Combustion* $(dH_{eff}60s)$: difference between heat release of the methane flame with the burning sample within the flame ($HR_{flame+\ sample}$) and heat release of the methane flame alone (HR_{flame}) during the first 60 seconds of combustion (integral of the *dHRR*) per unit of sample mass (gravimetric) or volume (volumetric):

$$dH_{eff}60s = HR_{60s(flame\ +\ sample)} - HR_{60s(flame)} \qquad [2.3]$$

$$dH_{eff}60s = \int_0^{60} dHRR \qquad [2.4]$$

In this study, $dH_{eff}60s$ was expressed (normalized) traditionally per unit of mass loss (mass of fuel consumed, $dH_{eff}60s.ML,\ kJ\ g^{-1}$), gravimetrically per unit of fresh mass of the sample $(dH_{eff}60s.GRAV,\ kJ\ g^{-1})$, and volumetrically per unit of volume of the sample $(dH_{eff}60s.VOL,\ kJ\ cm^{-3})$.

2.2.2.4 Flammability testing

Flammability tests were performed in the Protective Clothing and Equipment Research Facility at the University of Alberta using oxygen consumption calorimetry equipment modified for the study. (Fig. 2.8). Technical description of an oxygen consumption calorimetry method, procedure, and apparatus used for flammability testing is provided in Paskaluk, Ackerman, & Melnik (2015).

Figure 2.7 Oxygen consumption calorimeter used for the flammability testing.

Each set of flammability tests normally included the testing of the samples from the most recent day of the field sampling and from one of the previous field sampling days. Each

day of the field sampling was represented in the flammability tests by 3-5 trees out of 18 trees sampled on the test site (1-2 trees out of 6 for each of 3 slope positions were randomly selected for the testing). The flammability was tested for the total of 185 fuel samples: 3 to 5 trees were selected on each of the 11 sampling days and 3-4 samples per each tree were tested (new, 1-year, 2+year, and mixed shoot samples). For 138 of them (new, 1-year, and 2+year old shoots), a full set of laboratory work and data processing was performed: flammability tests, measurements of volume and biophysical characteristics, calorimetric content tests and calculations of the energy content. For the remaining 47 fuel samples (mixed shoot), only flammability tests were performed. Biophysical characteristics, calorimetric content, and energy content of mixed shoot samples were estimated as a weighted average of measured variables for new, 1-year, and 2+year old shoots composing the mixed shoot sample.

2.2.3 Evaluation of volume using a proposed constant volume method

Tests on evaluation of volume and biophysical characteristics of plant material (water content, dry matter content, density, and porosity) were performed in the fire laboratory at the Department of Renewable Resources of the University of Alberta. The volume of the sub-samples was estimated using a time- and cost-efficient *constant-volume* method developed during this study that allows measurements of volume of any given plant sample, with one measurement per sample (after mass of the container filled with water was evaluated), using a precision balance. A new technique was developed aiming to provide more accurate measurements of the volume of shoots and loose foliage compared to the traditional water displacement method. To establish volume, this new technique utilizes displacement of water by a sample from a container of constant inner volume. This was done by establishing the mass of a sealed standardized container fully filled with water and containing no air bubbles before performing the tests. After this, the mass of a sealed standardized container fully filled with water was considered constant. For each tested sample, mass measurement was taken with the sample displacing some water within the container, therefore reducing water mass but adding sample mass to the measurement.

The inner space of the sealed container (inner volume) was held constant. The proposed *constant-volume* method is based on the fact that the mass of the sealed container filled with water and a tested sample (mass of container, water, and sample, M_{cws}) (Fig. 2.9) is less than the mass of the sealed container filled with water alone (mass of container and water, M_{cw}) by the mass of water replaced by the sample (mass of water replaced, M_{wr}) and at the same time it is heavier by the mass of the tested sample (fresh mass of the tested sample, M_s):

$$M_{cws} = M_{cw} - M_{wr} + M_s \qquad [2.5]$$

Figure 2.8 Sealed container filled with water and a tested sample (loose foliage

Knowing that the mass of water at 20°C replaced by the sample (M_{wr}) represents volume of this sample (V) (density of water equals 1.00 g cm^{-3} at 20°C),

M_{wr} = V [2.6]

we can rewrite [2.5]:

$M_{cws} = M_{cw} - V + M_s$ [2.7]

The volume of the sample can be calculated by rearranging [2.7] and solving it for V:

$V = M_{cw} - M_{cws} + M_s$ [2.8]

Thus the volume of the fresh sample can be calculated as the mass of the sealed container filled with water only (M_{cw}) minus the mass of the same sealed container filled both with water and a tested sample (M_{cws}) plus the fresh mass of the tested sample (M_s). Since the fresh mass of the sample was known and the mass of the sealed container filled with water only was constant and known, the volume of the given sample was evaluated using a single measurement of the mass of the sealed container filled with water and the sample.

To avoid additional variability in the tests results due to variation in water solutions and hence variation in water density, distilled water was used for the tests. The mass of a sealed standardized container fully filled with water was periodically re-checked. A precision balance check was performed before, during, and after each set of measurements. The resolution of the proposed *constant-volume* volume measurement method was limited only by the resolution of mass measurements; in this study it was 0.01 grams. With density of plant material that was close to 1.00 on average, this produced 0.01ml resolution of volume measurements. The resolution of the traditional water displacement method that was tried in the beginning of this study was limited by the resolution of the two readings of

water level in a graduated cylinder (initial and final) of 0.1ml (marginal). The low resolution of the traditional water displacement method was caused by two reasons: (1) difficulties in using small-diameter measuring cylinder that is required for small sample size and (2) the plant material floating (inaccurate readings of water level).

2.2.4 Evaluation of biophysical properties

2.2.4.1 Water and dry matter content

Use of the air-tight, pre-weighed, numbered containers for taking sub-samples during flammability testing allowed for almost instant evaluation of the fresh mass, even though the mass of the container with the sample inside was measured 1-2 days after the sub-sample was taken. Air-tight sealed storage also resulted in minimal changes in volume, water content, density, and porosity during this delay. After the fresh mass and then the volume of the sub-samples was measured, samples were dried in open tin cans using the Sheldon manufacturing Inc., Model FX14-2 drying oven during 48 hours at 80℃ (Fig. 2.10).

Figure 2.9 Plant material prepared for drying was placed in the open tin cans (top image) and then into in the oven (bottom image).

Dry mass (dry matter content) measurements were performed immediately after completing drying in the oven. To prevent absorption of room air moisture by dried samples, each time only 5-10 tin cans with samples were taken out from the oven. The dry mass of the samples was determined to the nearest 10 mg using a precision balance. The dry matter content was expressed gravimetrically per unit of fresh mass (*DM.GRAV,* parts of 1) and volumetrically per unit of volume of the fresh sample (*DM.VOL,* g cm^{-3}). The water content of the sub-samples (shoot water content) was calculated as the difference in

fresh mass and dry mass. Shoot water content was expressed gravimetrically (Norum & Miller, 1984) on the dry mass basis (*SWC.GRAV,* %) and volumetrically as quantity of water in the unit of volume of the fresh sample (*SWC.VOL,* g cm^{-3}).

2.2.4.2 Fresh density

The fresh density of the sub-sample (*D,* g cm^{-3}) was calculated as the proportion of fresh mass to volume of the sample. It indicates the total mass of substances that are contained in 1 cm^3 of the sample's volume: that is, solid cell wall substance, as well as water and gases filling empty space (voids) within it. To characterize properties of the solid cell wall substance itself, excluding the space of voids filled with water (cell wall material alone in the cell space free of water) this study introduces volumetric-only "water-free" plant material characteristics: *density water-free (DWF,* g cm^{-3}) and *porosity water-free (PWF,* parts of 1).

2.2.4.3 Density water-free

Fresh plant material can be presented as a mixture of the complex geometry fragments: dry matter fragments (cell wall substance), voids filled by intercellar water solution, and voids filled with gases. The *DM.VOL* (commonly called dry density) represents mass of dry organic matter per unit of fresh plant material volume. The *DWF* also represents mass of this dry organic matter, but only per unit of volume that is not occupied by water (plant tissue volume minus volume of voids filled by water = volume occupied by dry organic matter and voids filled with gases). The substantial presence of the water-filled voids can be essential for some of the plant material properties and processes (such as fresh density, specific heat, thermal conductivity, and e.g. losses of energy to the unburned part of the fuel) and not so important for others. For instance, wood decomposition (pyrolysis), which determines the rate of flammable pyrolizates release and hence rate of heat release, is not so dependable on the presence of the water-filled voids. By the moment of the beginning of the pyrolysis the most of the water-filled voids are already opened to the fire environment by the excessive pressures inside the plant cells caused by the heat transfer

from the frontal flame. The opened by the flame voids are hence practically free of water. This suggests that the rate of the pyrolysis will be determined by the properties of the plant material modified by the ignition heat transfer as described above. The plant material in this case can be considered as a mixture of only the dry matter fragments and voids filled by gases – without water-filled voids, hence – separately from the rest of plant material volume filled by water. This represents the concept of the plant material free of water, 'water-free'. Its density and porosity (which can substantially differ from those for the initial fresh plant material composed of the mixture of dry matter content fragments, voids filled with gases, and water-filled voids) are defined and measured in this study as *PWF* and *DWF*.

For 1 cm^3 of fresh sample, volume of water-free cell wall substance (V_{wf}, cm^3) in 1 cm^3 of the fresh sample can be calculated if volume of water in 1 cm^3 of the fresh sample *(V_w, cm^3)* is known:

$$V_{wf} = 1 - V_w \qquad [2.9]$$

Since at 20℃ 1 cubic centimeter of water has a mass of exactly 1 gram, the volume of water (V_{water}) in [2.9] can be replaced by volumetric water content *(SWC.VOL):*

$$V_{wf} = 1\ (cm^3) - SWC.VOL\ (cm^3) \qquad [2.10]$$

The density of the cell wall material alone for the cell space free of water (*DWF, g* cm^{-3}*)* can be calculated as the mass of dry matter in one cubic centimeter of sample *(DM.VOL* * 1 cm^3*)* divided by water-free volume (V_{wf}) which this dry matter occupies (considering presence of water):

$$DWF = DM.VOL * 1\ cm^3 \ / \ V_{wf} \qquad [2.11]$$

Using [2.10] for V_{wf} in [2.11], density water-free was calculated:

$$DWF = DM.VOL * 1\ cm^3 / (1\ cm^3 - SWC.VOL) \quad [2.12]$$

2.2.4.4 Porosity water-free

The density of oven-dry solid cell wall substance DWF_0^w (density of the oven-dry cell walls material without any voids) of 1.53 $g\ cm^{-3}$ is used for calculations of the porosity (Siau, 1995). Knowing DWF_0^w, the proportion of missing volume because of voids in one cubic centimeter of cell wall substance (porosity of water-free, *PWF, parts of 1)* was calculated as the proportion of missing mass due to voids in one cubic centimeter of cell wall substance to mass of one cubic centimeter of solid cell wall substance without any voids:

$$PWF = (DWF_0^w - DWF) / DWF_0^w \quad [2.13]$$

or

$$PWF = (1.53\ g\ cm^{-3} - DWF) / 1.53\ g\ cm^{-3} \quad [2.14]$$

or

$$PWF = 1 - DWF / 1.53\ g\ cm^{-3} \quad [2.15]$$

2.2.5 Calorimetric content (gross heat of combustion)

Calorimetric content tests (oxygen bomb calorimetry) were performed in the burning laboratory at the Northern Forestry Centre of the Canadian Forest Service in Edmonton, Alberta. Calorimetric content (gross heat of combustion, H_{gross}, $kJ\ g^{-1}$) was measured using Parr model 1341 Plain Jacket calorimeter equipment and standard oxygen bomb calorimetry test method (Chrosciewicz, 1986a) (Fig. 2.11 and 2.12). Tree numbers for the current day of calorimetric content tests (15-20 tests per day) were selected randomly (using R-software). Knowing the mass of the water, its specific heat value, and its measured temperature change pattern due to combustion of live fuel, and mas of the fuel samples the calorimetric content of live fuel (H_{gross}) was then calculated. Water content of dried sub-samples was evaluated simultaneously with the oxygen bomb calorimetry tests; their test day average was used for H_{gross} calculations. Calorimetric content of the mixed shoot sample was calculated as weighted average of measured H_{gross} for new, 1-year, and 2+year samples according to their mass proportion in composition of a branch.

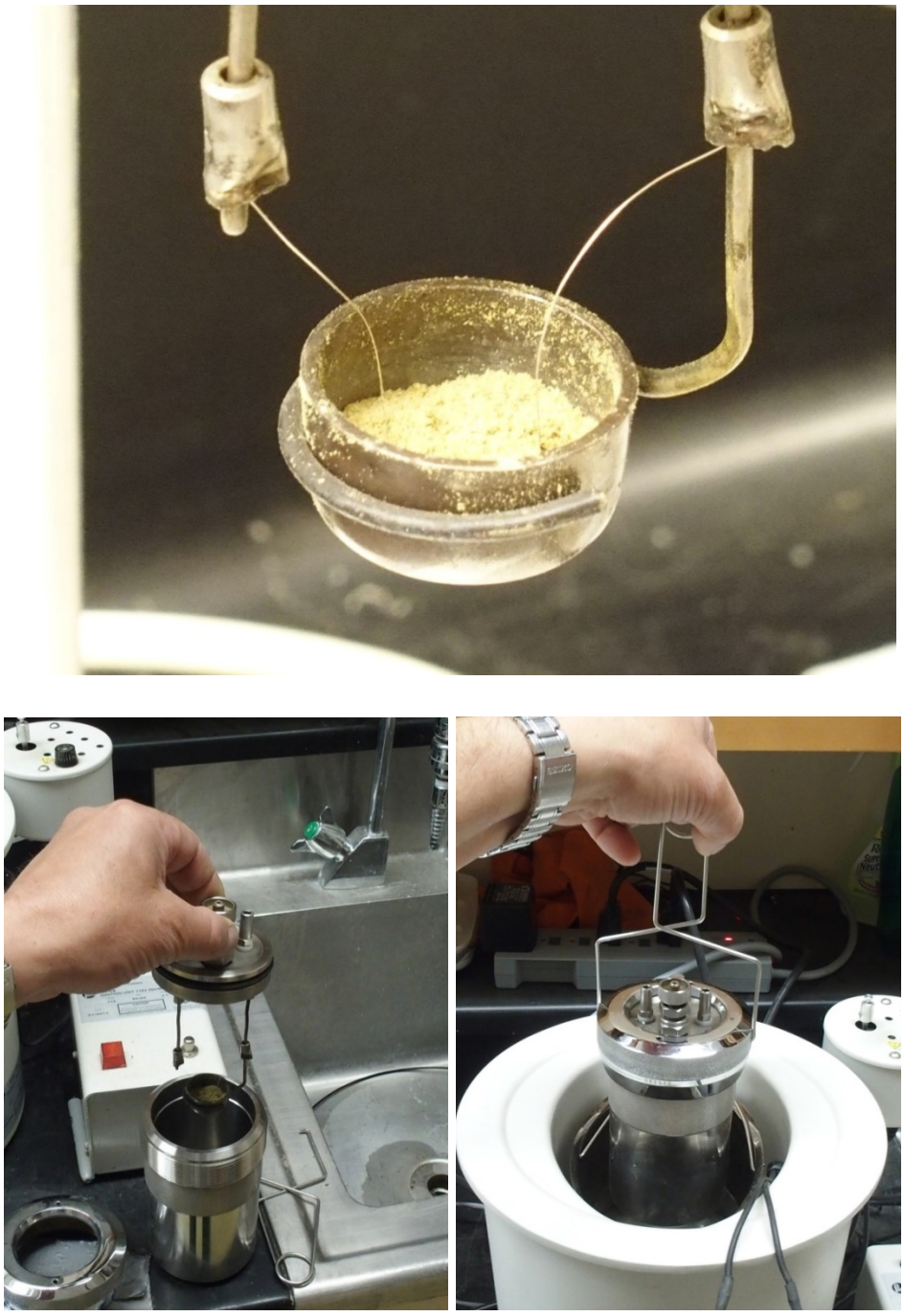

Figure 2.10 Tested grinded plant material in the crusible with inserted ignition wire (top image); body of the "bomb", its lead with attached crusible filled with 0.5-0.7 grams of fuel sample (bottom left image); "bomb" is immersed into the water (bottom right image).

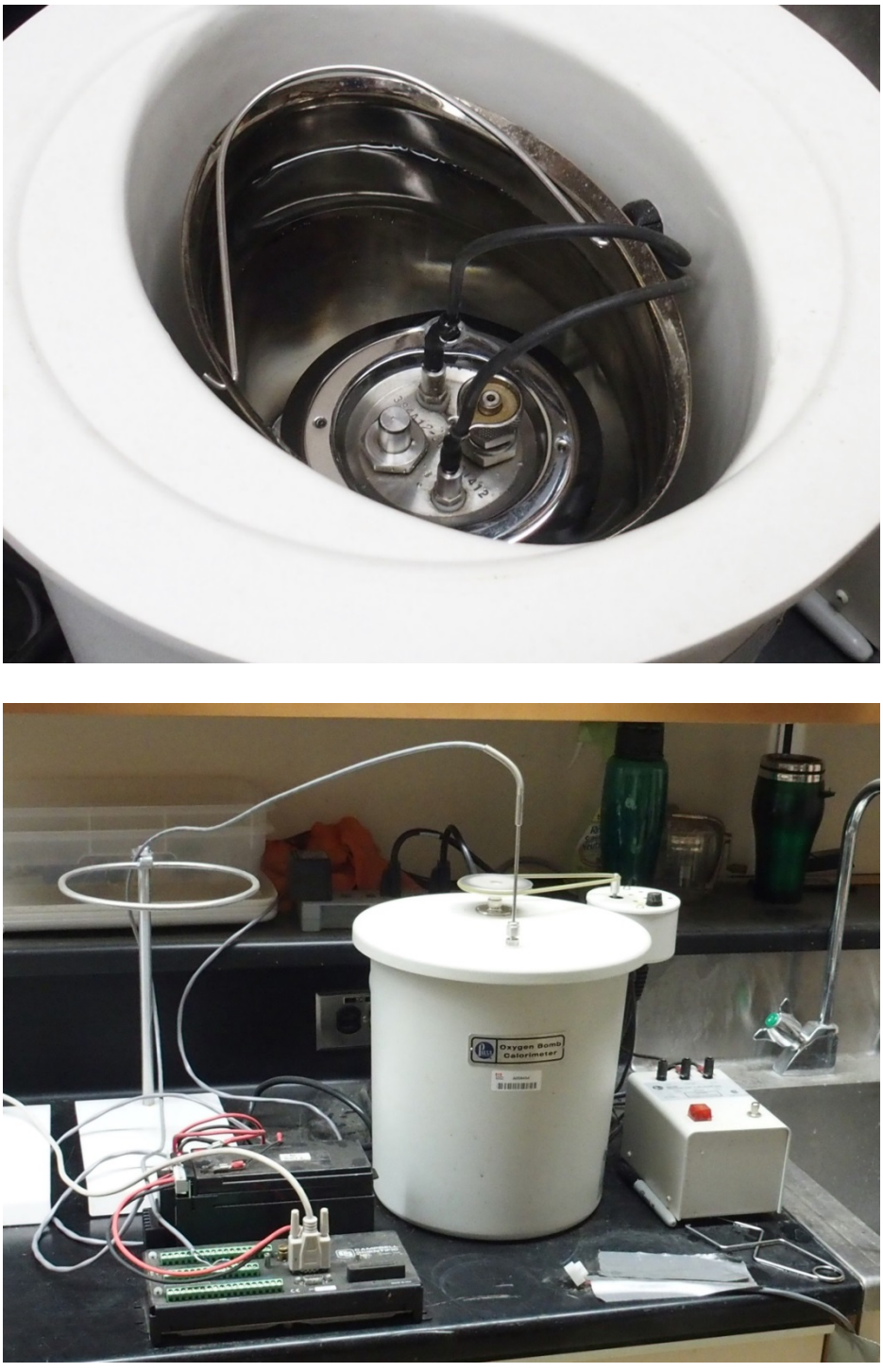

Figure 2.11 Electrical contacts for ignition of the tested sample are connected (top image); Parr model 1341 Plain Jacket calorimeter ready for the test (bottom image).

The oxygen bomb callorimetry tests were performed in March 2015 during 8 days of laboratory testing for this study. A benzoic acid test was performed once per test day. The precision of the method was evaluated by determining a 0.95 confidence interval using standard deviation of the values of gross heat of combustion acquired in the repeated benzoic acid tests. The actual range of variation and 0.95 confidence interval (as proportions to measured mean, %) were compared. The confidence interval was also compared to reported heat of combustion of standard sample benzoid acid (Jessup & Green, 1934).

2.2.6 Energy content

Gravimetric and volumetric energy content was determined for each fuel sample. As used in this study, *energy content (EC)* was defined as a theoretical maximal amount of energy which can be released with combustion in pure oxygen environment under the pressure of 30 atmospheres of oven-dry organic matter that was contained in the unit of live fuel's fresh mass (gravimetric approach) or volume (volumetric approach) before drying. According to this definition, the gravimetric energy content of live fuel per unit of fresh mass *(EC.GRAV,* kJ g^{-1}) was calculated for each fuel sample as the product of quantity of dry organic substance in the unit of fresh mass (dry matter content, *DM.GRAV,* parts of 1) and calorimetric content of this substance (*CC,* or H_{gross}, kJ g^{-1}):

$$EC.\ GRAV = DM.\ GRAV * CC \quad \text{or} \quad EC.\ GRAV = DM.\ GRAV * H_{gross} \qquad [2.16]$$

Volumetric energy content *(EC.VOL,* kJ cm^{-3}*)* is a theoretical amount of energy which can be released with combustion in pure oxygen environment under the pressure of 30 atmospheres of oven-dry organic matter that was contained in 1 cm^3 of the fresh plant material before drying. It was calculated as the product of quantity of dry organic

substance in the unit of volume (*DM.VOL,* g cm^{-3}) and calorimetric content of this substance *(CC*, or H_{gross}, kJ g^{-1}):

$$EC.VOL = DM.VOL * CC \quad \text{or} \quad EC.VOL = DM.VOL * H_{gross} \qquad [2.17]$$

2.3 DATA

2.3.1 Variables and datasets

Exploratory data analysis and statistical analysis were performed using the R statistical software version 3.2.5 (2016-04-14). Datasets for the 4 fuel sample types such as (1) *tree branch* (mixed shoot sample), (2) *new shoots,* (3) *1-year shoots,* and (4) *2+year shoots* were analyzed separately. The fuel sample types listed above (except tree branch) were also studied together as an additional (5) *all ages of shoots* dataset (2,3, and 4 combined). It represented a full range of variation in properties and flammability of shoots of white spruce. Using the *all ages of shoots* dataset violates the assumption of the independency of the data (samples representing *new shoots, 1-year shoots,* and *2+year old shoots* were taken from the same branch) if differences among these groups are studied. However, since the main goal of the study was to investigate if there is a physics-based model that would be able to explain variation in flammability regardless of age class, and to see if all data points of these separate groups of tissue type can be close to the single regression line, this combined *all ages of shoots* dataset was used. To evaluate the quality of the representation of the flammability of tree branches by *all ages of shoots* model, the additional (6) *all fuel sample types* dataset was also used. It comprised (1) *tree branch* (mixed shoot sample), (2) *new shoots,* (3) *1-year shoots,* and (4) *2+year shoots* datasets. Data were processed and analyzed using both gravimetric and volumetric approaches.

In a volumetric approach, measured variables were expressed per unit of volume of plant tissue, instead of being expressed per unit of dry or fresh mass in a gravimetric approach.

Gravimetric shoot water content *(SWC.GRAV)*, for instance, was measured as a proportion of mass of water contained in the sample to dry mass of the sample (%). Gravimetric dry matter content *(DM.GRAV)* was measured as a proportion of mass of dry organic matter to fresh mass of the sample (parts of 1). Instead, volumetric shoot water content *(SWC.VOL)* and volumetric dry matter content *(DM.VOL)* were measured as a proportion of mass of water and dry matter content, respectively, to the volume of the fresh sample (g cm^{-3}).

The predictands (response variables) –flammability of live fuel – were measured as a gravimetric and volumetric differential effective heat of combustion at 60 seconds: $dH_{eff}60s.GRAV$ (parts of 1, fresh mass basis) and $dH_{eff}60s.VOL$ (g cm^{-3}), respectively. They were investigated in relation to the biophysical-chemical and calorimetrical properties of live plant tissue affecting its flammability (predictors, or independent variables, in Table 2.1)

Table 2.1 Gravimetric and volumetric predictor variables used in the statistical analysis.

Predictors (Independent variables)	Gravimetric		Volumetric	
	Abbreviation	Units	Abbreviation	Units
Shoot water content	*SWC.GRAV*	% (dry mass basis)	*SWC.VOL*	g cm^{-3}
Dry organic matter content	*DM. GRAV*	Parts of 1 (fresh mass basis)	*DM.VOL*	g cm^{-3}
Calorimetric content	*CC*	$kJ\ g^{-1}$ (dry mass basis)		
Energy content	*EC.GRAV*	kJ g^{-1} (fresh mass basis)	*EC.VOL*	kJ cm^{-3}
Fresh density			*D*	g cm^{-3}
Density water-free			*DWF*	g cm^{-3}
Porosity water-free			*PWF*	Parts of 1

The units of the volumetric variables were found to be more consistent than those for gravimetric variables since all of them are expressed as a proportion of a measured value to the volume of the sample (Table 2.1). The traditional (commonly used in fire modelling) gravimetric variables are expressed on the dry mass basis and on the fresh mass basis. The volumetric approach allowed for use of the additional variables such as *D, DWF,* and *PWF* that are absent in the traditional gravimetric approach, potentially providing better representation of the properties of live fuel. While an independent variable such as calorimetric content is seemingly missing in the volumetric approach *(CC,* Table 2.1), it was actually included in the calculations of the volumetric energy content *(EC.VOL*) using the equation [2.17].

2.3.2 Data exploration

2.3.2.1 Preliminary data check

The preliminary check of the data for errors in data entry and for missing data was performed by examination of the data sets, and by using graphical techniques in R programming language and software environment for statistical computing and graphics version 3.2.5 (2016-04-14). If one or more variables were found to be missed, the whole data point (properties and flammability of the particular tissue type for the given tree number and day of the sampling) was excluded from the analysis. Unusual values, outliers, were detected using boxplots and the values of standard deviation for the given sample. Since there was only moderate deviation from the 1.5 interquartile range (IQR) and no a priori reasons (for example, non-standard test conditions), these values were not excluded from the analysis.

2.3.2.2 Data distribution

The gravimetric and volumetric seasonal mean, median, minimum and maximum values, range, interquartile range, variance, and standard deviation were determined separately for each of the 6 datasets discussed earlier (section 2.3.1), using the exploratory statistics in R. The shape of the distribution was investigated using boxplots and histograms.

2.3.2.3 Time series

Time series were investigated separately for the 5 groups of tissue types. Each data point for the particular tissue type was calculated as the daily average of the corresponding measured values of the plotted variable. Due to limited sample size (3-5 randomly selected trees out of 18 on each day of field sampling) and due to prolonged storage time for May and June samples (and hence increased water losses by each plant specimen during its storage in a refrigerator), the actual seasonal values of water content of new shoots in the very beginning of the season were most likely underestimated.

2.4 ANALYSIS AND MODELLING

2.4.1 Properties and flammability of different types of plant material

To determine if measured values of properties and flammability of live plant material varied significantly between the 4 plant fuel sample types (tree branch (mixed shoot sample), new shoots, 1-year shoots, and 2+year old shoots) one-way Analysis of Variance (ANOVA) was used. The assumption of data normality (for ANOVA and for a parametric correlation and the linear regression analyses) was checked by examining the normality of residuals. The assumption of homogeneity of variances was checked using side-by-side comparison of boxplots for multiple groups. The assumption of linearity was examined using scatterplots of the corresponding variables. The assumption of the random sampling

was met by the experimental design and in particular by the previously described procedure of tree branch separation on shoots and random selection of shoots of a given age for the preparation of the fuel samples and sub-samples for evaluation of live fuel properties.

2.4.2 Modelling flammability of live fuel

In order to evaluate the relative importance of water, dry matter, calorimetric, and energy contents, as well as fresh density, density water-free, and porosity water-free (predictors) in determining flammability measured as differential effective heat of combustion (predictand), Pearson's correlation analysis was performed. Depending on the results, predictor variables, important in determining flammability, were selected for flammability modelling. For the gravimetric and volumetric approaches, flammability modelling was performed using linear one-variable regression analysis. For the volumetric approach only, more complicated models were considered and multivariable non-linear regression analysis was performed using *nls*-function of R-software for multivariable model's parameters optimization. Model frames used for the multivariable analysis were designed aiming to produce a better representation of the physical-chemical process of live fuel – frontal flame interaction. The models that showed the best statistical quality of flammability prediction were further tested against the measured seasonal flammability data. The performance of the single-variable and multi-variable models in the explanation of the flammability was compared using the R-squared adjusted for the number of the predictors in the model (adjusted R^2)

The fitted nonlinear regression flammability models showing the best statistical quality were checked against the measured values of flammability through the season and compared with the seasonal trend of live fuel flammability assumed by the FBP model. The modelled time series of flammability was calculated using the measured values of the independent variables for mixed shoot samples (representing a separate tree branch of the given tree) in each flammability model. The seasonal trend of live fuel flammability

assumed by the FBP model was reproduced using the relative scale from the seasonal trend of live fuel flammability illustrated by Turner & Lawson, (1978) and expressed as a crown spread factor (CSF) (Van Wagner, 1974).

3 RESULTS

The main characteristics and seasonal changes in live fuel flammability expressed as change in energy release to the frontal flame and measured as gravimetric and volumetric differential effective heat of combustion (predictand variables) (section 3.2), fuel consumption (section 3.3), and variation in factors affecting flammability (predictor variables, section 3.1) are further discussed.

3.1 PREDICTOR VARIABLES

3.1.1 Proportion of different age shoots

The properties and flammability of a whole tree branch vary through the vegetative season with changes in the properties of shoots of different age and in their mass proportions in the composition of the tree branch. For white spruce, after emergence of new growth, the proportion by mass of new shoots increased from 0%-10% at the end of May to 20%-30% at the end of October 2014. The proportion of older shoots declined from 35% to 20% for 1-year old shoots and from 65% to 55% for 2+year old shoots due to the increase in the proportion of new shoots (Fig. 3.1).

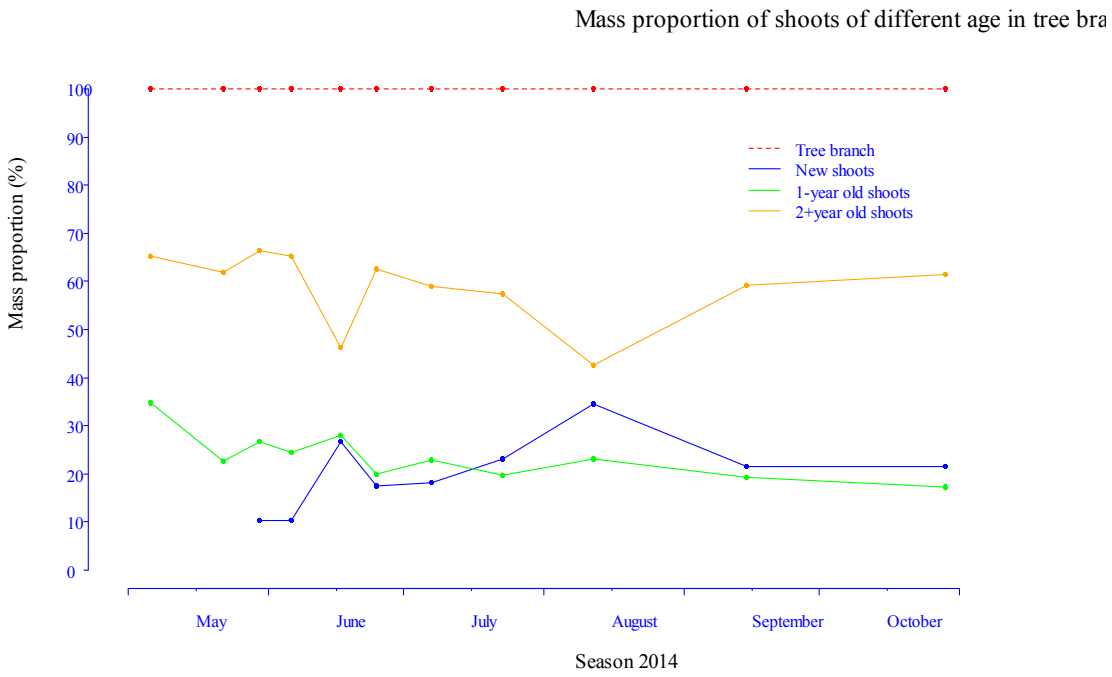

Figure 3.1 Seasonal changes in the proportions of shoots of different age by mass in a tree branch composition for white spruce in 2014. The red dashed line and the solid blue, green, and orange lines represent: tree branches, new, 1-year, and 2+year old shoots respectively.

3.1.2 Shoot water content

3.1.2.1 Gravimetric – *SWC.GRAV*

The mean seasonal values for gravimetric shoot water content (*SWC.GRAV)* in white spruce (Fig 3.2) were significantly different between groups of fuel sample type such as tree branches (mixed shoot sample), new, 1-year, and 2+year old shoots (ANOVA, $p < 0.001$, $F = 60.081$, $n = 181$). New shoots showed the highest seasonal values for SWC.GRAV, largest dispersion, and lower normality of the data distribution compared with other tissue type groups. To a smaller degree, this also affected a mixed shoot sample representing a tree branch.

For all ages of shoots, *SWC.GRAV* varied from 71.4% to 376.8% during the vegetative season of 2014 (Table 3.1). New shoots had the highest seasonal variation (standard

deviation 86.6%). The *SWC.GRAV* seasonal mean ranged from the lowest to highest as follows: 2+year shoots (89.3%), 1-year shoots (103.7%), and new shoots (198.5%). The mean *SWC.GRAV* for tree branches (mixed shoot sample) was 103.3%, which is slightly lower compared with 1-year old shoots.

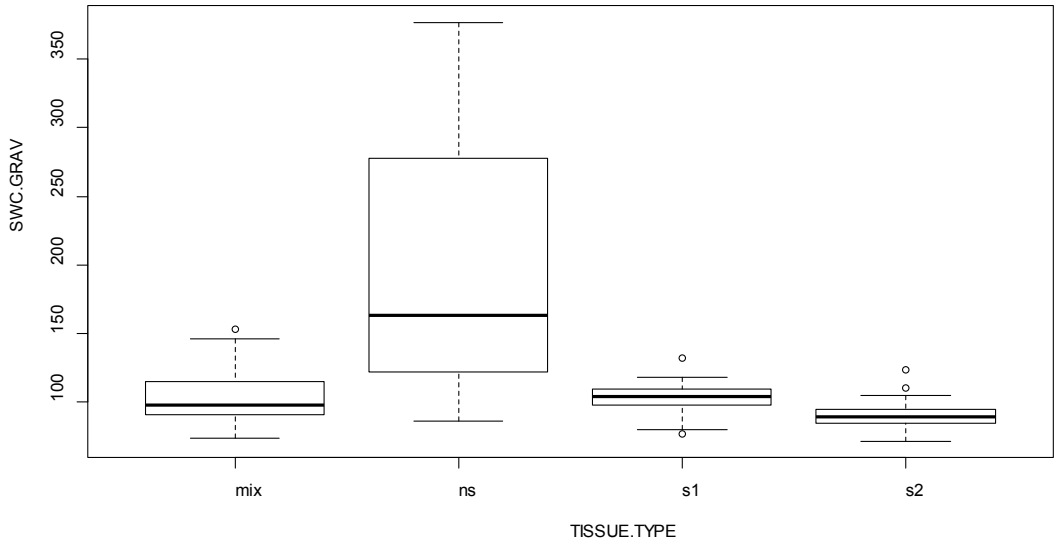

Figure 3.2 Box plots of seasonal variation in gravimetric shoot water content *(SWC.GRAV)* for tree branches of white spruce (mix, mixed shoot sample) in 2014 and for its constituent parts: new (ns), 1-year (s1), and 2+year old shoots (s2). A horizontal line within the box (the interquartile range, IQR) indicates the median. Whiskers are shown at 1.5 IQR. Circles indicate observed values outside of the 1.5 IQR.

Table 3.1 Seasonal minimum, maximum, range, mean, and standard deviations of gravimetric shoot water content *(SWC.GRAV)*.

Fuel sample type	Minimum *SWC.GRAV,* %, dry mass basis	Maximum *SWC.GRAV,* %, dry mass basis	Range, %, dry mass basis	Mean (standard deviation), %, dry mass basis	Sample size
Tree branch (mixed shoot sample)	73.7	152.8	79.1	103.3 (17.9)	47
New shoots	86.2	376.8	290.6	198.5 (86.6)	42
1-year shoots	76.5	132.1	55.6	103.7 (10.0)	48
2+year shoots	71.4	123.8	52.4	89.3 (9.9)	48
All ages of shoots	71.4	376.8	305.4	127.5 (67.6)	138

For white spruce in 2014, the gravimetric shoot water content showed two seasonal minimums for tree branches (mixed shoot sample) at the end of May and in mid-August. It also had one distinct seasonal maximum through mid-June (Fig. 3.3). The SWC.GRAV of new shoots was substantially higher compared with older growth, from the time of emergence of new shoots at the end of May until mid-August.

The *SWC.GRAV* of new shoots at the end of May and in early June was lower compared with mid-June, while, theoretically, it should be the highest at the very beginning of their growth and gradually decrease through the season. Most likely, due to longer storage time and the subsequent increased loss of water content before testing, the water content of new shoots (the most sensitive to dehydration) in May and early June was underestimated, showing a peak in mid-June.

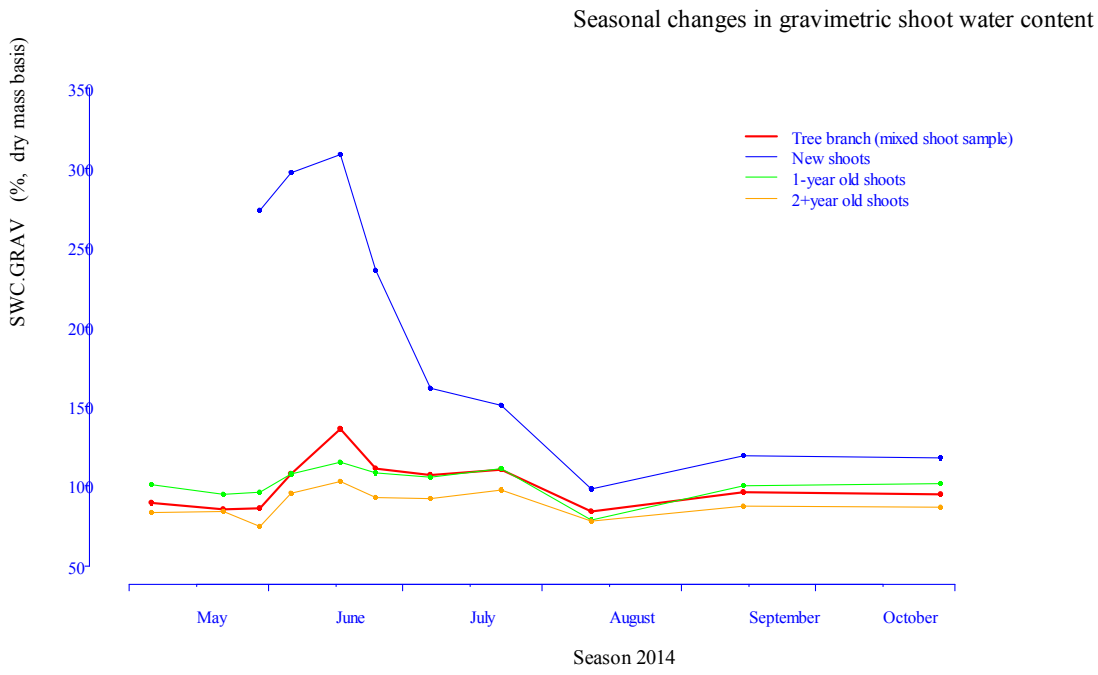

Figure 3.3 Seasonal variation in gravimetric shoot water content *(SWC.GRAV)* for white spruce in 2014. Red, blue, green, and orange lines represent tree branches (mixed shoots sample), new, 1-year, and 2+year old shoots respectively.

3.1.2.2 Volumetric – *SWC.VOL*

The mean seasonal values for volumetric shoot water content *(SWC.VOL)* were significantly different between groups of fuel sample type: tree branch (mixed shoot sample), new, 1-year, and 2+year old shoots (ANOVA, $p < 0.001$, $F = 33.564$, $n = 181$). The values of *SWC.VOL* and their seasonal variation were noticeably higher for new shoots than for older shoots or tree branches (Fig 3.4), but to a lesser degree compared with *SWC.GRAV* (Fig 3.2). For all groups of tissue type, the *SWC.VOL* data showed a higher normality of data distribution compared with *SWC.GRAV*.

SWC.VOL varied from 0.31g cm^{-3} to 0.66 g cm^{-3} for all ages of shoots during 2014 (Table 3.2). New shoots had the highest seasonal variation (standard deviation 0.08 g cm^{-3}). The mean *SWC.GRAV* for new shoots (0.52 g cm^{-3}) was substantially higher than for 1-year old shoots (0.44 g cm^{-3}), 2+year old shoots (0.41 g cm^{-3}), and tree branches

(0.43 g cm^{-3}). Unlike *SWC.GRAV* (Table 3.1), minimum *SWC.VOL* was practically the same for all groups of tissue type: 0.32 g cm^{-3} for new and 2+year old shoots, 0.31 g cm^{-3} for 1-year old shoots, and 0.33 g cm^{-3} for tree branches (Table 3.2). This suggests that volumetric water content, if compared with gravimetric water content, is probably a better indicator of the minimum availability of soil moisture caused by drought.

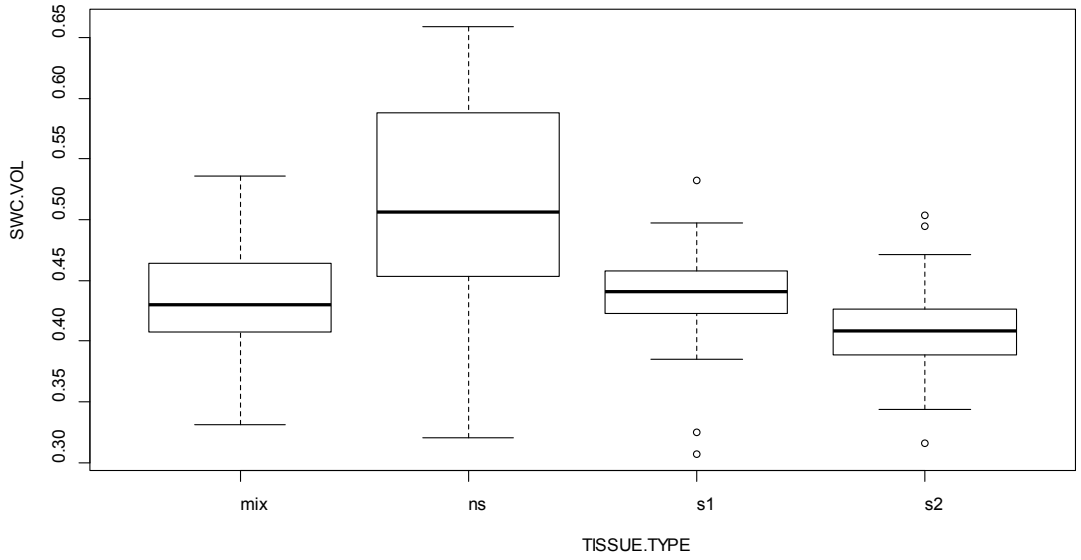

Figure 3.4 Box plots of seasonal variation in volumetric shoot water content *(SWC.VOL)* for tree branches (mix, mixed shoot sample), and for its constituent parts: new (ns), 1-year (s1), and 2+year old shoots (s2). A horizontal line within the box (the interquartile range, IQR) indicates the median. Whiskers are shown at 1.5 IQR. Circles indicate observed values outside of the 1.5 IQR.

Table 3.2 Seasonal minimum, maximum, mean, and standard deviations of volumetric shoot water content *(SWC.VOL)*.

Fuel sample type	Minimum *SWC.VOL*, g cm^{-3}	Maximum *SWC.VOL*, g cm^{-3}	Range, g cm^{-3}	Mean (standard deviation), g cm^{-3}	Sample size
Tree branch (mixed shoot sample)	0.33	0.54	0.21	0.43 (0.05)	47
New shoots	0.32	0.66	0.34	0.52 (0.08)	42
1-year shoots	0.31	0.53	0.23	0.44 (0.04)	48
2+year shoots	0.32	0.50	0.18	0.41 (0.04)	48
All ages of shoots	0.31	0.66	0.35	0.45 (0.07)	138

The volumetric shoot water content for white spruce in 2014 showed two seasonal minimums for tree branches (mixed shoot sample): at the beginning of May (or earlier, for which period no data exist) and a much more marked minimum in mid-August (Fig. 3.5). It also showed one distinct seasonal maximum through mid-June. The *SWC.VOL* of new shoots was substantially higher compared with older growth from the time of emergence of new shoots at the end of May until the end of July. For new shoots, *SWC.VOL* at the very beginning of the season (end of May and early June) was lower compared with mid-June, when theoretically it should be higher. The water content of new shoots (the most sensitive to dehydration) in May and early June was most likely underestimated due to longer storage time and the increased loss of water content before testing. This resulted in a peak in the water content of new shoots in mid-June.

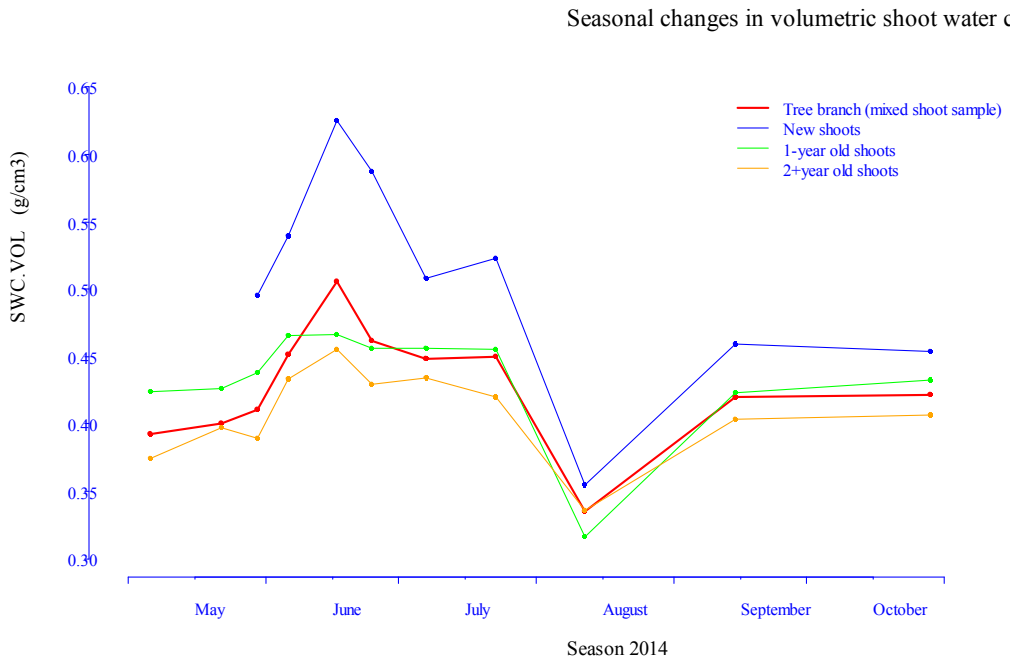

Figure 3.5 Seasonal variation in volumetric shoot water content *(SWC.VOL)*. Solid red, blue, green, and orange lines represent tree branches (mixed shoot sample), new, 1-year, and 2+year old shoots respectively.

3.1.3 Dry matter content

3.1.3.1 Gravimetric – *DM.GRAV*

The values for mean gravimetric dry matter content *(DM.GRAV)* were significantly different between groups of fuel sample type (ANOVA, $p < 0.001$, $F = 80.973$, $n = 181$). New shoots showed the lowest seasonal *DM.GRAV* values, largest dispersion, and lower normality of the data distribution compared with older shoots and tree branches (Fig 3.6).

For all ages of shoots, *DM.GRAV* varied from 0.21 to 0.58 (parts of 1, fresh mass basis) during the vegetative season of 2014 (Table 3.3). New shoots had the highest seasonal variation (standard deviation 0.10). A seasonal average of *DM.GRAV* for new shoots (0.36) was substantially lower than for older growth (0.49 for 1-year and 0.53 for 2+year old shoots). *DM.GRAV* for tree branches (0.50) was slightly higher compared with 1-year old shoots.

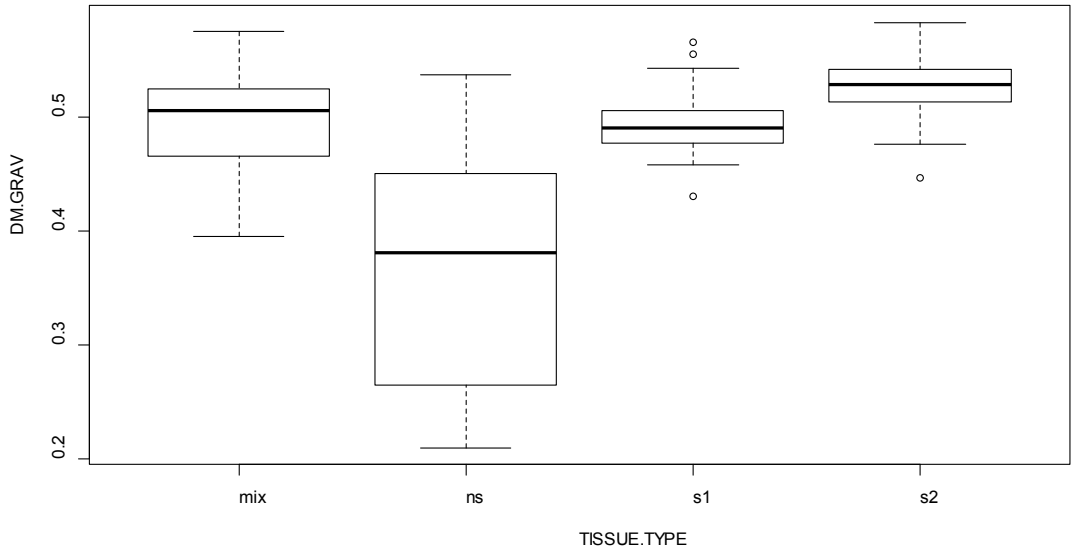

Figure 3.6 Box plots of seasonal variation in gravimetric dry matter content for tree branches (mix, mixed shoot sample), new (ns), 1-year (s1), and 2+year (s2) old shoots. A horizontal line within the box (the interquartile range, IQR) indicates the median. Whiskers are shown at 1.5 IQR. Circles indicate observed values outside of the 1.5 IQR.

Table 3.3 Seasonal minimum, maximum, mean, and standard deviations of gravimetric dry matter content *(DM.GRAV)*.

Fuel sample type	Minimum *DM.GRAV,* fresh mass basis, parts of 1	Maximum *DM.GRAV,* fresh mass basis, parts of 1	Range, fresh mass basis, parts of 1	Mean (standard deviation), fresh mass basis, parts of 1	Sample size
Tree branch (mixed shoot sample)	0.40	0.58	0.18	0.50 (0.04)	47
New shoots	0.21	0.54	0.33	0.36 (0.10)	42
1-year shoots	0.43	0.57	0.14	0.49 (0.02)	48
2+year shoots	0.45	0.58	0.14	0.53 (0.03)	48
All ages of shoots	0.21	0.58	0.37	0.47 (0.09)	138

DM.GRAV had two seasonal maximums for tree branches at the end of May and in mid-August. The lowest seasonal values of *DM.GRAV* were measured through mid-June and mid-July (Fig. 3.7). The *DM.GRAV* of new shoots was substantially lower compared with older growth until the beginning of August.

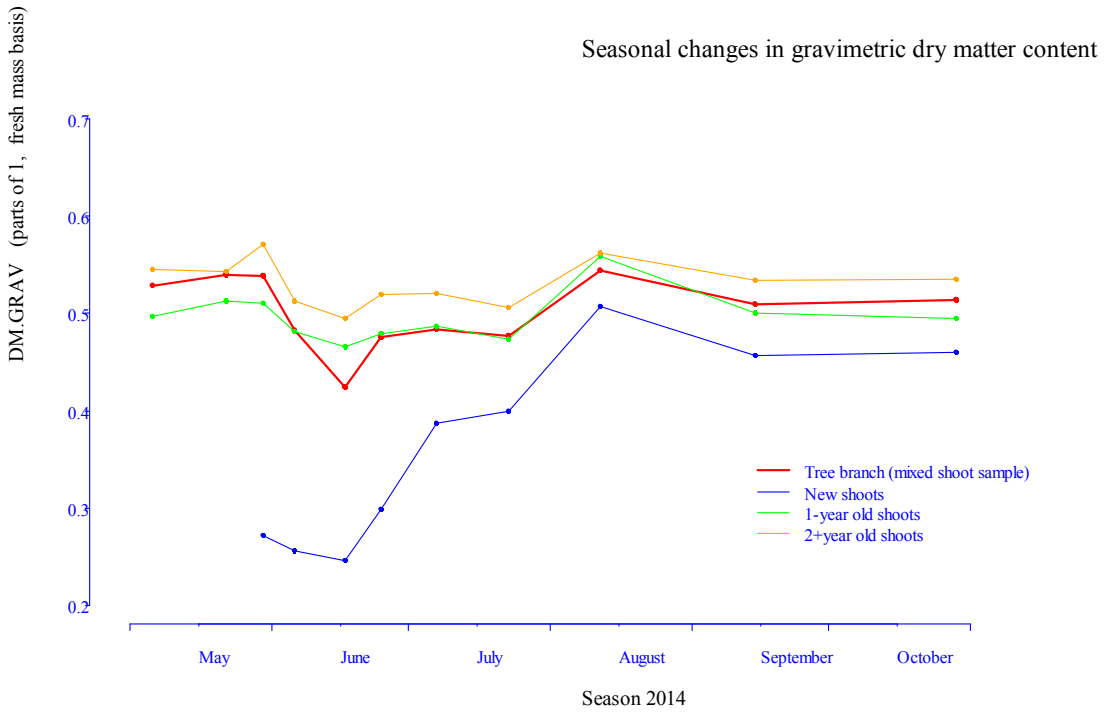

Figure 3.7 Seasonal variation in gravimetric dry matter content *(DM.GRAV)*. Red, blue, green, and orange lines represent tree branches (mixed shoot sample), new, 1-year, and 2+year old shoots respectively.

3.1.3.2 Volumetric – *DM.VOL*

The mean seasonal values of volumetric dry matter content *(DM.VOL)* were significantly different between groups of fuel sample type (ANOVA, $p < 0.001$, $F = 101.46$, $n = 181$). Similarly to *DM.GRAV* (Fig 3.6), for new shoots, seasonal variation in *DM.VOL* was higher, values of and normality of the data distribution were lower compared with older shoots and tree branches (Fig 3.8).

For all ages of shoots, *DM.VOL* varied from 0.15 g cm^{-3} to 0.57 g cm^{-3} during the season of 2014 (Table 3.4). A seasonal average of *DM.VOL* for new shoots of 0.29 g cm^{-3} was substantially lower than for older growth (0.42 g cm^{-3} for 1-year and 0.46 g cm^{-3} for 2+year old shoots). The *DM.VOL* for tree branches (0.43 g cm^{-3}) was slightly higher compared with 1-year old shoots.

Similarly to *DM.GRAV* (Fig. 3.7), the lowest seasonal values of *DM.VOL* for tree branches (Fig. 3.9) were measured through mid-June with slight increase in the beginning of July. However, seasonal variation in *DM.VOL* was noticeably different compared with *DM.GRAV* for the rest of the season. The *DM.VOL* showed a second seasonal minimum for tree branches through mid-August. By contrast, when measured on a fresh mass basis, *DM.GRAV* indicated a seasonal maximum in dry matter content through mid-August (Fig. 3.7) due to the small proportion of water in the fresh mass of shoots as indicated by the seasonal minimum in *SWC.GRAV* during that time period (Fig.3.3). The *DM.VOL* for new shoots was noticeably lower compared with older shoots and tree branches until the beginning of August.

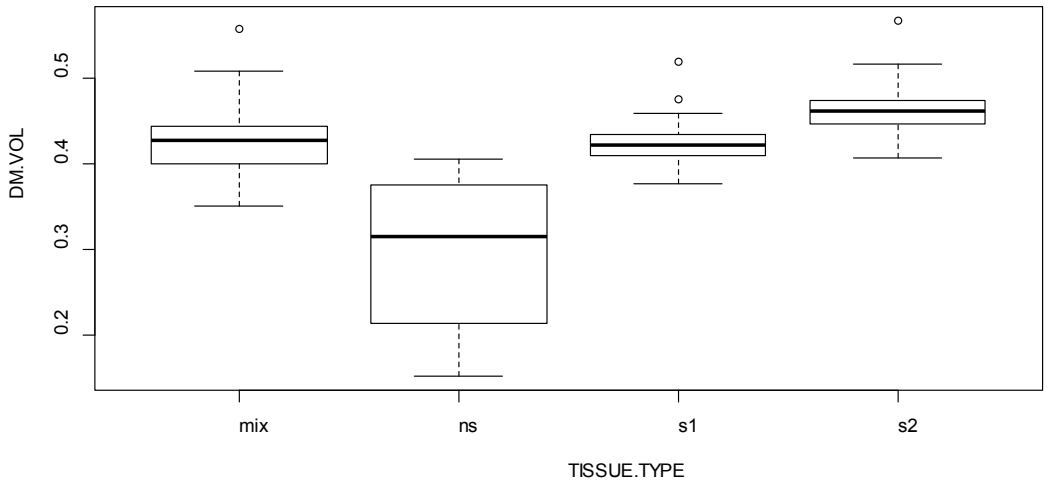

Figure 3.8 Box plots of seasonal variation in volumetric dry matter content *(DM.VOL)* for tree branches (mix, mixed shoot sample), new (ns), 1-year (s1), and 2+year (s2) old shoots. A horizontal line within the box (the interquartile range, IQR) indicates the median. Whiskers are shown at 1.5 IQR. Circles indicate observed values outside of the 1.5 IQR.

Table 3.4 Seasonal minimum, maximum, mean, and standard deviations of volumetric shoots dry matter content *(DM.VOL)*

Fuel sample type	Minimum *DM.VOL*, g cm^{-3}	Maximum *DM.VOL*, g cm^{-3}	Range, g cm^{-3}	Mean (standard deviation), g cm^{-3}	Sample size
Tree branch (mixed shoot sample)	0.35	0.56	0.21	0.43 (0.09)	47
New shoots	0.15	0.41	0.25	0.29 (0.08)	42
1-year shoots	0.38	0.52	0.14	0.42 (0.02)	48
2+year shoots	0.41	0.57	0.16	0.46 (0.03)	48
All ages of shoots	0.15	0.57	0.42	0.40 (0.09)	138

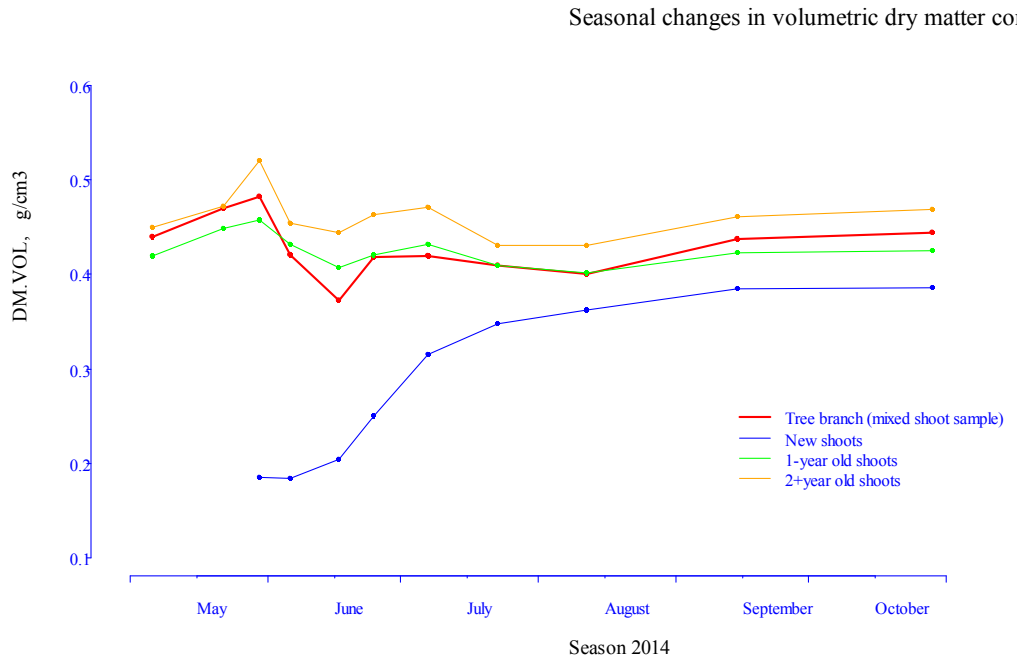

Figure 3.9 Seasonal variation in volumetric dry matter content *(DM.VOL)*. Red, blue, green, and orange lines represent tree branches (mixed shoot sample), new, 1-year, and 2+year old shoots respectively.

3.1.4 Calorimetric content – *CC*

Unlike other independent variables, the values for mean calorimetric content *(CC*, gross heat of combustion) were not significantly different between groups of plant tissue (ANOVA, p = 0.03869, F = 2.8527, n = 181). Seasonal values, variation, and normality of the data distribution were similar for all groups of fuel sample type (Fig. 3.10). *CC* varied from 18.64 kJ g^{-1} to 22.75 kJ g^{-1} for all ages of shoots during the vegetative season of 2014 (Table 3.5). Calorimetric content seasonal average ranged from highest to lowest as follows: 1-year old (21.08 kJ g^{-1}), new (20.81 kJ g^{-1}), and 2+year old shoots (20.64 kJ g^{-1}). The *CC* for tree branches (20.76 kJ g^{-1}) was slightly lower compared with new shoots.

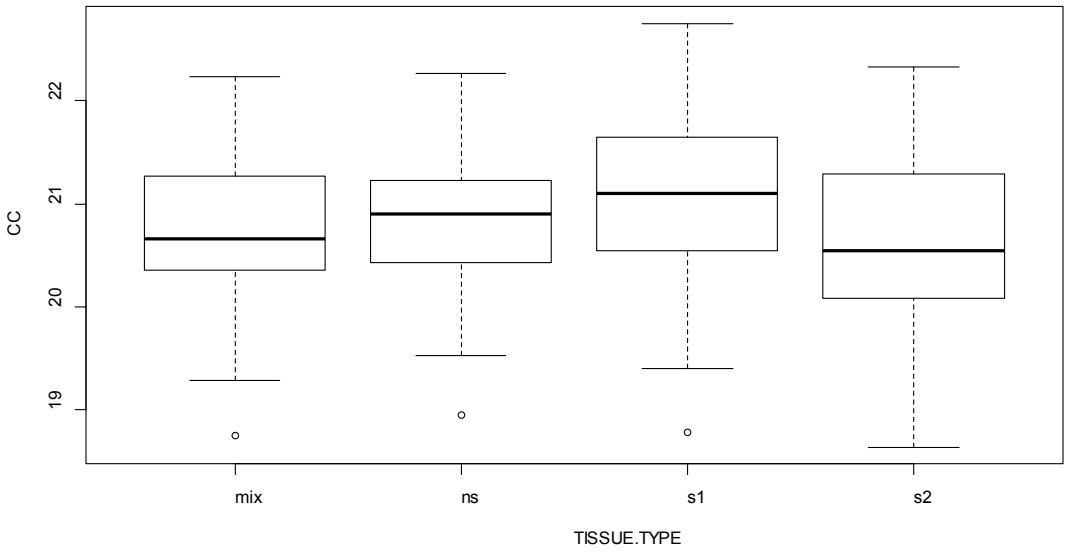

Figure 3.10 Box plots of seasonal variation in calorimetric content *(CC*, gross heat of combustion) for tree branches (mix, mixed shoot sample), new (ns), 1-year (s1), and 2+year (s2) old shoots. A horizontal line within the box (the interquartile range, IQR) indicates the median. Whiskers are shown at 1.5 IQR. Circles indicate observed values outside of the 1.5 IQR.

Using benzoic acid tests data (Appendix 3), the calorimetric content (gross heat of combustion) mean and standard deviation were calculated at 26.02 kJ g^{-1} and 0.76 kJ g^{-1} respectively (Table 3.5). For benzoic acid tests, the standard error of the mean was

estimated at 0.27 kJ g^{-1}. As a measure of the precision of the method, the proportion of the 0.95 confidence interval (0.64 kJ g^{-1}, estimated using the standard error of the mean discussed above) to benzoic acid heat of combustion mean (26.02 kJ g^{-1} in Table 3.5) was estimated to be 2.5%. This was substantially lower than the proportion of the actual range of variation in gross heat of combustion (Table 3.5) for all ages of shoots (4.11 kJ g^{-1}) to measured mean (20.85 kJ g^{-1}) that was estimated to be 19.7%. Also, since 0.95 confidence interval was estimated to range from 25.38 kJ g^{-1} to 26.66 kJ g^{-1}, it therefore included the value of benzoic acid heat of combustion reported by Jessup & Green, (1934) of 26.419 kJ g^{-1}. These suggest the appropriate accuracy (2.5%, as discussed above) of the methodology used for calorimetric content evaluation.

Table 3.5 Seasonal minimum, maximum, mean, and standard deviations of calorimetric content (*CC*, gross heat of combustion) for fresh shoots and branches of white spruce compared to benzoic acid tests results

Fuel type	Minimum *CC,* kJ g^{-1} (dry mass basis)	Maximum *CC,* kJ g^{-1} (dry mass basis)	Range, kJ g^{-1} (dry mass basis)	Mean (standard deviation), kJ g^{-1} (dry mass basis)	Sample size
Tree branch (mixed shoot sample)	18.75	22.24	3.49	20.76 (0.73)	47
New shoots	18.95	22.27	3.32	20.81 (0.66)	42
1-year shoots	18.78	22.75	3.97	21.08 (0.85)	48
2+year shoots	18.64	22.33	3.69	20.64 (0.83)	48
All ages of shoots	18.64	22.75	4.11	20.85 (0.81)	138
Benzoic acid	25.02	27.04	2.02	26.02 (0.76)	8

The seasonal pattern of variation in *CC* showed maximums in mid-May, mid-June, at the end of July, and in mid-September (Fig. 3.11). The most substantial minimum in *CC* occurred in mid-August, simultaneously to seasonal minimums for *DM.VOL* (Fig. 3.9) and *SWC.VOL* (Fig. 3.5). The pattern of the seasonal changes in calorimetric content was noticeably different for new shoots compared to older growth. Calorimetric content was practically the same for 1-year and 2+year shots and tree branches (mixed shoot sample) before leaf-out at the end of May; it was noticeably higher for 1-year shoots and lower for 2+year old shoots compared to tree branches for the rest of the season. In general, all groups of tissue type showed slight growth in the calorimetric content through the vegetative season.

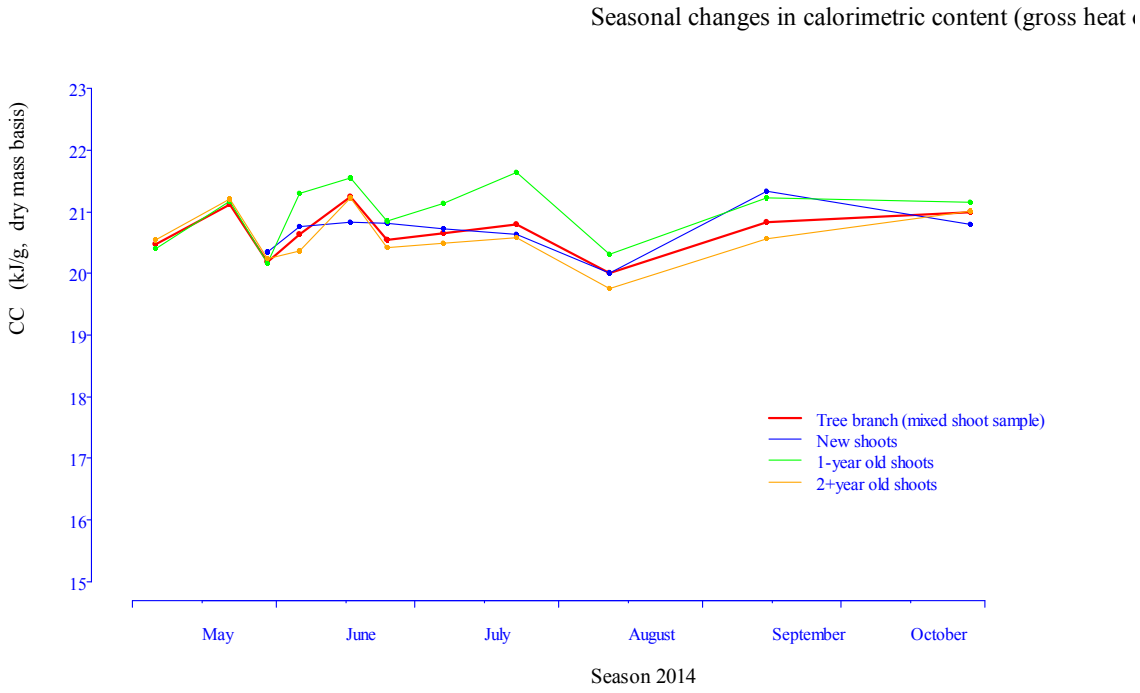

Figure 3.11 Seasonal variation in calorimetric content *(CC,* gross heat of combustion). Red, blue, green, and orange lines represent tree branches (mixed shoot sample), new, 1-year, and 2+year old shoots respectively.

The increase in the calorimetric content in the beginning of May (Fig. 3.11) is caused by the beginning of spring physiological activity of plants and accumulation of energy-reach chemical substances in the older growth. The calorimetric content drops with transferring energy-reach chemical substances from older growth to new buds in the end of May before

leave-out. In the beginning-mid of June, the calorimetric content increases both for old and new growth due to high photosynthetic activity of plants. In central Alberta, carbon fixation activity and growth (and hence calorimetric content) are limited to amount of precipitation starting July (Downing & Pettapiece, 2006). This was confirmed in 2014: in general, for new and older growth, calorimetric content *(CC)* declines starting July towards late-summer drought in mid August (critically low volumetric water content as it is seen in Fig. 3.5). The mid-June and end of July peaks in *CC* (Fig. 3.11) exactly corresponds to peaks in volumetric shoot water content *(SWC.VOL)* in Fig. 3.5. The late-August and September recovery in *CC* (Fig. 3.11) correspond to recovery in *SWC.VOL* (Fig. 3.5).

3.1.5 Energy content

3.1.5.1 Gravimetric – *EC.GRAV*

The values for mean gravimetric energy content *(EC.GRAV)* were significantly different between groups of fuel sample type (ANOVA, $p < 0.001$, $F = 77.115$, $n = 181$). For new shoots, the variation in *EC.GRAV* was noticeably higher; seasonal values and normality of the data distribution were lower compared with older shoots and tree branches (Fig 3.12).

For all ages of shoots, *EC.GRAV* varied from 4.46 kJ g^{-1} to 12.06 kJ g^{-1} (fresh mass basis,) during the vegetative season of 2014 (Table 3.6). New shoots had the highest seasonal variation (standard deviation 2.07 kJ g^{-1}). The seasonal *EC.GRAV* mean for new shoots (7.55 kJ g^{-1}) was substantially lower than for older growth (10.37 kJ g^{-1} for 1-year and 10.92 kJ g^{-1} for 2+year old shoots). The *EC.GRAV* mean for tree branches (10.27 kJ g^{-1}) was slightly lower compared with 1-year old shoots.

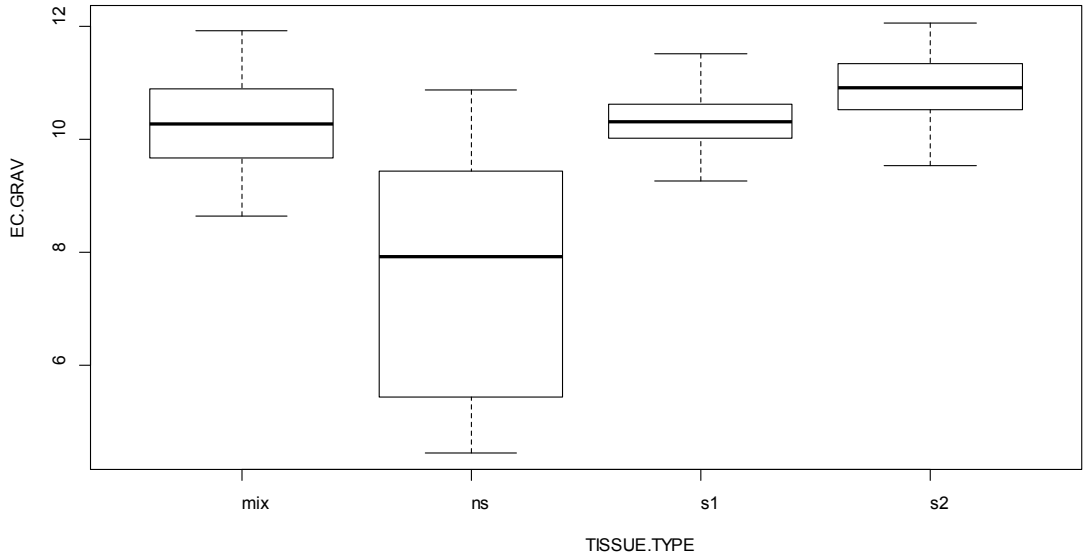

Figure 3.12 Box plots of seasonal variation in gravimetric energy content *(EC.GRAV)* for tree branches (mix, mixed shoot sample), new (ns), 1-year (s1), and 2+year (s2) old shoots. A horizontal line within the box (the interquartile range, IQR) indicates the median. Whiskers are shown at 1.5 IQR. Circles indicate observed values outside of the 1.5 IQR.

Table 3.6 Seasonal minimum, maximum, mean, and standard deviations of gravimetric energy content *(EC.GRAV).*

Fuel sample type	Minimum *EC.GRAV,* fresh mass basis, kJ g^{-1}	Maximum *EC.GRAV,* fresh mass basis, kJ g^{-1}	Range, fresh mass basis, kJ g^{-1}	Mean (standard deviation), fresh mass basis, kJ g^{-1}	Sample size
Tree branch (mixed shoot sample)	8.64	11.93	3.29	10.27 (0.81)	47
New shoots	4.46	10.88	6.42	7.55 (2.07)	42
1-year shoots	9.27	11.51	2.24	10.37 (0.52)	48
2+year shoots	9.54	12.06	2.52	10.92 (0.57)	48
All ages of shoots	4.46	12.06	7.60	9.70 (1.89)	138

The seasonal trend for *EC.GRAV* (Fig. 3.13) was very similar to that for *DM.GRAV* (Fig. 3.7). Gravimetric energy content showed two seasonal maximums for tree branches in mid-May and in mid-August. The lowest seasonal values of *EC.GRAV* were measured through mid-June and mid-July. The *EC.GRAV* of new shoots was substantially lower compared with older growth until the beginning of August.

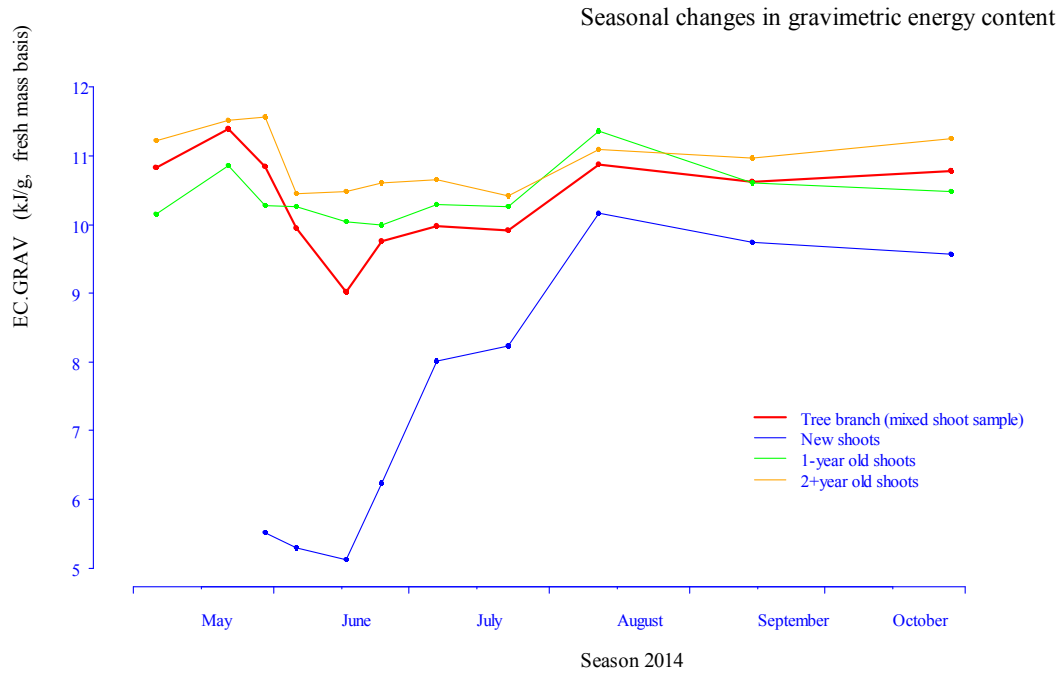

Figure 3.13 Seasonal variation in gravimetric dry matter content *(EC.GRAV)*. Red, blue, green, and orange lines represent tree branches (mixed shoot sample), new, 1-year, and 2+year old shoots respectively.

3.1.5.2 Volumetric – *EC.VOL*

The mean seasonal values for volumetric energy content *(EC.VOL)* were significantly different between groups of fuel sample type (ANOVA, $p < 0.001$, $F = 92.587$, $n = 181$). The values of *EC.VOL* and normality of the data distribution were lower for new shoots compared with older shoots and tree branches; seasonal variation for new shoots was noticeably higher (Fig 3.14).

For all ages of shoots, *EC.VOL* varied from 3.24 kJ cm^{-3} to 10.92 kJ cm^{-3}during the season of 2014 (Table 3.7). Seasonal variation in *EC.VOL* was the highest for new shoots (standard deviation of 1.81 kJ cm^{-3}). The seasonal *EC.VOL* mean for new shoots of 6.13 kJ cm^{-3} was substantially lower than for 1-year (8.95 kJ cm^{-3}) and 2+year old shoots (9.52 kJ cm^{-3}). The *EC.VOL* seasonal mean for tree branches (8.82 kJ cm^{-3}) was slightly lower compared with 1-year old shoots.

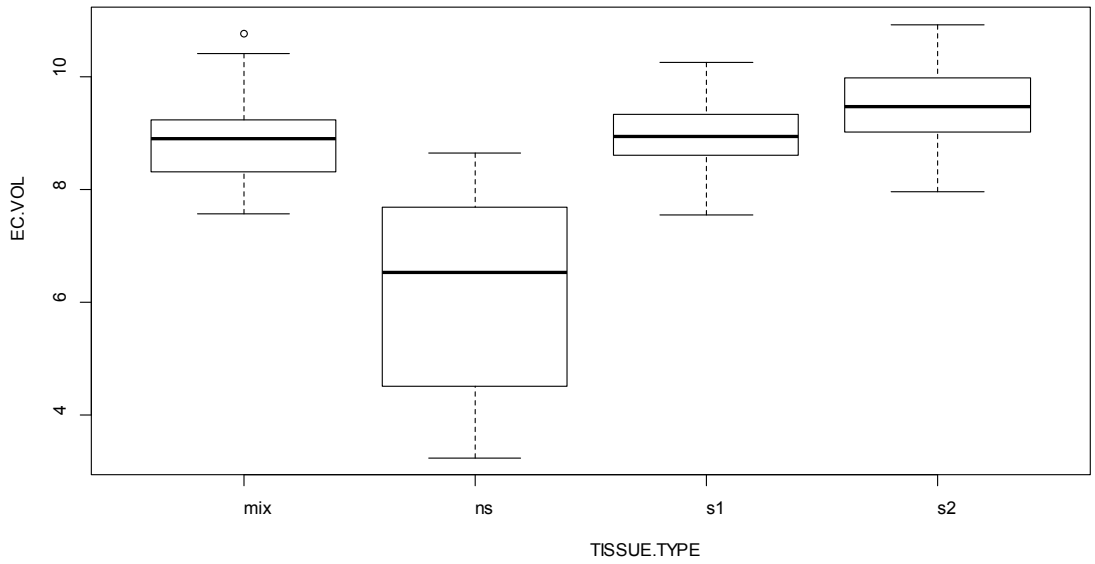

Figure 3.14 Box plots of seasonal variation in volumetric energy content *(EC.VOL)* for tree branches (mix, mixed shoot sample), new (ns), 1-year (s1), and 2+year (s2) old shoots. A horizontal line within the box (the interquartile range, IQR) indicates the median. Whiskers are shown at 1.5 IQR. Circles indicate observed values outside of the 1.5 IQR.

Table 3.7 Seasonal minimum, maximum, mean, and standard deviations of volumetric energy content *(EC.VOL)*.

Fuel sample type	Minimum *EC.VOL,* kJ cm^{-3}	Maximum *EC.VOL,* kJ cm^{-3}	Range, kJ cm^{-3}	Mean (standard deviation), kJ cm^{-3}	Sample size
Tree branch (mixed shoot sample)	7.56	10.75	3.19	8.82 (0.75)	47
New shoots	3.24	8.64	5.40	6.13 (1.81)	42
1-year shoots	7.54	10.24	2.70	8.95 (0.56)	48
2+year shoots	7.96	10.92	2.96	9.52 (0.64)	48
All ages of shoots	3.24	10.92	7.68	8.29 (1.83)	138

The seasonal pattern of variation in *EC.VOL* (Fig. 3.15) was noticeably different compared with *EC. GRAV* (Fig. 3.13). The lowest seasonal values of *EC.VOL* for tree branches were measured through mid-June and mid-August. By contrast, when measured gravimetrically on a fresh mass basis, *EC.GRAV* showed a seasonal maximum through mid-August (Fig. 3.13) due to a smaller proportion of water (hence a higher proportion of dry matter) in the fresh mass of shoots as indicated by the lowest seasonal minimum in *SWC.VOL* during that time period (Fig.3.5). The *EC.VOL* for new shoots was noticeably lower compared with older shoots and tree branches until the beginning of August.

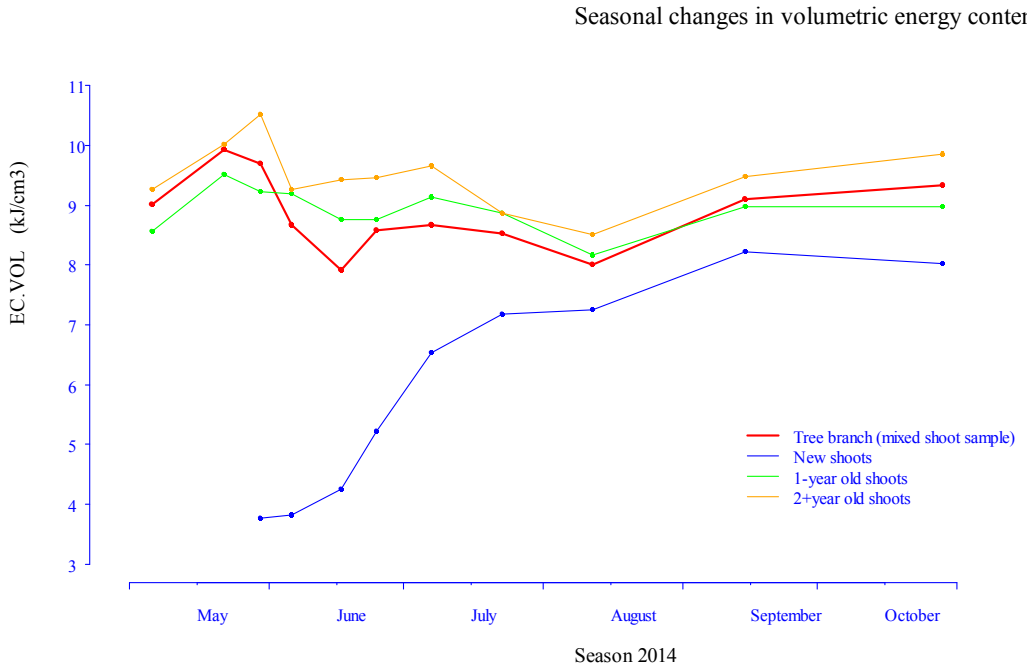

Figure 3.15 Seasonal variation in volumetric energy content *(EC.VOL)*. Red, blue, green, and orange lines represent tree branches (mixed shoot sample), new, 1-year, and 2+year old shoots respectively.

3.1.6 Fresh density – *D*

Values for mean fresh density *(D)* were significantly different between groups of fuel sample type (ANOVA, $p < 0.001$, $F = 14.162$, $n = 181$). For new shoots, variation in *D* was higher; seasonal values and normality of the data distribution were lower compared with older shoots and tree branches (Fig 3.16).

Fresh density for all ages of shoots varied from 0.62 g cm^{-3} to 0.99 g cm^{-3} during the vegetative season of 2014 (Table 3.8). New shoots had the highest seasonal variation (standard deviation 0.07 g cm^{-3}). The seasonal average of *D* was lower for new shoots (0.81 g cm^{-3}) than for older growth (0.86 g cm^{-3} for 1-year and 0.87 g cm^{-3} for 2+year old shoots). The *D* for tree branches (0.86 g cm^{-3}) was the same as for 1-year old shoots.

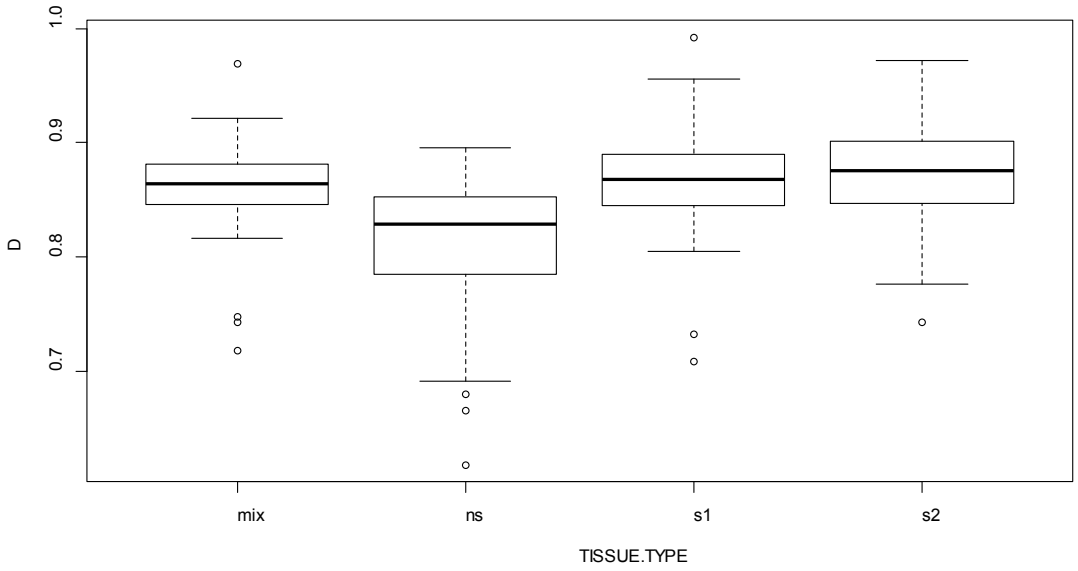

Figure 3.16 Box plots of seasonal variation in fresh density *(D)* for tree branches (mix, mixed shoot sample), new (ns), 1-year (s1), and 2+year (s2) old shoots. A horizontal line within the box (the interquartile range, IQR) indicates the median. Whiskers are shown at 1.5 IQR. Circles indicate observed values outside of the 1.5 IQR.

Table 3.8 Seasonal minimum, maximum, mean, and standard deviations of white spruce shoots fresh density *(D)*.

Fuel sample type	Minimum *D,* g cm^{-3}	Maximum *D,* g cm^{-3}	Range, g cm^{-3}	Mean (standard deviation), g cm^{-3}	Sample size
Tree branch (mixed shoot sample)	0.72	0.97	0.25	0.86 (0.04)	47
New shoots	0.62	0.90	0.28	0.81 (0.07)	42
1-year shoots	0.71	0.99	0.28	0.86 (0.04)	48
2+year shoots	0.74	0.97	0.23	0.87 (0.05)	48
All ages of shoots	0.62	0.99	0.37	0.85 (0.06)	138

For all tissue type groups, fresh density showed a gradual growth until the end of May, slight decline until the end of July and then a substantial minimum in mid-August followed by slight growth towards the end of the season (Fig. 3.17). Fresh density of new shoots was substantially lower compared with other tissue type groups until mid-July. The dip in fresh density for all classes of sample in August occurred simultaneously with the second seasonal late-summer dip in volumetric water content (drought conditions indicated by the extreme low *SWC.WOL* values in Fig.3.5) suggesting that fresh density was affected by drought and associated decline in concentration of water in the plant tissue.

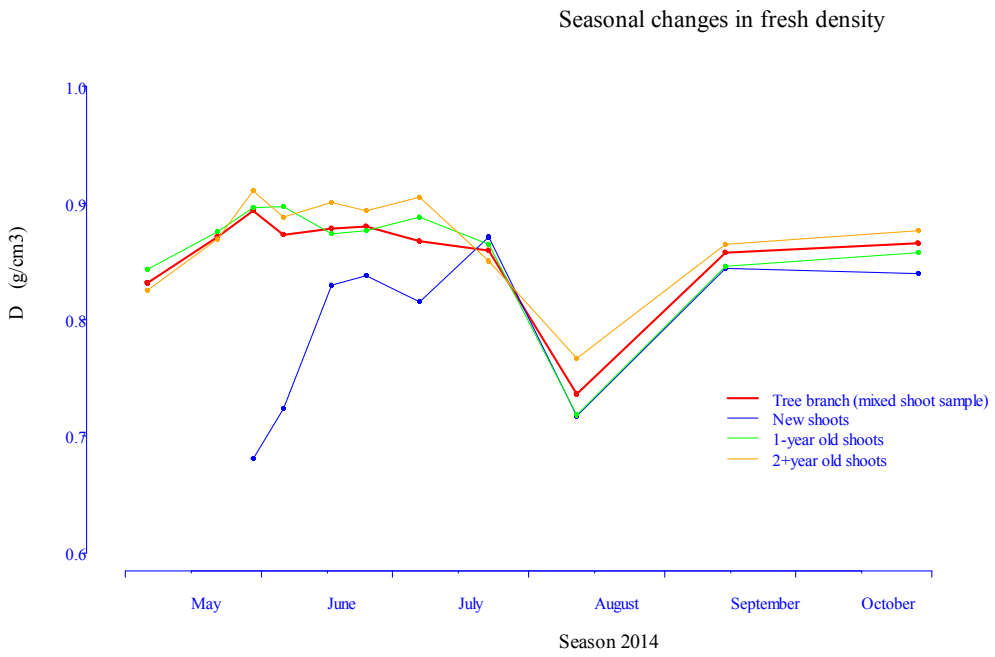

Figure 3.17 Seasonal variation in fresh density *(D)*. Red, blue, green, and orange lines represent tree branches (mixed shoot sample), new, 1-year, and 2+year old shoots respectively.

3.1.7 Density water-free – *DWF*

The mean seasonal values for density water-free *(DWF)* (Fig. 3.18) were significantly different between groups of fuel sample type (ANOVA, $p < 0.001$, $F = 44.667$, $n = 181$). In general, *DWF* showed very similar characteristics to *D* (Fig. 3.16) having, however, noticeably lower values. The values of *DWF* and the normality of the data distribution were lower for new shoots compared with older shoots and tree branches; seasonal variation for new shoots was noticeably higher.

For all ages of shoots, *DWF* varied from 0.31 g cm^{-3} to 0.98 g cm^{-3}during the season of 2014 (Table 3.9) with a seasonal mean of 0.72 g cm^{-3}, which was noticeably lower compared with *D* (0.85 g cm^{-3}). The seasonal *DWF* mean for new shoots of 0.60 g cm^{-3} was substantially lower than for 1-year (0.76 g cm^{-3}) and 2+year old shoots (0.79 g cm^{-3}). The *DWF* seasonal mean for tree branches (0.75 kJ g cm^{-3}) was slightly lower compared with 1-year old shoots.

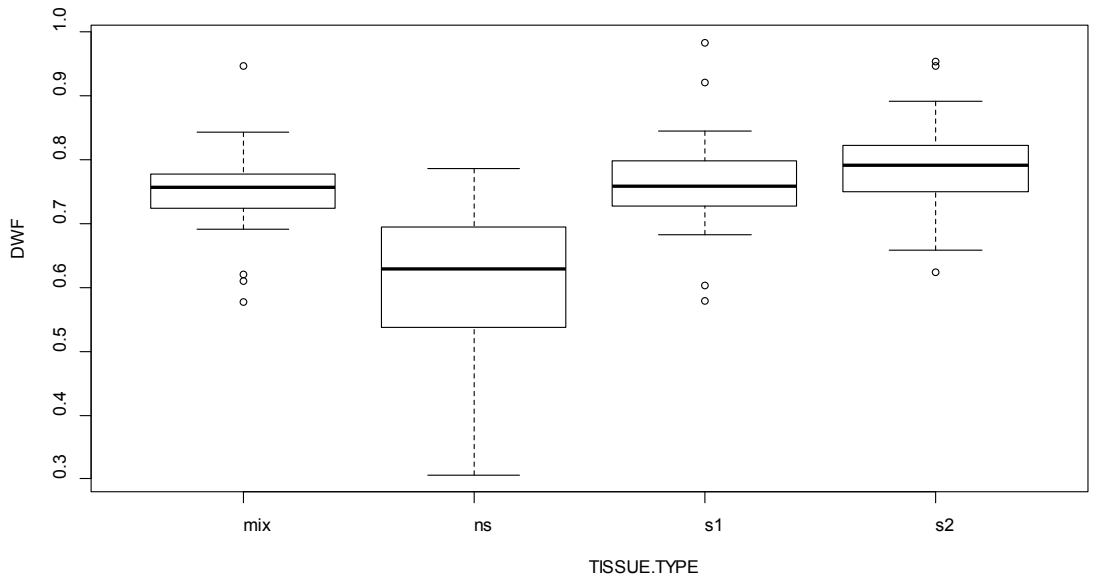

Figure 3.18 Box plots of seasonal variation in density water-free *(DWF)* for tree branches (mix, mixed shoot sample), new (ns), 1-year (s1), and 2+year (s2) old shoots. A horizontal line within the box (the interquartile range, IQR) indicates the median. Whiskers are shown at 1.5 IQR. Circles indicate observed values outside of the 1.5 IQR.

The seasonal pattern in density water-free (Fig. 3.19) was similar to the seasonal pattern of fresh density (Fig. 3.17). For new shoots, however, unlike *D* (Fig. 3.17)*, DWF* showed gradual constant growth in the first half of the vegetative season before a drop in mid-August. The timing of this drop in *DWF* in mid-August coincides with seasonal minimums in *SWC.VOL* (Fig. 3.5)*, DM.VOL* (Fig. 3.9)*,* and *EC.WOL* (Fig. 3.15). The *DWF* of new shoots was substantially lower compared with other tissue type groups until mid-July. Similar to fresh density (as was discussed in the section 3.1.6, Fig. 3.17), density water-free for all classes of sample (Fig. 3.19) was affected by drought in mid-August (Fig.3.5).

Table 3.9 Seasonal minimum, maximum, mean, and standard deviations of density water-free *(DWF)*

Fuel sample type	Minimum *DWF,* g cm^{-3}	Maximum *DWF,* g cm^{-3}	Range, g cm^{-3}	Mean (standard deviation), g cm^{-3}	Sample size
Tree branch (mixed shoot sample)	0.58	0.95	0.37	0.75 (0.06)	47
New shoots	0.31	0.79	0.48	0.60 (0.12)	42
1-year shoots	0.58	0.98	0.40	0.76 (0.09)	48
2+year shoots	0.62	0.95	0.33	0.79 (0.07)	48
All ages of shoots	0.31	0.98	0.68	0.72 (0.12)	138

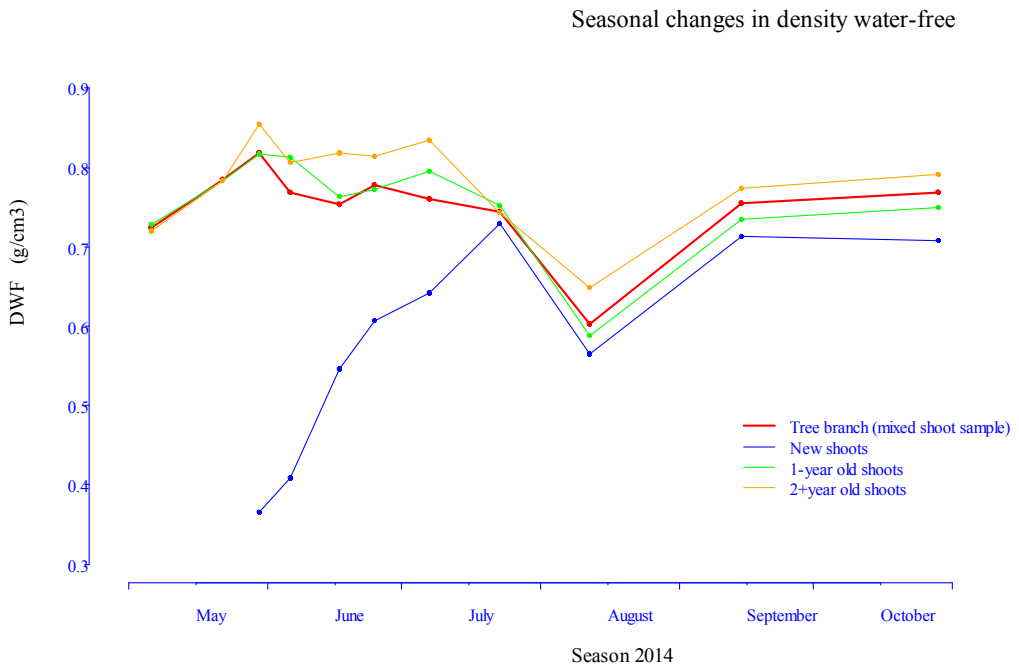

Figure 3.19 Seasonal variation in density water-free *(DWF)*. Red, blue, green, and orange lines represent tree branches (mixed shoot), new, 1-year, and 2+year old shoots respectively.

3.1.8 Porosity water-free – *PWF*

The mean seasonal values for porosity water-free *(PWF)* were significantly different between groups of fuel sample type (ANOVA, $p < 0.001$, $F = 44.667$, $n = 181$). The values of *PWF* were higher and the normality of the data distribution was lower for new shoots compared with older shoots and tree branches; seasonal variation for new shoots was noticeably higher as well (Fig 3.20).

The *PWF* varied from 0.36 ( ) to 0.80 ( ) for all ages of shoots during the season of 2014 (Table 3.10) with a seasonal mean of 0.50 ( ). The seasonal *PWF* mean for new shoots of 0.61 ( ) was higher than for 1-year (0.50) and 2+year old shoots (0.49). The *PWF* seasonal mean for tree branches (0.51) was slightly higher compared with 1-year and 2+year old shoots.

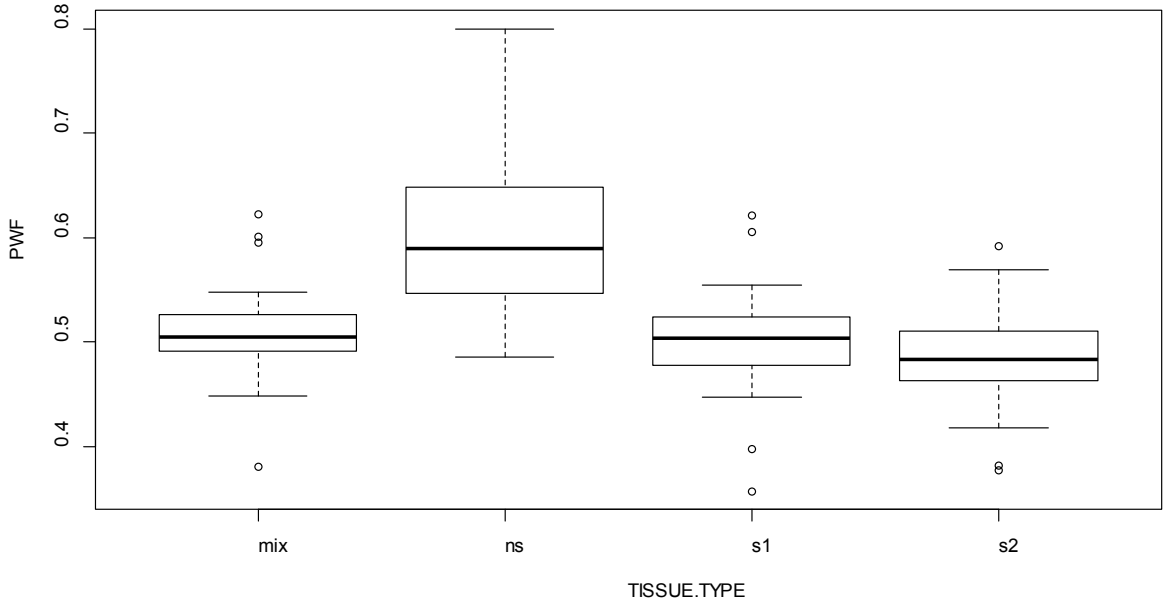

Figure 3.20 Box plot of seasonal variation in porosity water-free *(PWF)* for tree branches (mix, mixed shoot sample), new (ns), 1-year (s1), and 2+year (s2) old shoots. A horizontal line within the box (the interquartile range, IQR) indicates the median. Whiskers are shown at 1.5 IQR. Circles indicate observed values outside of the 1.5 IQR.

Table 3.10 Seasonal minimum, maximum, mean, and standard deviations of porosity water-free *(PWF)*.

Fuel sample type	Minimum *PWF,* parts of 1 (part of volume)	Maximum *PWF,* parts of 1 (part of volume)	Range, parts of 1 (part of volume)	Mean (standard deviation), parts of 1 (part of volume)	Sample size
Tree branch (mixed shoot sample)	0.38	0.62	0.24	0.51 (0.04)	47
New shoots	0.49	0.80	0.31	0.61 (0.08)	42
1-year shoots	0.36	0.62	0.26	0.50 (0.04)	48
2+year shoots	0.38	0.59	0.21	0.49 (0.04)	48
All ages of shoots	0.36	0.80	0.44	0.53 (0.08)	138

The seasonal pattern in porosity water-free (Fig. 3.21) was opposite to the seasonal pattern of density water-free (Fig. 3.19). The *PWF* of new shoots was substantially higher compared with other tissue type groups until mid-July; it showed a gradual monotonic decline in the first half of the vegetative season before a mid-August spike. The seasonal maximum in *PWF* in mid-August (Fig. 3.21) coincides with seasonal minimums in *SWC.VOL* (Fig. 3.5)*, DM.VOL* (Fig. 3.9)*,* and *EC.WOL* (Fig. 3.15). It can be explained by the substantial decline in concentration of water in the plant tissue caused by drought as indicated by the extreme low shoot water content in mid-August (Fig.3.5).

For new shoots at the very beginning of the vegetative season, *PWF,* as the proportion of voids filled by gases in the cell wall substance, reached 80% (Table 3.10). With maximum water contents of new shoots, the cell wall substance occupied only approximately 30% of cell volume because another 70% was filled by water (Table 3.2, maximum *SWC.VOL* for new shoots of 0.66 g cm^{-3}). Therefore, the combined actual proportion of the voids filled by gases (porosity water-free) and by water (porosity filled by water, or volumetric water content) in the plant cell volume can be higher than 90%. This means that for new shoots at the beginning of the season, only 0.1 cm^3 of solid cell wall substance (solid dry organic matter without any voids) is mixed with 0.9 cm^3 of water and gases, composing 1.0 cm^3 of volume of the tissue of new shoots. The cells of the new shoots of white spruce in the beginning of the season with a PWF daily mean close to 0.80 (Fig. 3.21) are actually inflated by water and gases!

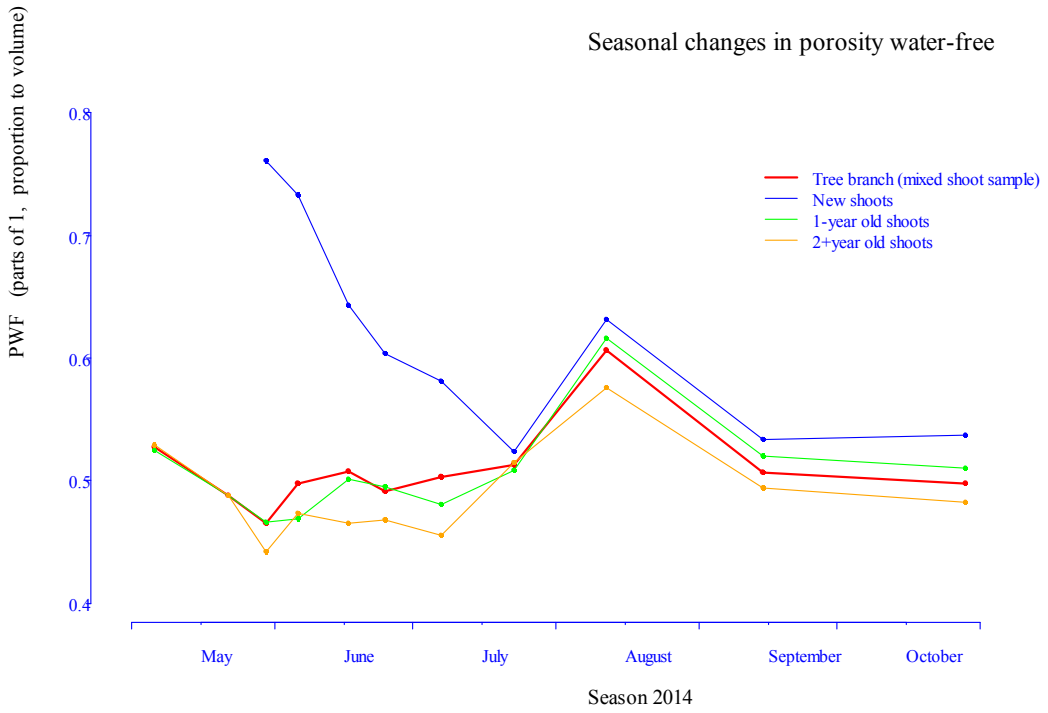

Figure 3.21 Seasonal variation in porosity water-free *(PWF)* for white spruce in 2014. Red, blue, green, and orange lines represent tree branches (mixed shoot sample), new, 1-year, and 2+year old shoots respectively.

3.2 PREDICTAND VARIABLES – FLAMMABILITY OF LIVE FUEL

3.2.1 Gravimetric flammability – $dH_{eff}60s.GRAV$

The predictand variables (gravimetric and volumetric flammability of live fuel) were measured in this study as the gravimetric and volumetric differential effective heat of combustion, respectively. The values for the mean gravimetric differential effective heat of combustion $(dH_{eff}60s.GRAV)$ were significantly different between groups of fuel sample type (ANOVA, $p < 0.001$, $F = 47.649$, $n = 181$). For new shoots, the variation in $dH_{eff}60s.GRAV$ was noticeably higher (Fig 3.22); seasonal values and normality of the data distribution were lower compared with older shoots and tree branches.

For all ages of shoots, $dH_{eff}60s.GRAV$ varied from -6.33 kJ g^{-1} to 7.10 kJ g^{-1} (fresh mass basis) during the vegetative season of 2014 (Table 3.11). New shoots had the highest seasonal variation in $dH_{eff}60s.GRAV$ (standard deviation 3.68 kJ g^{-1}). The seasonal $dH_{eff}60s.GRAV$ mean for new shoots (0.23 kJ g^{-1}) was substantially lower than for older growth (4.75 kJ g^{-1} for 1-year and 4.76 kJ g^{-1} for 2+year old shoots). The $dH_{eff}60s.GRAV$ mean for tree branches (4.39 kJ g^{-1}) was slightly lower compared with 1-year and 2+year old shoots.

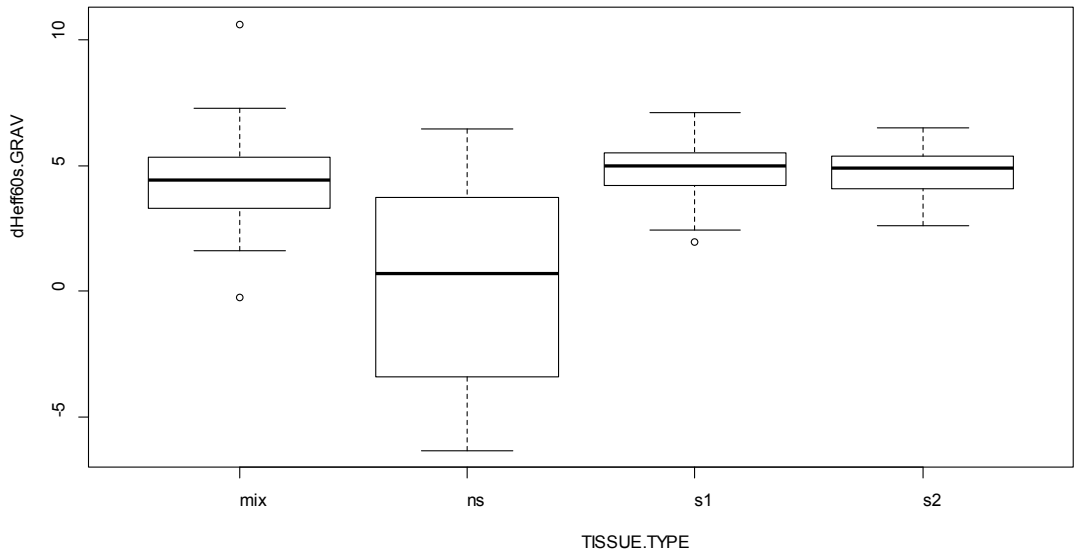

Figure 3.22 Box plot of seasonal variation in gravimetric differential effective heat of combustion ($d\boldsymbol{H_{eff}}60s.GRAV$) for tree branches (mix, mixed shoot sample), new (ns), 1-year (s1), and 2+year (s2) old shoots. A horizontal line within the box (the interquartile range, IQR) indicates the median. Whiskers are shown at 1.5 IQR. Circles indicate observed values outside of the 1.5 IQR.

Table 3.11 Seasonal minimum, maximum, mean, and standard deviations of gravimetric differential effective heat of combustion ($dH_{eff}60s.GRAV$).

Fuel sample type	Minimum $dH_{eff}60s.GRAV$, fresh mass basis, kJ g^{-1}	Maximum $dH_{eff}60s.GRAV$, fresh mass basis, kJ g^{-1}	Range, fresh mass basis, kJ g^{-1}	Mean (standard deviation), fresh mass basis, kJ g^{-1}	Sample size
Tree branch (mixed shoot sample)	-0.24	10.63	10.87	4.39 (1.79)	47
New shoots	-6.33	6.48	12.81	0.23 (3.68)	42
1-year shoots	1.98	7.10	5.12	4.75 (1.19)	48
2+year shoots	2.61	6.49	3.88	4.76 (0.86)	48
All ages of shoots	-6.33	7.10	13.43	3.38 (3.03)	138

The seasonal trend of $dH_{eff}60s.GRAV$ (Fig. 3.23) was in general similar to that for *EC.GRAV* (Fig. 3.13) and for *DM.GRAV* (Fig. 3.7). The lowest seasonal values of $dH_{eff}60s.GRAV$ were measured through mid-June and end of July. The $dH_{eff}60s.GRAV$ showed three seasonal maximums for tree branches in the very beginning of May (or earlier, for which period no data exists), the beginning of July, and in mid-August. The timing of the third seasonal spike in $dH_{eff}60s.GRAV$ in mid-August coincided with the second seasonal minimum in *SWC.GRAV* (Fig. 3.3). The $dH_{eff}60s.GRAV$ for new shoots was substantially lower compared with older growth until the beginning of August (Fig. 3.23). It showed a decline from the end of May to mid-June: due to longer storage time and the increased loss of water content for new shoots (the most sensitive to dehydration) before testing (as discussed earlier in the section 3.1.2), the $dH_{eff}60s.GRAV$ for new shoots in May and early June was most likely overestimated.

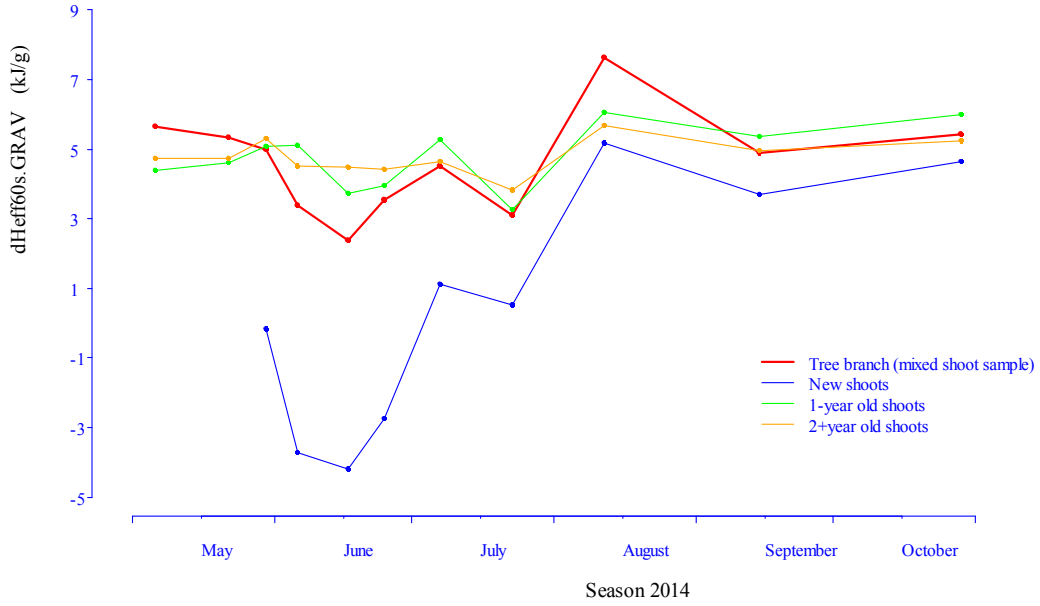

Figure 3.23 Seasonal variation in gravimetric differential effective heat of combustion ($d\boldsymbol{H}_{eff}60s.GRAV$). Red, blue, green, and orange lines represent tree branches (mixed shoot sample), new, 1-year, and 2+year old shoots respectively.

3.2.2 Volumetric flammability – $dH_{eff}60s.VOL$

The volumetric flammability of live fuel was measured as volumetric differential effective heat of combustion. Values for mean volumetric differential effective heat of combustion $(dH_{eff}60s.VOL)$ were significantly different between groups of fuel sample type (ANOVA, $p < 0.001$, $F = 53.601$, $n = 181$). For new shoots, variation in $dH_{eff}60s.VOL$ was noticeably higher; seasonal values and normality of the data distribution were lower compared with older shoots and tree branches (Fig 3.24).

For all ages of shoots, $dH_{eff}60s.VOL$ varied from -5.47 kJ cm^{-3} to 6.79 kJ cm^{-3} during the vegetative season of 2014 (Table 3.12). Seasonal variation in $dH_{eff}60s.VOL$ was the highest for new shoots (standard deviation 2.97 kJ cm^{-3}). The seasonal $dH_{eff}60s.VOL$

mean for new shoots (0.20 kJ cm^{-3}) was substantially lower than for 1-year (4.10 kJ cm^{-3}) and for 2+year old shoots (4.14 kJ cm^{-3}). The $dH_{eff}60s.VOL$ mean for tree branches (3.74 kJ cm^{-3}) was slightly lower compared with 1-year and 2+year old shoots.

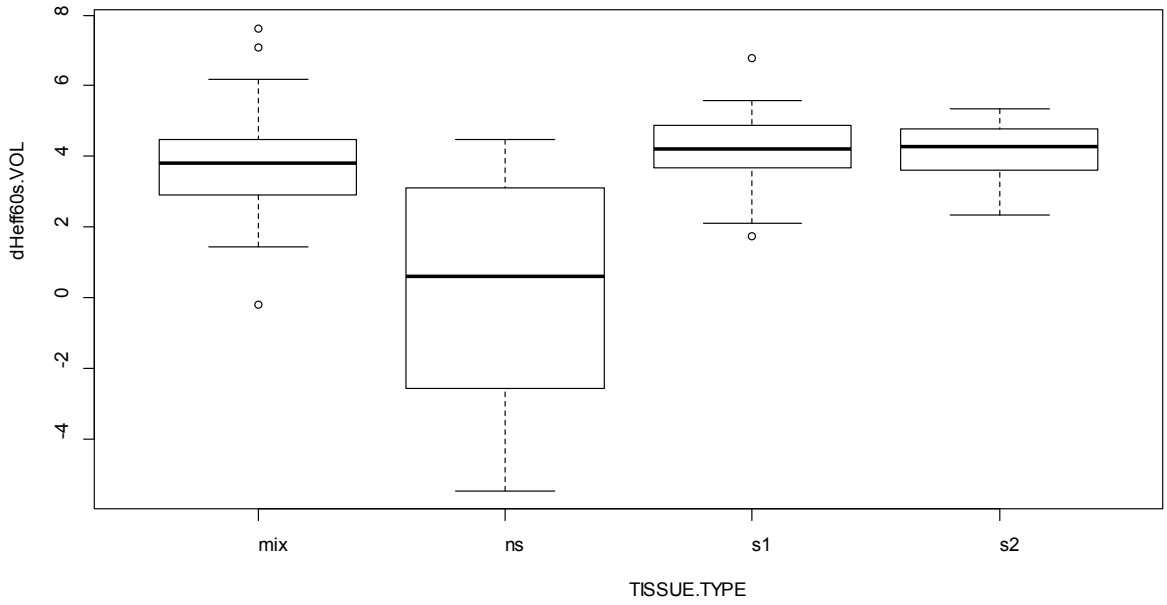

Figure 3.24 Box plot of seasonal variation in volumetric differential effective heat of combustion ($d\boldsymbol{H_{eff}}60s.VOL$) for tree branches (mix, mixed shoot sample), new (ns), 1-year (s1), and 2+year (s2) old shoots. A horizontal line within the box (the interquartile range, IQR) indicates the median. Whiskers are shown at 1.5 IQR. Circles indicate observed values outside of the 1.5 IQR.

Table 3.12 Seasonal minimum, maximum, mean, and standard deviations of volumetric differential effective heat of combustion ($dH_{eff}60s.VOL$)

Fuel sample type	Minimum $dH_{eff}60s.VOL$, kJ cm^{-3}	Maximum $dH_{eff}60s.VOL$, kJ cm^{-3}	Range, kJ cm^{-3}	Mean (standard deviation), kJ cm^{-3}	Sample size
Tree branch (mixed shoot sample)	-0.21	7.62	7.83	3.74 (1.43)	47
New shoots	-5.47	4.47	9.95	0.20 (2.97)	42
1-year shoots	1.72	6.79	5.07	4.10 (1.04)	48
2+year shoots	2.35	5.33	2.98	4.14 (0.72)	48
All ages of shoots	-5.47	6.79	12.26	2.93 (2.54)	138

The pattern of seasonal changes in $dH_{eff}60s.VOL$ (Fig. 3.25) was almost identical to that for $dH_{eff}60s.GRAV$ (Fig. 3.23). It was also, in general, similar to that for *EC.VOL* (Fig. 3.15) and for *DM.VOL* (Fig. 3.9) except during August. The lowest seasonal values of *dHeff60s.VOL* for tree branches were measured through mid-June and the end of July. It showed three seasonal maximums: the very beginning of May (or earlier, for which period no data exists), the beginning of July, and mid-August. The timing of the third seasonal spike in $dH_{eff}60s.VOL$ in mid-August coincides with the second seasonal minimum in *SWC.VOL* (Fig. 3.5).

The $dH_{eff}60s.VOL$ for new shoots (Fig. 3.25) was substantially lower compared with older growth until the beginning of August. It showed a decline from the end of May to mid-June. Due to longer storage time and the increased loss of water content for new shoots (the most sensitive to dehydration) before testing, as discussed earlier in the section 3.1.2, the $dH_{eff}60s.VOL$ for new shoots in May and early June was most likely overestimated.

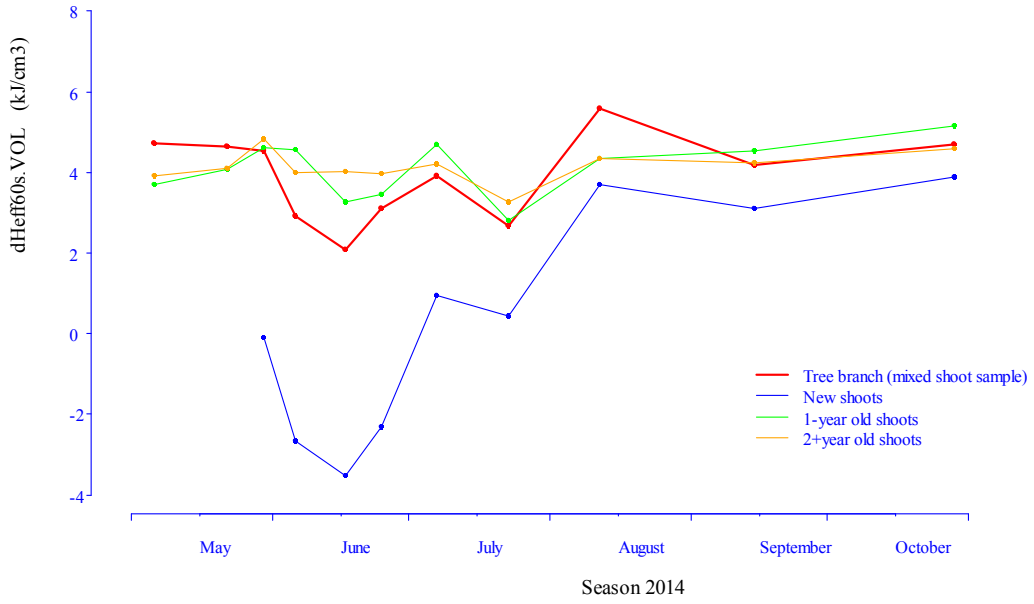

Figure 3.25 Seasonal variation in volumetric differential effective heat of combustion *($dH_{eff}60s.VOL$).* Red, blue, green, and orange lines represent tree branches (mixed shoot sample), new, 1-year, and 2+year old shoots respectively.

3.3 FUEL CONSUMPTION – *M.LOSS*

Fuel consumption, or rate and total amount of fuel mass consumed (mass loss, *M.LOSS)* is the important characteristics of combustion, since it is directly related to rate and total amount of energy released. For new shoots, variation in *M.LOSS* was noticeably higher; values and normality of the data distribution were lower compared with older shoots and tree branches (Fig 3.26). The *M.LOSS* varied from 43.7% to 99.8% with seasonal average of 87.1% for all ages of shoots (Table 3.13). Values of mean *M.LOSS* did not show a statistically significant difference between the fuel ages. Mean *M.LOSS* was measured at 82.7% for new shoots, 85.1% for 2+ year shoots, and 94.1% for 1-year old shoots. *M.LOSS* for tree branches (20.76 kJ g^{-1}) was slightly higher (88.1%) compared with 2+year old shoots.

The maximum *M.LOSS* values for all groups of tissue type were very close to 100% (99.8% for new and 1-year, 99.2% for 2+year old shoots, and 96.6% for tree branches). This cannot be correct, since, for different types of natural fuels (in ascending order: softwood, hardwood, shrub, herbaceous, succulent, and ground) ash content varied from 2.33% to 13.22% (Rivera et al., 2012). Moreover, several data points on mass loss higher than 100% were not used in the analysis (it is impossible to burn more fuel than it was initially). A possible reason for this is load cell calibration and re-zeroing issues due to accumulation of ash and partially burned needles on the surfaces of the methane burner and the load cell, due to the design of a sample holder where wire mesh was used.

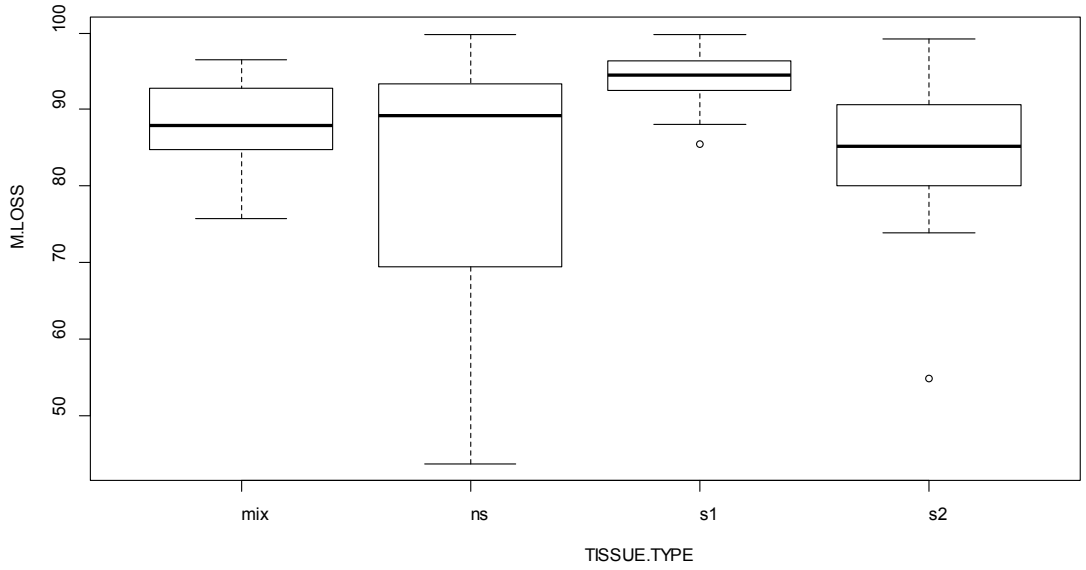

Figure 3.26 Box plots of seasonal variation in fuel sample fresh mass consumption *(M.LOSS,* %) for tree branches (mix, mixed shoot sample), new (ns), 1-year (s1), and 2+year (s2) old shoots. A horizontal line within the box (the interquartile range, IQR) indicates the median. Whiskers are shown at 1.5 IQR. Circles indicate observed values outside of the 1.5 IQR.

Table 3.13 Seasonal minimum, maximum, mean, and standard deviations of fresh mass consumption (mass loss, *M.LOSS,* %)

Fuel sample type	Minimum *M.LOSS,* %	Maximum *M.LOSS,* %	Range, %	Mean (standard deviation), %	Sample size
Tree branch (mixed shoot sample)	75.7	96.6	20.9	88.1 (5.3)	40
New shoots	43.7	99.8	56.1	82.7 (14.8)	28
1-year shoots	85.5	99.8	14.3	94.1 (3.3)	31
2+year shoots	54.9	99.2	44.3	85.1 (8.1)	48
All ages of shoots	43.7	99.8	56.1	87.1(10.5)	107

3.4 INTERCORRELATION MATRIX

3.4.1 Mass loss-based approach

For *all ages of shoots* dataset, flammability expressed traditionally as a proportion of energy release to mass loss (per unit of *mass of fuel consumed,* rather than per unit of the *initial fresh mass)* differential effective heat of combustion, $dH_{eff}60s.ML$, was strongly correlated with *EC.GRAV* (r = 0.90), *DM.GRAV* (r = 0.91), *and SWC.GRAV* (r = -0.90), as shown in Fig. 3.27. These three predictor variables were, however, strongly intercorrelated (r = 0.98, r = -0.96, r = -0.97). The $dH_{eff}60s.ML$ was weakly correlated with calorimetric content *(CC,* gross heat of combustion, r = -0.02).

Data distribution for *all ages of shoots* dataset (Fig. 3.27) show a slight bimodality for dry matter content and energy content since *all ages of shoots* dataset comprises *new shoots, 1-year shoots,* and *2+year old shoots* datasets; new shoots have distinct properties, including dry matter and energy contents (see section 3.1). As was discussed earlier in the section 2.3.1, since the main target of the study was a development of a model that would be able to explain variation in flammability regardless of age class, the *all ages of shoots* data set was mainly used for analysis. The bimodality in data distribution is also present for dry matter and energy contents using gravimetric (Fig. 3.28) and volumetric (Fig. 3.29) approaches.

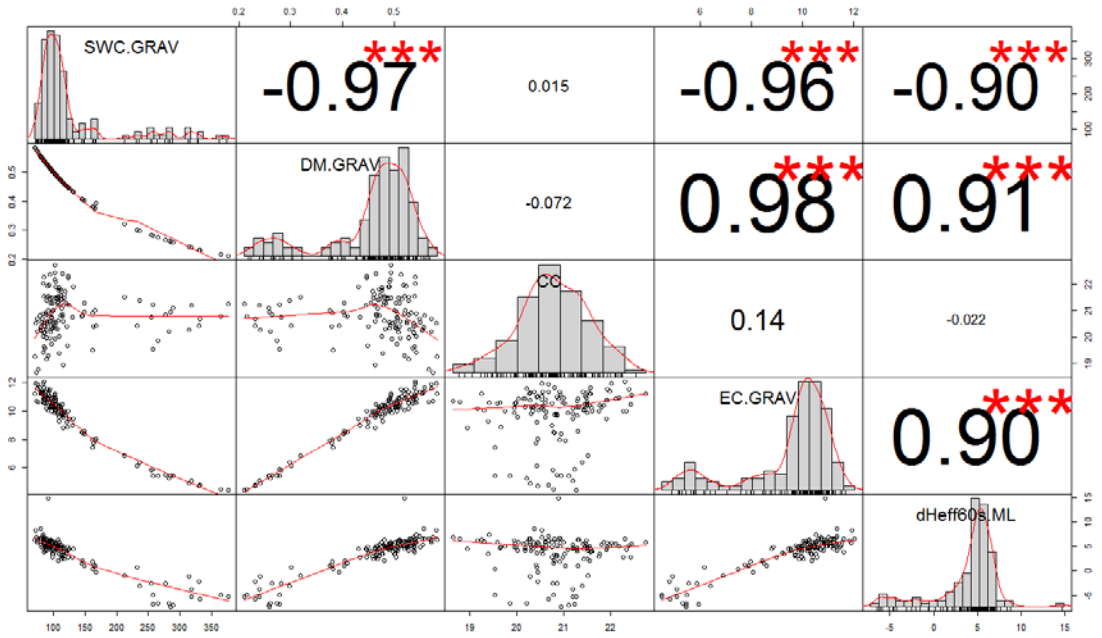

Figure 3.27 Relationship of flammability expressed traditionally as a proportion of energy release to mass loss (per unit of mass of fuel consumed, differential effective heat of combustion, $d\boldsymbol{H}_{\boldsymbol{eff}}60s.ML$, bottom right) with gravimetric predictor variables (from lower-right to top-left): energy content *(EC.GRAV),* calorimetric content *(CC*, gross heat of combustion), dry matter content *(DM.GRAV),* and shoot water content *(SWC.GRAV),* (all ages of shoot data set). The number of asterisks indicate the level of statistical significance: '***' – p-value is less than 0.001; '**' – p-value is less than 0.01; "*' – p-value is less than 0.05.

3.4.2 Gravimetric approach

Gravimetric flammability expressed as a proportion of energy release to the *initial fresh mass* of the fuel sample (per unit of fuel mass, gravimetric differential effective heat of combustion, $dH_{eff}60s.\ GRAV$) showed slightly better relationship with predictor variables (Fig. 3.28) compared with flammability expressed per unit of mass of fuel consumed ($dH_{eff}60s.ML$), (Fig. 3.27). The $dH_{eff}60s.\ GRAV$ was strongly correlated with *EC.GRAV* (r = 0.91), *DM.GRAV* (r = 0.92), and *SWC.GRAV* (r = -0.91). These predictor variables were strongly intercorrelated (r = 0.98, r = -0.96, r = -0.97). The $dH_{eff}60s.\ GRAV$ was weakly correlated with calorimetric content (*CC,* gross heat of combustion, r = 0.01)

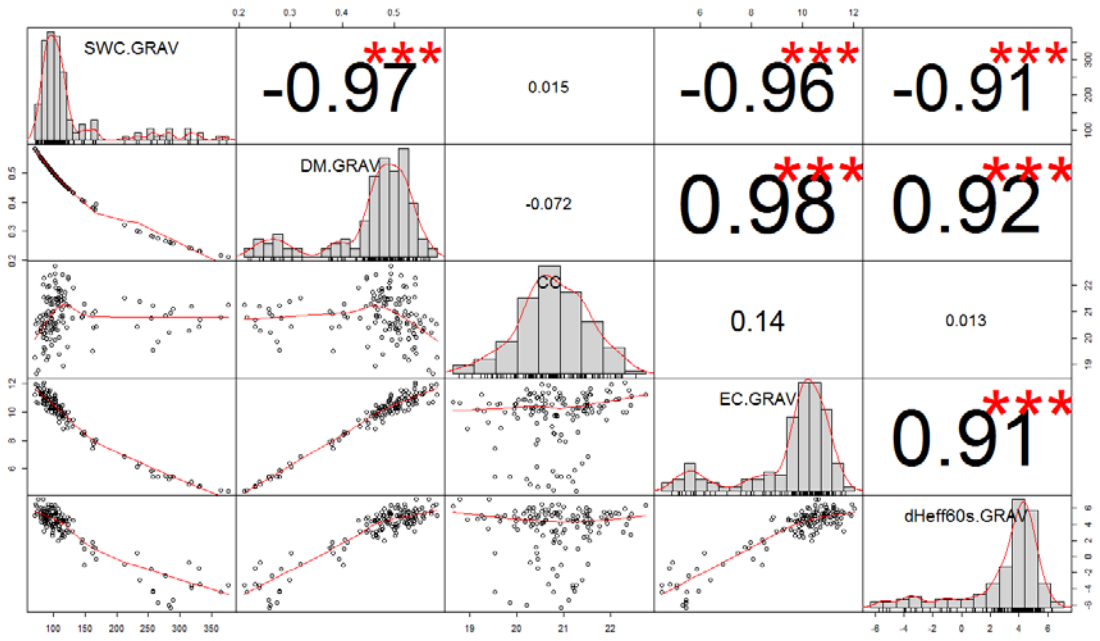

Figure 3.28 Relationship of flammability expressed gravimetrically as a proportion of energy release to the initial mass of the fuel sample (per unit of fuel mass, gravimetric differential effective heat of combustion, $d\boldsymbol{H_{eff}}60s.GRAV$, bottom right) with gravimetric predictor variables (from lower-right to top-left): energy content *(EC.GRAV),* calorimetric content *(CC,* gross heat of combustion), dry matter content *(DM.GRAV),* and shoot water content *(SWC.GRAV),* (all ages of shoot data set). The number of asterisks indicate the level of statistical significance: '***' – p-value is less than 0.001; '**' – p-value is less than 0.01; '*' – p-value is less than 0.05.

3.4.3 Volumetric approach

Volumetric flammability expressed as a proportion of energy release to the *initial volume* of the fresh fuel sample (per unit of fuel volume, volumetric differential effective heat of combustion, $dH_{eff}60s.VOL$) (Fig. 3.29) showed only slightly lower correlation with predictor variables compared with $dH_{eff}60s.ML$ (Fig. 3.27) *and* $dH_{eff}60s.\ GRAV$ (Fig. 3.28). The $dH_{eff}60s.VOL$ was strongly correlated with *EC.VOL* (r = 0.88), *DM.VOL* (r = 0.89), and *SWC.VOL* (r = 0.80). The *EC.VOL* was strongly intercorrelated with *DM.VOL* (r = 0.98) as well as with *SWC.VOL* (r = 0.70), *PWF* (r = -0.89), and *DWF* (r = 0.89). Volumetric flammability did not show a strong relationship with fresh density (r = 0.38), however, it was strongly affected by porosity water-free (r = -0.70) and density water-free (r = 0.70). The latter two variables showed strong collinearity (r = 1.00). Same as $dH_{eff}60s.ML$ (Fig. 3.27) and $dH_{eff}60s.\ GRAV$ (Fig. 3.28), $dH_{eff}60s.VOL$ (Fig. 3.29) was weakly correlated with calorimetric content *(CC,* r = 0.03).

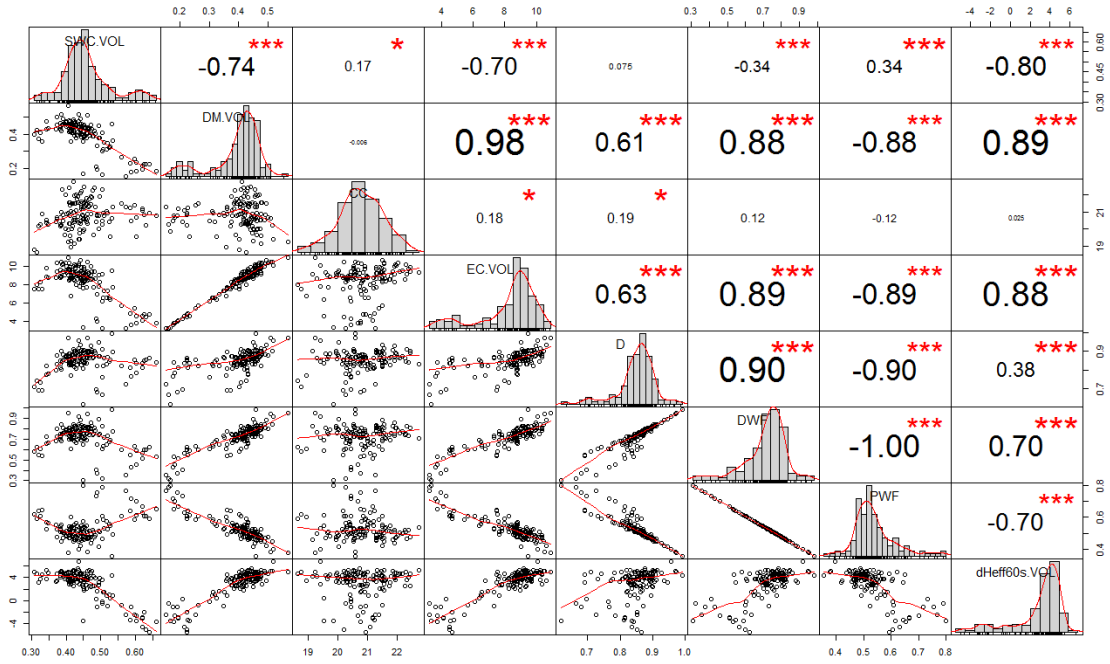

Figure 3.29 Relationship of volumetric flammability expressed as a proportion of energy release to the initial volume of the fuel sample (volumetric differential effective heat of combustion, $dH_{eff}60s.VOL$, bottom right) with predictor variables (from lower-right to top-left): porosity water-free *(PWF),* density water-free *(DWF),* fresh density *(D),* energy content *(EC.VOL),* calorimetric content *(CC,* gross heat of combustion), dry matter content *(DM.VOL), and* shoot water content *(SWC.VOL,* (all ages of shoot data set). The number of asterisks indicate the level of statistical significance: '***' – p-value is less than 0.001; '**' – p-value is less than 0.01; "*' – p-value is less than 0.05.

4 DISCUSSION AND MODEL DEVELOPMENT

The four most important questions in the further development of the physics-based theory of the wildland fire spread are uncertainty with fuel particle heat exchange, definition of the ignition, role and proportion in the ignition heat transfer of radiation and convection, and combustion of live fuel (Finney et al., 2012). While the issues mentioned above related to fuel particle ignition and the dominant way of the ignition heat transfer (radiative or convective) are also partially addressed, the main focus of this study is the uncertainty with the combustion and flammability of live fuel. The flammability was considered in the study as an effect of live fuel burning within the frontal flame on the energy release of the combined system of flames and was tested directly in a flame. The range of variation, factors (including ways of modelling), and seasonal trend of live fuel flammability were investigated.

4.1 FLAMMABILITY AS EFFECT ON FRONTAL FLAME

4.1.1 Characteristics of flammability of live fuel

Flammability can be defined as potential fire behaviour response of the given fuel to the potential (maximum) conditions of the fire environment. Flammability, therefore, can be described by characteristics of (I) *ignition* (ignitibility), (II) *consumption* (consumability), and (III) *energy release* (combustibility and sustainability) (Anderson, 1970; Martin, 1994) of the live fuel in the conditions of the frontal flame of maximal intensity. To allow realistic representation in the tests of these characteristics of the flammability, they were measured in the conditions that are similar to those in the fire front, that is, – directly in the flame. Testing of a plant material directly in the flame has previously been used for assessment flammability of live fuel measured as ignition delay time (Jolly & Butler, 2013). However, for live fuel flammability testing, as energy release response to fire

conditions, it was firstly used in this study (Melnik et al., 2015). While assessment and modelling of live fuel (III) energy release was the main focus of the study, the important results on the investigation of live fuel (I) ignition and (II) consumption are also discussed in the following sub-sections.

4.1.1.1 Ignition

The delayed and inconsistent ignition and subsequent inaccuracy of the results of the traditional oxygen consumption calorimetry tests are caused by the insufficient radiative-only ignition heat transfer and the direction of the ignition heat transfer that is opposite to flame propagation direction (see section 1.4.4 for details). In this study, combined radiative and convective ignition energy transfer, of sufficient intensity and adequate direction that coincided with the direction of flame propagation through the sample, was used since flammability of the live plant material was tested directly in the flame. While radiative heat transfer dominates near the ground and hence is more suitable for testing flammability of dead fuel, in the upper part of the plant canopy (represented mostly by live fuel) the mode of heat transfer is combined radiative and convective. Testing flammability of live fuel directly in the flame therefore eliminates the necessity to solve a theoretical question on the dominance of radiative or convective ignition heat transfer with flame propagation through upper (live) part of the vegetative canopy, which is still under investigation (Albini, 1985; Anderson, 1969; Van Wagner, 1977; Beer, 1991; Frankman et al., 2013). Mitigation of the variability and inconsistency in the live fuel ignition caused by variability in the spatial structure of a tree branch was provided by using of the concept of the thin fuel sample (Melnik et al., 2015) as described earlier in this study (Section 2.2.1, Fig. 2.5 and Fig. 2.6). All these provided heating rates of approximately 20-30 °C sec^{-1} resulting in consistent ignition. Each fuel sample ignited at 5-20 sec time and showed approximately 45 sec flaming combustion time (Paskaluk, Ackerman, &Melnik, 2015). Similar characteristics of ignition were reported for the flame-front (Frankman et al., 2013; Wotton et al., 2012). The effects of the characteristics of live fuel (water, dry matter contents, chemical composition, density, and porosity) on the ignition delay time, however, require of separate detailed investigation and were not considered in this study.

4.1.1.2 Fuel consumption

The use high-intensity ignition heat transfer (the nominal energy release of the calibrated methane burner of 500 kW m^{-2}) of the correct direction and the application of the thin fuel sample concept resulted in not only fast and consistent ignition, but also in almost complete consumption of the fuel samples that consisted of roundwood (twigs) thinner than 1 cm in diameter with the attached foliage (shoots). According to Stocks et al., (2004), the same live plant material was consumed by frontal flame; average time of its interaction with the frontal flame was reported approximately 60 sec (Frankman et al., 2013; Wotton et al., 2012). The average proportion of fresh shoots (twigs 1-9 mm in diameter with attached foliage) consumed during 60 seconds of combustion in the tests was 87.1% for all ages of shoots (Table 3.13). Though the heat flux to the samples was not measured, almost complete consumption of the tested fresh shoots suggests that the intensity, direction, and type of ignition heat transfer in the tests were close to those in the flame-front with measured in field conditions peak radiative and convective ignition heat flux of 220-340 kW m^{-2} (Frankman et al., 2013).

4.1.1.3 Energy release

The use of the proposed test method provided not only more realistic representation of the characteristics of the ignition and consumption of the live fuel, it also allowed for evaluation of energy release proportional to fresh mass or volume, instead of mass loss (mass of fuel consumed). Moreover, the flammability of live fuel was defined and measured not as its energy content, but as an effect of the burning live fuel on the energy release of the frontal flame, hence – on the frontal flame propagation scale. These two stated above subjects require more detailed consideration and are discussed in the following sections.

4.1.2 Energy release per unit of fresh mass or volume instead of mass loss

Most fire models still use theoretical (maximal) heat of combustion of oven-dry fuel in the pure oxygen environment (gross heat of combustion, H_{gross}) that is hence substantially higher than energy release in the oxygen-deficient environment of the flame-front. The oxygen consumption calorimetry methods more realistically represent combustion since plant material is tested in the atmospheric air environment and incomplete combustion is partially accounted. The flammability of fresh plant material is evaluated as effective heat of combustion *(H_{eff})* and measured as a proportion of total energy release to mass loss (energy release per unit of mass of fuel consumed) (Babrauskas, 2006; Madrigal et al., 2011). In these studies, the energy release was normalized to mass loss rather than to initial mass or volume of the fuel sample due to the partial rather than complete consumption of fresh tested samples. This presents three problems. Firstly, due to high water content that is typical for live fuel, loss of mass in the initial phase of combustion indicates mostly mass of water evaporated rather than mass of dry organic matter consumed. Secondly, as measured by this approach, energy release represents only the part of the fuel that ignites most easily (typically foliage) showing partial (selective) consumption. Hence the energy release of foliage and twigs burning together in real conditions is not represented and remains unknown. Finally, this theoretically more precise approach, in which energy release depends on mass consumed, does not indicate or predict the energy release of the unit of mass, or volume, of the given plant material. Depending on the proportion of the consumption, the result can be very different for these two approaches (energy release per unit of mass loss versus energy release per unit of the initial mass or volume of the sample). If, for example, initial mass of the fuel sample was 1.0 kg and consumption of 50% of its fresh mass (0.5 kg) produced 10.0 MJ of energy, mass loss approach shows the energy release per unit of fuel consumed of 20.0 MJ kg^{-1} (10.0 MJ/ 0.5 kg). At the same time, actual energy release per unit of the initial mass of the fuel sample was only 10.0 MJ kg^{-1} (10.0 MJ/ 1.0 kg). The main issue with use of the mass loss-based approach for evaluation of the energy release is that it requires separate quite complex modelling of fuel consumption.

Due to the almost complete consumption of the fuel samples in the tests, the assessment of flammability as proportion to fresh mass or to volume was possible instead of proportion to mass loss. Mass loss, or mass of fuel consumed, is directly related to the energy release from the burning fuel (Anderson, 1970) and is commonly used in oxygen consumption calorimetry methods where the effective heat of combustion is expressed as a proportion of energy release to mass loss (per unit of mass of fuel consumed) (Babrauskas, 2006). However, according to the results of this study, where flammability was evaluated as an effect on the intensity of the frontal flame rather than the energy release of the fuel element burning separately, using the mass loss approach did not improve the results.

Gravimetric differential effective heat of combustion *($dH_{eff}60s.\ GRAV$)* expressed as a proportion of energy release to the initial mass of the fuel sample (per unit of fuel mass), showed even slightly better relationship with predictor variables (water, dry matter, and energy contents, Fig. 3.28, Section 3.4) compared with flammability expressed traditionally as a proportion of energy release to mass loss *($dH_{eff}60s.ML$),* (Fig. 3.27). Volumetric differential effective heat of combustion *($dH_{eff}60s.VOL$)* expressed as a proportion of energy release to the initial volume of the fuel sample (per unit of fuel volume) (Fig. 3.29) showed only slightly lower correlation with predictor variables compared with mass loss-based $dH_{eff}60s.ML$ (Fig. 3.27). Due to these findings and also considering that the proposed gravimetric and volumetric approaches allow for evaluation of energy release knowing the initial mass or volume of the fuel (and hence allows for evaluation of the potential energy release in the potentially maximal conditions of the fire environment without evaluation of fuel consumption), only these two approaches were used in the flammability modelling. The mass loss-based approach was excluded from the analysis.

The possibility of measuring energy release as a proportion to fresh mass or volume using the proposed method suggests that assessment and modelling of the *potential* (maximal) heat release contribution of live or dead fuel into the frontal flame can be performed when the amount of these fuels in the vegetative canopy is known without consideration or modelling of fuel consumption. A potential energy release in the extreme weather conditions therefore can be evaluated on the scale of the forest stand and used as a

numerical measure of its flammability allowing for development of the energy release- and stand characteristics-based fuel classification (see Further Research and Applications sections 4.6.3 – 4.6.5 for more details).

4.1.3 Flammability as effect on the frontal flame energy release

Testing of flammability directly in the flame allowed for evaluation of the flammability of live fuel on the frontal flame propagation scale as an energy source (generation) component of the energy balance of the frontal flame. The two-way interaction of the live fuel flame with the frontal flame and for the resulting increased losses for both flames due to incomplete combustion in the flames interaction zone were accounted for since flammability was defined and measured as the change in energy release to the frontal flame in the result of this interaction. The change in energy release in the frontal flame was evaluated as the difference in the energy release of the incoming methane intensity which resulted from the interaction with the burning live fuel sample. The change in energy release in the frontal flame was not always positive. The test results confirmed the existence and, in some cases, significance of the negative effect of live fuel on the energy release of the frontal flame caused by incomplete combustion for both flames in the flames interaction zone. In other words, the addition of live fuel into the flame, depending on the fuel's properties, can positively or negatively impact the energy release from the methane flame. Since flammability of live fuel is defined in this study as the change in the energy release of the frontal flame, it will be either positive or negative depending on the resulting change in the intensity of the flame.

4.1.4 Negative flammability?

The existing oxygen consumption methods consider combustion of live fuel on a separate fuel element scale. Current methods do not represent well the interaction of the flame of the recently ignited element with the system of the flames of other elements already burning and composing the frontal flame. The increased losses in this interaction of flames are not captured. Measured traditionally, flammability is always positive because it represents the energy release of the burning fuel sample tested separately, and energy release cannot be negative. Previous studies on the flammability of live fuel and their applications in fire modelling are based on the assumption that change in energy release (increase only) to the frontal flame in the result of consumption of each next ignited fuel element equals to the energy releases of this element if measured separately. Considering flame propagation scale, it may be incorrect due to, in some cases, either more substantial (in the case of live fuel) reduction in energy release with incomplete combustion in the flames interaction zone (live fuel element's flame and frontal flame) or growth in energy release with higher temperatures for the interacting flames under sufficient oxygen supply. For the flame of the live fuel element burning within the frontal flame, losses may be higher than measured in the traditional tests due to lower oxygen concentration and higher water vapor concentration in the flames interaction zone. Besides, for the frontal flame, reduction in energy release with incomplete combustion caused by the high water content of live fuel and oxygen deficiency in the flames interaction zone may be substantial as well. Therefore, theoretically, the intensity of the frontal flame can drop due to interaction with live fuel of high water content. This was confirmed by the results.

In the beginning of the vegetative season the flammability of new shoots and a whole tree branch of white spruce, measured using the method proposed in this study and expressed as gravimetric and volumetric differential effective heat of combustion ($dH_{eff}60s.GRAV$ and $dH_{eff}60s.VOL$) showed negative values of flammability (Table 3.11and Fig. 3.23; Table 3.12 and Fig. 3.25). In this study, flammability represents a change in energy release to the frontal flame caused by interaction with flame of live fuel sample during an average flame-front residence time of 60 seconds (Melnik et al., 2015; Paskaluk, Ackerman,

&Melnik, 2015). The flammability of the live fuel element is negative if the resulting intensity of the frontal flame after passing live fuel element flame is lower than before interaction with the live fuel element. *Therefore, as measured in the tests, negative values of flammability mean a substantial reduction in the energy release of the frontal flame, as a result of interaction of the frontal flame with the flame of the burning live fuel in the flames interaction zone during an average flame-front residence time of 60 seconds.*

Measured in the tests the substantial negative values of the flammability of new shoots (or their energy release contribution) is an experimental confirmation of the substantial reduction in energy release due incomplete combustion in the interaction zone of the flame of the burning live fuel and the frontal flame. This empirically proves an assumption of the study that the high water content of live fuel has a substantial negative effect on the resulting intensity of the frontal flame. The negative effect on the energy release and intensity of the frontal flame was substantial. For all ages of shoot, gravimetric $dH_{eff}60s.GRAV$ varied from negative 6.33 kJ g^{-1} to positive 7.10 kJ g^{-1}, (Table 3.11), while volumetric $dH_{eff}60s.VOL$ varied from negative 5.47 kJ cm^{-3} to positive 6.79 kJ cm^{-3}, (Table 3.12). New shoots in the beginning of the season actually suppressed energy release of the frontal flame. This effect is illustrated on the top image in Fig 4.1. (top image). In the flames' interaction zone above the fuel sample, the outgoing flame (represented by mixture of gases of the methane flame and of the flame of the burning live fuel flame) is practically absent due to high concentrations of water vapor and due to oxygen deficiency for both of the flames. Combustion occurs, however, outside of the flames' interaction zone due to higher oxygen supply (above-right of the fuel sample). With a positive effect on the energy release of the incoming flame (1-year shoots), the resulting intensity of the outgoing flame (methane flame plus sample's flame) in the flames interaction zone above the sample (bottom image in Fig 4.1.) is noticeably higher compared with new shoots.

Figure 4.1 Live fuel burning within the methane flame at several seconds after ignition: new shoots (top image) and 1-year shoots (bottom image)

4.2 RANGE OF VARIATION IN LIVE FUEL FLAMMABILITY

4.2.1 Upper limit of flammability

The potential theoretical limit of the energy release of live fuel (calorimetric content, *CC)* was measured using oxygen bomb calorimetry (gross heat of combustion) from 18 kJ g^{-1} to 23 kJ g^{-1} for foliage and twigs of hardwood species (Rivera et al., 2012). This agrees with the results of this study, where *CC* ranged from 18.64 kJ g^{-1} to 22.75 kJ g^{-1} (Table 3.5) for all ages of shoots of white spruce. Considering that the maximum proportion of dry matter in live fuel was 54-58% of fresh mass (Table 3.3), the upper limit of the gravimetric energy content (*EC.GRAV*) should be expected to be not higher than 54-58% of upper limit of *CC* (22.75 kJ g^{-1}). This corresponds to the results: maximum *EC.GRAV* was measured 10.88 kJ g^{-1} for new shoots, 11.51 kJ g^{-1} for 1-year shoots, 12.06 kJ g^{-1} for 2+year shoots, and 11.93 kJ g^{-1} for tree branches (Table 3.6). Due to incomplete combustion, the energy release contribution of live fuel to the frontal flame energy release should be lower than these numbers. This was confirmed by the results: maximum $dH_{eff}60s.GRAV$ was measured 6.48 kJ g^{-1} for new shoots, 7.10 kJ g^{-1} for 1-year shoots, 6.49 kJ g^{-1} for 2+year shoots, and 10.63 kJ g^{-1} for tree branches (Table 3.11).

Considering that the maximum proportion of dry matter in live fuel was 41-57% depending on tissue type (Table 3.4), it is reasonable to expect maximum volumetric energy content *(EC.VOL)* to be not higher than 41-57% of maximum *CC* (22.75 kJ g^{-1}) since *EC.VOL,* by the definition, is *CC* per unit of volume). According to the results, maximum *EC.VOL* was measured 8.64 kJ cm^{-3} for new shoots, 10.24 kJ cm^{-3} for 1-year shoots, 10.92 kJ cm^{-3} for 2+year shoots, and 10.75 kJ cm^{-3} for tree branches (Table 3.7). Due to incomplete combustion and the associated reduction in energy release in the flames interaction zone, the energy release contribution of live fuel to the frontal flame energy release should be lower than these numbers. This was also confirmed by the test results: maximum $dH_{eff}60s.VOL$ was measured 4.47 kJ cm^{-3} for new shoots, 6.79 kJ cm^{-3} for 1-

year shoots, 5.33 kJ cm^{-3} for 2+year shoots, and 7.62 kJ cm^{-3} for tree branches (Table 3.12).

4.2.2 Range of flammability variation

The variation in flammability, defined as the energy release contribution to intensity of the frontal flame, was substantially larger than when measured using the traditional oxygen bomb calorimetry techniques and compared with that is assumed by the current fire behaviour models. Since maximum calorimetric content *(CC)* for live fuel (foliage and twigs of hardwoods) was reported 23 kJ g^{-1} (Rivera et al., 2012), a theoretical range of energy release variation is 23 kJ g^{-1} (from 0 to 23 kJ g^{-1}). The energy release of live fuel in that study was reported to vary from 18 to 23 kJ g^{-1}. That is only 22% of the theoretically possible variation (23 kJ g^{-1}). The variation in energy release for the frontal flame as measured in this study gravimetrically, $dH_{eff}60s.GRAV$ was substantially larger: 13.43 kJ g^{-1} for all ages of shoot (from negative 6.33 to positive 7.10), (Table 3.11), showing 58% of the theoretically possible range. Measured volumetrically (though not fully comparable with gravimetric *CC),* the $dH_{eff}60s.VOL$ variation range was 12.26 kJ cm^{-3} (from negative 5.47 to positive 6.79), (Table 3.12) showing 53% of the theoretically possible range. These results suggest that the actual range of variation in the flammability of live fuel is 2-3 times larger than is measured using the existing test techniques and hence is underestimated by the current fire modelling systems.

In fire modelling, the substantial seasonal and natural disturbances-caused changes in the ability of live fuel to burn and release energy that drives wildfire initiation, growth, propagation, and behaviour are considered as minor secondary changes or constant. In the FBP CFFDRS System for instance, the intensity of the simultaneous combustion of live and dead fuel is calculated using the constant averaged net heat of combustion (gross heat of combustion measured by oxygen bomb calorimetry minus energy absorption for water evaporation) of dry dead fuel alone at 18 kJ g^{-1}. The accuracy of the fire models could be substantially higher if more realistic data on the range of variation of live fuel

flammability were considered. Moreover, changes in live fuel flammability are accounted for regardless of the age of live plant material consumed and the proportions of this plant material in the composition of tree branches and the plant canopy.

4.2.3 Variation in flammability depending on shoots age

The gravimetric and volumetric flammability of new growth (new shoots) was substantially lower compared with old growth due to high negative values in the beginning of the season (Fig 3.23 and 3.25). For new shoots, gravimetric flammability *($dH_{eff}60s.GRAV$)* varied from -6.33 kJ g^{-1} to 6.48 kJ g^{-1} with a seasonal mean 0.23 kJ g^{-1}. For 1-year shoots $dH_{eff}60s.GRAV$ varied from 1.98 kJ g^{-1} to 7.10 kJ g^{-1} with a seasonal mean 4.75 kJ g^{-1}; for 2+year shoots $dH_{eff}60s.GRAV$ varied from 2.61 kJ g^{-1} to 6.49 kJ g^{-1} with a seasonal mean 4.76 kJ g^{-1} (Table 3.11). Volumetric flammability *($dH_{eff}60s.VOL$)* of new shoots varied from -5.47 kJ cm^{-3} to 4.47 kJ cm^{-3} with a seasonal mean 0.20 kJ cm^{-3}. For 1-year shoots $dH_{eff}60s.VOL$ varied from 1.72 kJ cm^{-3} to 6.79 kJ cm^{-3} with a seasonal mean 4.10 kJ cm^{-3}; for 2+year shoots $dH_{eff}60s.VOL$ varied from 2.35 kJ cm^{-3} to 5.33 kJ cm^{-3} with a seasonal mean 4.14 kJ cm^{-3} (Table 3.12). The test results showed minor differences in the flammability of old growth (1-year compared with 2+year old shoots). For 1-year and 2+year old shoots respectively, the seasonal average was 4.75 kJ g^{-1} versus 4.76 kJ g^{-1} measured as $dH_{eff}60s.GRAV$ and 4.10 kJ cm^{-3} versus 4.14 kJ cm^{-3} measured as $dH_{eff}60s.VOL$ (Table 3.11 and 3.12). The substantial difference in flammability of new shoots compared with older shoots and more substantial seasonal variation in the flammability of new shoots suggests their essential importance in the determining flammability of live fuel and the resulting fire growth, propagation, and behaviour. The flammability of new shoots should be evaluated separately and paid the most of the attention in live flammability assessment and modelling.

4.3 FACTORS AND MODELLING OF FLAMMABILITY

The factors that determine the flammability of live fuel (predictors) are biophysical and chemical properties such as water content, dry matter content, chemical composition, calorimetric content, energy content, density and porosity. The seasonal trend of live fuel flammability for white spruce was previously established by field sampling and laboratory testing and will be compared with the modelled values. The ways and results of flammability modelling using single and then multivariate predictors are discussed in the following sections.

4.3.1 Factors of live fuel flammability variation (single-variable models)

4.3.1.1 Water content

Water content is one the most important variables strongly negatively affecting the flammability of live fuel Smith, 2005; Van Wagner, 1963; Babrauskas, 2006). The fire suppression properties of water are obvious even without experimental studies, since it is widely used in fire management to impair combustion. Water content represents the amount of suppressing reagent in the composition of live plant tissue: the higher it is, the lower is the ability to burn, or flammability. This was confirmed by the test results. For all ages of shoots (new, 1-year, and 2+year old) plotted together, the gravimetric flammability of live fuel, defined as the energy release contribution of burning fuel to the intensity of the frontal flame and experimentally measured as a differential effective heat of combustion ($dH_{eff}60s.GRAV$), was strongly negatively related to water content (Fig. 4.2). The $dH_{eff}60s.GRAV$ varied from positive 7.10 $kJ\ g^{-1}$ to negative 6.33 $kJ\ g^{-1}$ (Table 3.11) with increase in shoot water content *(SWC.GRAV)* from 71.4% to 376.8% (Table 3.1). For new shoots with water content higher than 210% (dry weight basis) flammability was negative. Flammability of new shoots was noticeably lower than flammability of 1-year and 2+year old shoots.

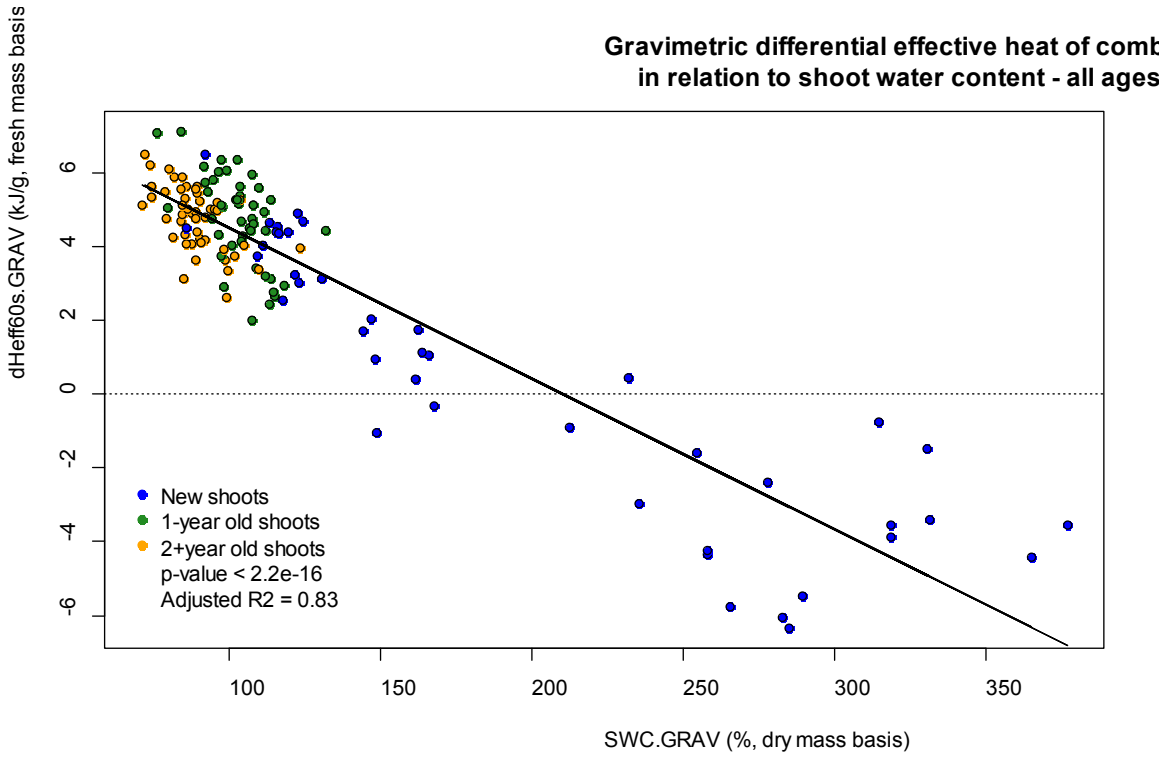

Figure 4.2 Gravimetric flammability of white spruce measured as differential effective heat of combustion *($dH_{eff}60s.GRAV$)* in relation to gravimetric shoot water content *(SWC.GRAV)* for all ages of shoots. Blue, green, and orange colors represent new, 1-year, and 2+year old shoots respectively.

The volumetric flammability of shoots ($dH_{eff}60s.VOL$) showed a negative relationship with volumetric shoot water content *(SWC.VOL)* for all ages of shoots (Fig. 4.3). The $dH_{eff}60s.VOL$ varied from positive 6.79 kJ cm^{-3} to negative 5.47 kJ cm^{-3} (Table 3.12) with increase in *SWC.VOL* from 0.31 g cm^{-3} to 0.66 g cm^{-3} (Table 3.2). For new shoots with water content higher than 0.55 g cm^{-3} flammability was negative. Flammability of new shoots was noticeably lower than flammability 1-year and 2+yearold shoots.

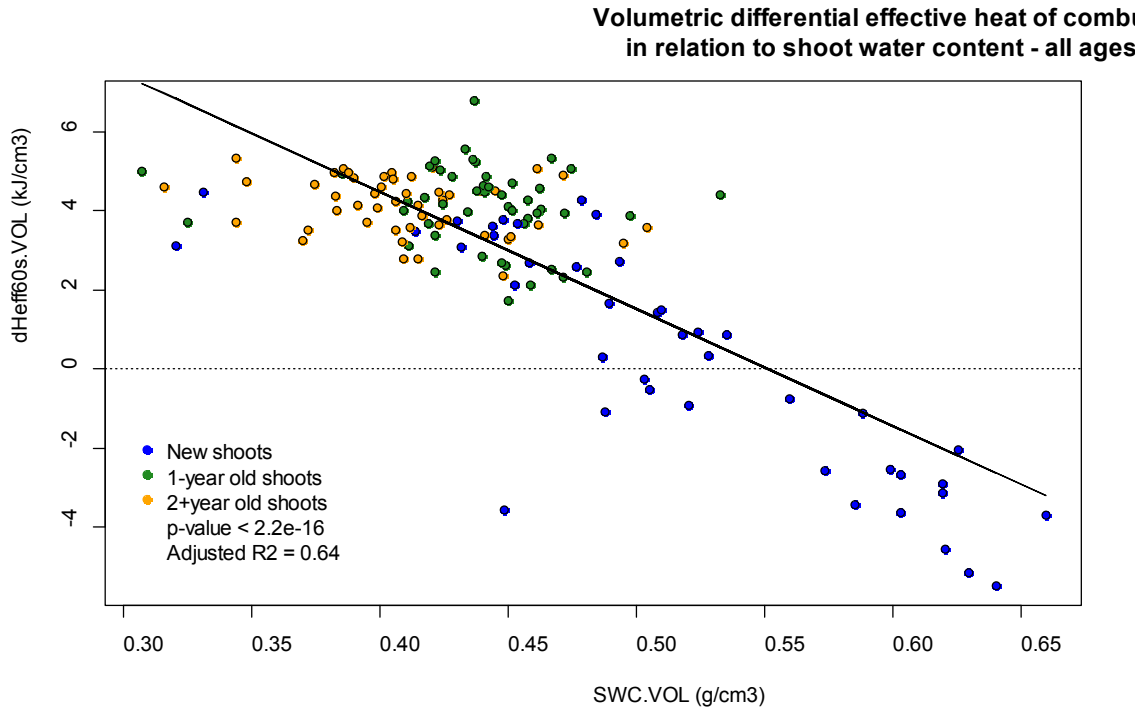

Figure 4.3 Volumetric flammability of shoots of white spruce measured as differential effective heat of combustion *(dH_{eff} 60s.VOL)* in relation to volumetric shoot water content *(SWC.VOL)* for all ages of shoots dataset. Blue, green, and orange colors represent new, 1-year, and 2+year old shoots respectively.

The *SWC.VOL* explained, however, only 64 % of variation in flammability showing strong linear relationship with flammability only for its range from 0.45 g cm^{-3} and higher (Fig. 4.3). The relationship was weak for lower values of water content suggesting the importance of variables other than water content in explaining the flammability. Volumetric water content, if expressed in the same way as gravimetric (proportion of water content to dry matter content) gave practically the same statistical quality in explaining variation in flammability (adjusted $R^2 = 0.82$) (Fig. 4.4) as gravimetric water content (Fig. 4.2). This indicates on the importance of dry matter content in the explaining the flammability of live fuel: "… if there is no solid, there is no fuel, there is no fire…"

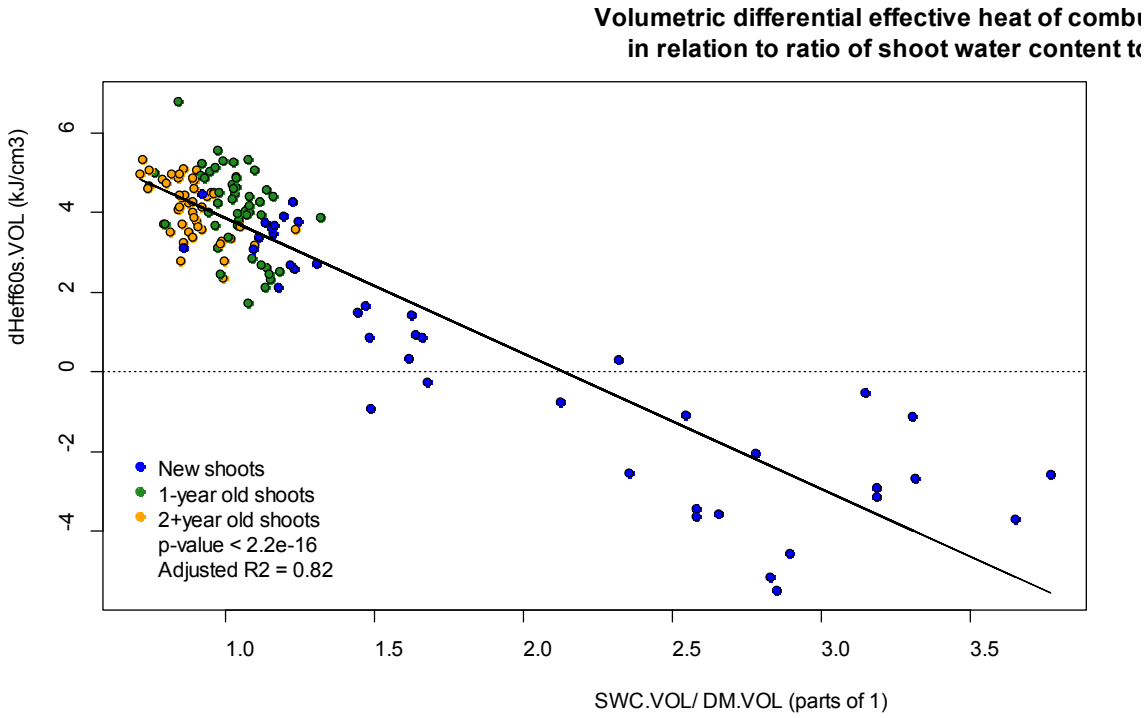

Figure 4.4 Volumetric flammability of shoots of white spruce measured as differential effective heat of combustion *($dH_{eff}60s.VOL$)* in relation to ratio of volumetric shoot water content *(SWC.VOL)* and dry matter content *(DM.VOL)* for all ages of shoots dataset. Blue, green, and orange colors represent new, 1-year, and 2+year old shoots respectively.

Gravimetric and volumetric flammability of tree branches (mixed shoot sample) was marginally explained by water content (adjusted $R^2 = 0.51$ in Fig. 4.5 and 4.6). The water content of shoots alone was insufficient to explain the range of variation in flammability for 1-year and 2-year old shoots measured gravimetrically and volumetrically (adjusted R^2 of 0.30, 0.31, 0.01, and 0.07 respectively, in Fig. 4.5 and 4.6). Seasonal and drought-related changes in flammability cannot be explained only by variation in water content since physiological changes in photosynthetically-active 1-year and 2+year old shoots cause substantial changes in dry matter content, chemical composition, and energy content. This suggests the importance of these characteristics of plant tissue in the explanation of the flammability of live fuel.

For new shoots, substantially better linear relationship of flammability with water content expressed gravimetrically (adjusted R^2 of 0.77 in Fig. 4.5, top-right graph) seemingly indicates the prevalence of changes in water content compared with other factors.

However, similarly to *all ages of shoot* dataset (Fig. 4.3), relationship of the flammability with water content for *new shoots* data set expressed volumetrically (adjusted R^2 of 0.70 in Fig. 4.6, top-right graph) showed strong linear relationship with flammability only for its range from 0.45 g cm^{-3} and higher. The relationship was weak for lower values of water content suggesting the importance of variables other than water content (dry matter content, chemical composition, and energy content, as was discussed above for 1-year and 2+year old shoots) in the explaining of the flammability of new shoots. The higher ability of the gravimetric approach in predicting flammability using water content compared with volumetric can be explained by fixed inclusion in the gravimetric water content metric of the another variable – dry matter content (by the definition, gravimetric water content is ratio of water mass to dry matter mass). This advantage in the flammability prediction using single-variable models may indicate less flexibility (sensitivity) of gravimetric water content when using multivariable models.

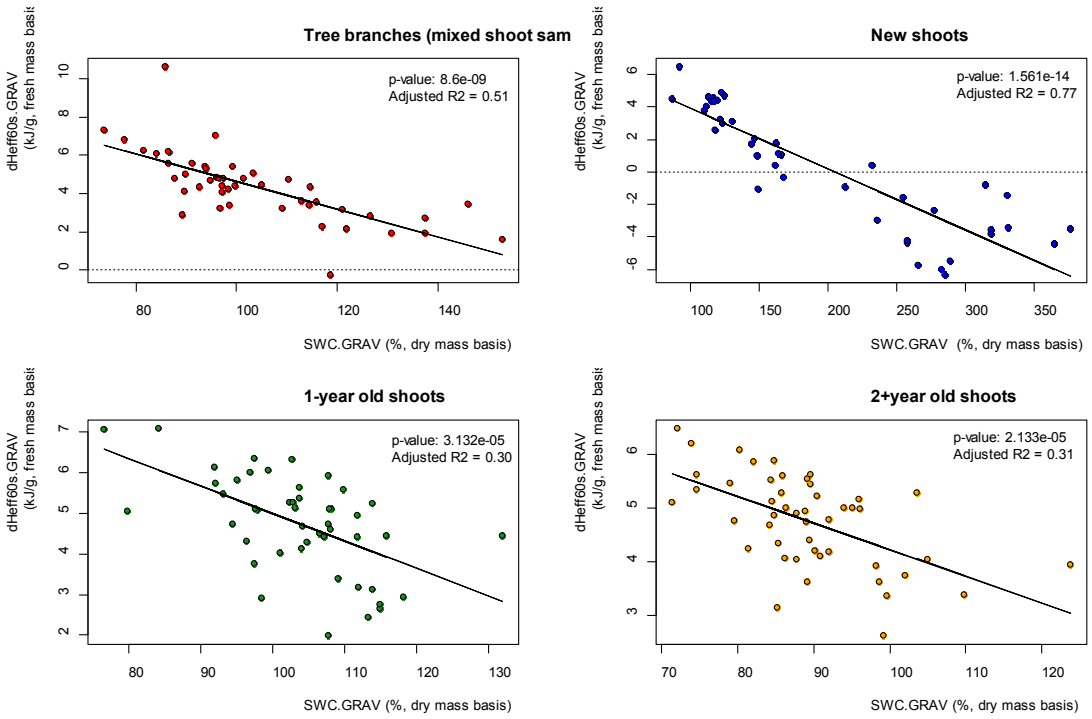

Figure 4.5 Gravimetric flammability *($dH_{eff}60s.GRAV$)* in relation to shoot water content *(SWC.GRAV)* for tree branches and all ages of shoots of white spruce plotted separately. Red, blue, green, and orange colors represent tree branches, new, 1-year, and 2+year old shoots respectively.

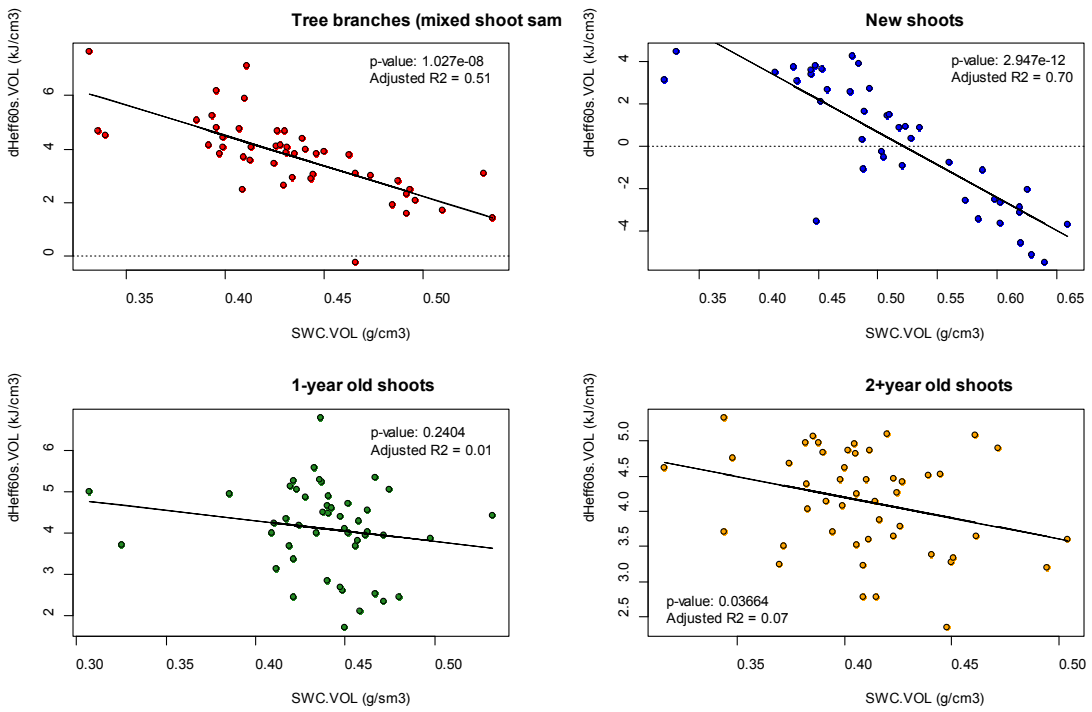

Figure 4.6 Volumetric flammability *($dH_{eff}60s.VOL$)* in relation to shoot water content *(SWC.VOL)* for tree branches and all ages of shoots of white spruce plotted separately. Red, blue, green, and orange colors represent tree branches, new, 1-year, and 2+year old shoots respectively.

4.3.1.2 Dry matter content and energy content

For the gravimetric and volumetric approach, flammability was strongly negatively affected by water content and was directly related to dry matter content, energy content, and ratio of energy content to water content. (Fig 4.7). They represent the amount of combustible organic substance in the fuel, the energy it contains, and the proportion of the energy to water content respectively. The higher the value of those variables, the higher is the potential fire behaviour response of live fuel. Previous studies showed a similar positive relation between flammability and density, dry matter content, energy content, and chemical composition (Jolly et al., 2014; Dickinson & Kirkpatrick, 1985; Jolly et al., 2012)

In general, the gravimetric approach explained flammability slightly better than volumetric. For the gravimetric approach, dry matter content, energy content, and ratio of

energy content of water content did not show noticeably better results in the explanation of the flammability compared with water content: 84%, 83%, and 75% versus 83%, respectively (Fig 4.7, left column of graphs). In contrast, volumetric dry matter content, energy content, and their ratio showed noticeably higher compared with volumetric water content ability in the explanation of the flammability: 79%, 78%, and 79% versus 64%, respectively (Fig 4.7, right column of graphs).

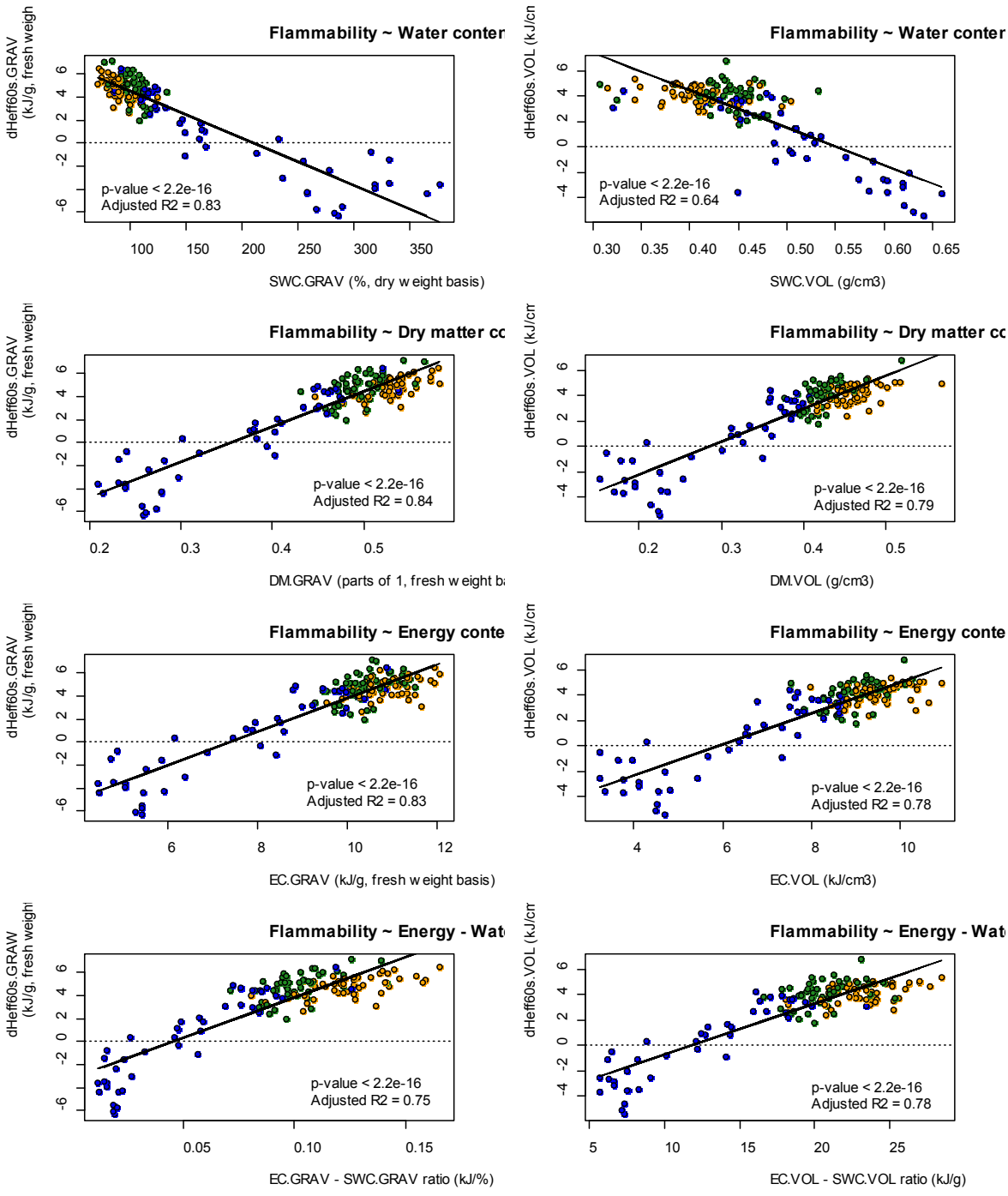

Figure 4.7 Gravimetric *($dH_{eff}60s.GRAW$)* and volumetric *($dH_{eff}60s.VOL$)* flammability in relation to water content, dry matter content, energy content, and energy content to water content ratio for all ages of shoots of white spruce. Blue, green, and orange colors represent new, 1-year, and 2+year old shoots respectively.

4.3.1.3 Additional volumetric variables affecting flammability

In order to improve prediction of flammability using the volumetric approach, variables that are solely volumetric, such as density *(D),* density water-free *(DWF),* and porosity water-free *(PWF),* were also used in the analysis. Density is an important factor affecting flammability (Jolly et al., 2014). Density alone, however, showed a weak positive relationship with $dH_{eff}60s.VOL$ explaining only14% of flammability variation (Fig 4.8). According to the results, variation in flammability was better explained by the characteristic of live plant tissue proposed in this study, such as density water-free (adjusted $R^2 = 0.48$ in Fig 4.9) and porosity water-free (adjusted $R^2 = 0.48$ in Fig 4.10) rather than by the traditional fresh density.

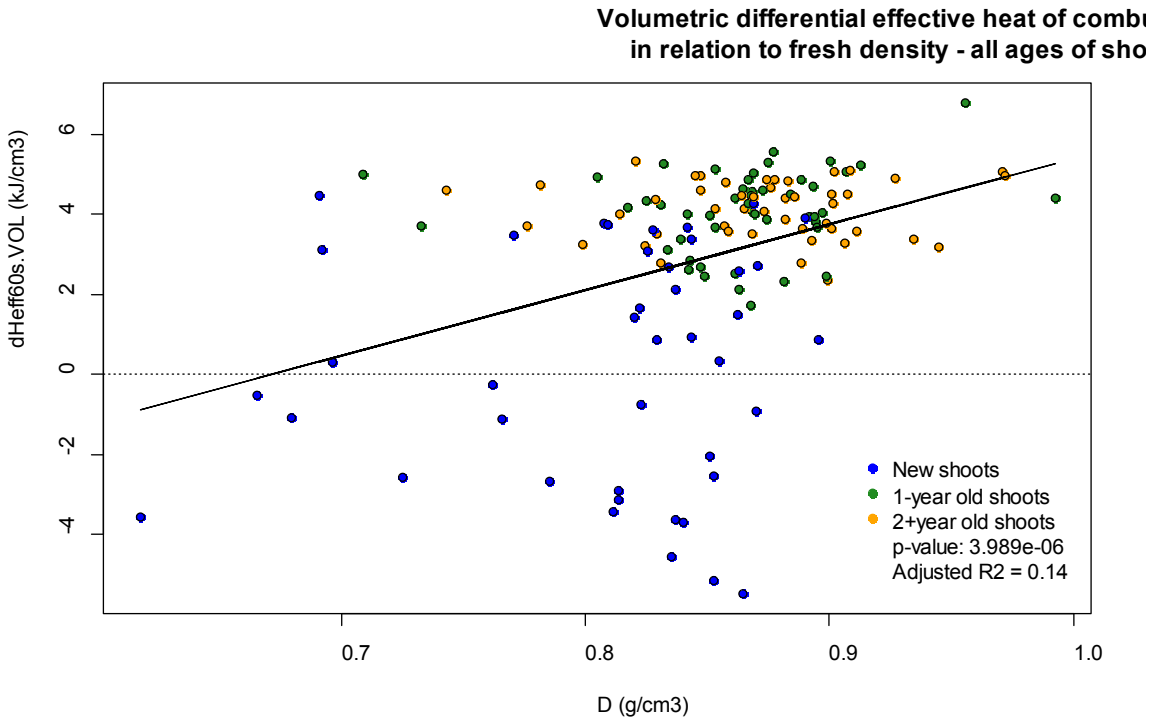

Figure 4.8 Relationship between volumetric flammability *($dH_{eff}60s.VOL$)* and fresh density *(D).* Blue, green, and orange colors represent new, 1-year, and 2+year old shoots respectively.

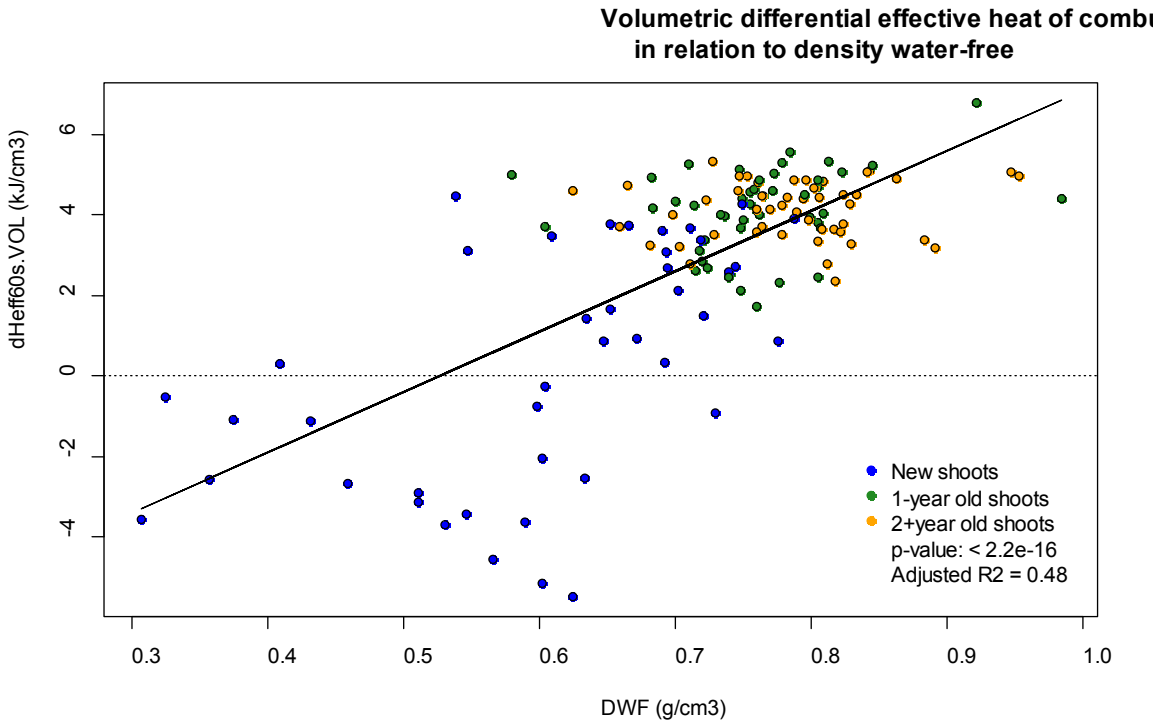

Figure 4.9 Relationship between volumetric flammability *($dH_{eff}60s.VOL$)* and density water-free *(DWF)*. Blue, green, and orange colors represent new, 1-year, and 2+year old shoots respectively.

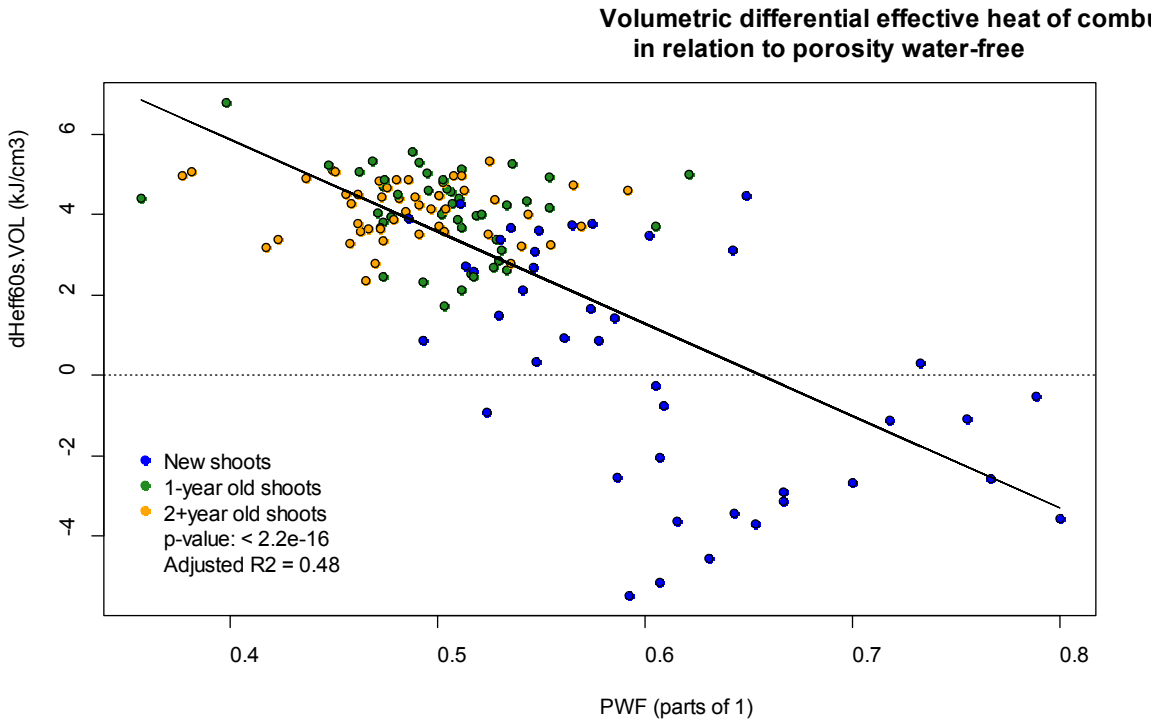

Figure 4.10 Relationship between volumetric flammability *($dH_{eff}60s.VOL$)* and porosity water-free *(PWF)*. Blue, green, and orange colors represent new, 1-year, and 2+year old shoots respectively.

4.3.2 Multi-variable model of live fuel flammability

4.3.2.1 Flammability modelling approach – gravimetric or volumetric?

The flammability of live fuel was satisfactorily predicted using single-variable models, where gravimetric variables such as water content, dry matter content, and energy content explained 83%, 84%, and 83% of flammability variation, respectively (Fig. 4.7). Volumetric water content, dry matter content, and energy content explained 64%, 79%, and 78% of variation in flammability, respectively. Seemingly, due to simplicity and the slightly higher statistical quality of the gravimetric single-variable models, the gravimetric approach should be used for assessment and modelling of live flammability. The gravimetric approach, however, is not compatible with remote sensing. Satellite and

airborne sensors are unable to detect, for instance, the proportion of water content to dry mass (a measure of the gravimetric water content). Also, gravimetric measurements have limited mass-to-mass physical meaning; such variables as density, porosity, and surface-to-volume ratio are absent.

Unlike gravimetric, the volumetric approach is fully compatible with remote sensing techniques. It accounts not only for mass-to-mass proportions of the substances composing the fuel, but also for spatial mass-volume-surface area proportions. Since combustion is not only mass, but also space-determined process both in solid and gaseous phases, the volumetric approach, therefore, theoretically could better represent combustion and flammability of live fuel. Another important reason for using the volumetric approach is the complexity of biophysical and chemical characteristics of live plant material which have been measured with a great variety of measures and units. For example, gravimetric water content is measured as a proportion to dry matter content (dry mass). The gravimetric dry matter content in plant tissue is measured as a proportion to fresh tissue mass (fresh mass) that, again, includes water mass. In order to compare or use these two variables in further analysis, the method needs to account somehow for the fact that the traditional contents of water and dry matter represent amounts of these two substances as proportions to mass of two different physical objects: of tissue without water (to dry mass) and of tissue with water in it, (to fresh mass) respectively.

The volumetric approach unifies all variables as amounts of any substance or energy (water, dry organic substance, chemical composition, energy content, etc.) in plant tissue as concentrations – per unit of volume of fresh plant tissue. It provides, therefore, a mathematically undistorted measure of the proportions, or concentration, of these components in live plant tissue composition. The volumetric approach was used in the flammability studies only partially by using dry mass density (van Altena et al., 2012) and fresh plant material density (Jolly et al., 2014). For all variables (including water, dry matter, calorimetric, and energy contents, fresh density, density water-free, and porosity water-free), the volumetric approach was first applied in this study (Paskaluk, Ackerman, &Melnik, 2015, Melnik et al., 2015). As an attempt to improve the results of the single-

variable models, all these volumetric variables were further used in the development of the multivariable live fuel flammability model for white spruce.

4.3.1.2 Selection of input variables for live fuel flammability model

As was discussed earlier in section 1.3.1, the important variables affecting flammability of live fuel are water content, dry matter content, chemical composition, calorimetric content, density, and porosity. This was also confirmed by the results of the correlation analysis. Pearson correlation coefficient *(r)* of relationship of $dH_{eff}60s.VOL$ with *SWC.VOL, DM.VOL, DWF, PWF* were -0.80, 0.89, 0.70, and -0.70, respectively (Fig. 3.28). Though *DWF* and *PWF* were strongly interrelated (r = 1.00), they were both used in the modelling of flammability due to their completely different effects on combustion processes and its characteristics. Correlation of $dH_{eff}60s.VOL$ with fresh density *(D) was* lower, but still substantial enough *(r* = 0.38) to include this variable into the modelling. One traditional variable that was missed from the analysis – chemical composition *(Ch)* – and one newly introduced in this study variable – energy content per unit of volume *(EC.VOL)* – need an additional discussion.

4.3.1.3 Energy content instead of dry matter content and chemical composition

The large number of variables that must be used to fully represent chemical composition, variability in the results, as well as the general complicity and high cost of methods of chemical analysis make it difficult to use variables characterizing chemical composition in the modelling of flammability. In this research, dry matter content *(DM.VOL)* and multiple variables characterizing chemical composition *(Ch)* were replaced by a single variable – energy content of live fuel *(EC.VOL).* The *EC.VOL* showed the second highest correlation with $dH_{eff}60s.VOL$ (r of 0.88) after *DM.VOL (r* = 0.89), which was noticeably higher than for *SWC.VOL (r* = -0.80) (Fig. 3.28).

Changes in flammability caused by variation in dry matter content and chemical composition can be fully represented by variation in energy content of live fuel.

Theoretically, with given spatial structure, flammability is determined by the amounts of water and flammable substances in a unit of fuel dry mass, fresh mass, or volume as well as by the variety and characteristics of these substances (chemical composition). According to this, $dH_{eff}60s.VOL$ can be explained by variation in volumetric shoot water content *(SWC.VOL)* (amount of suppressing reagent), dry matter content *(DM.VOL)* (total amount of flammable organic substances), and chemical composition *(Ch)* (proportions of different flammable organic substances in the dry matter content that have different calorimetric and combustion characteristics), fresh density *(D),* density water-free *(DWF),* and porosity water-free *(PWF).*

$$dH_{eff}60s.VOL = f\,(SWC.VOL, \mathbf{DM.VOL, Ch,} D, DWF, PWF) \quad [4.1]$$

SWC.VOL represents amount of water per unit of volume of live fuel and strongly negatively affects flammability of live fuel (Fig. 4.3). This is caused by reactants (oxygen and flammable volatilized products of pyrolysis) dilution by water vapor and by energy absorption for water evaporation as well as for fuel and products of combustion temperature increase (water has the highest heat capacity among all components of live plants). Energy absorption hold down the temperature of chemical reaction of oxidation (combustion) and therefore causes a decrease in rate of a chemical reaction (intensity).

Dry matter content *(DM.VOL)* in [4.1], as the total amount of flammable organic substances per unit of volume of live fuel (energy source of combustion), and chemical composition, *Ch,* as proportions of these flammable organic substances that have different calorimetric content, together, therefore, characterize the energy content per unit of fuel volume *(EC.VOL, kJ* cm^{-3}*):*

$$EC.VOL = f\,(\mathbf{DM.VOL, Ch}) \quad [4.2]$$

Volumetric energy content (EC.VOL), is a maximal theoretical amount of heat per unit of fuel volume. It determines a potential energy release response to fire conditions of the flame front and hence the flammability of live fuel. According to the results, the flammability of fuel samples was directly related to *EC.VOL* (Fig. 4.7). Using the expression [2.14], *EC.VOL* can be calculated as the product of dry matter content (*DM.VOL,* representing mass of dry organic substance in the unit of fresh fuel volume) and calorimetric content (*CC,* or *gross* heat of combustion, H_{gross}, representing energy that will be released by the unit of mass of this dry organic substance). According to [4.2], ***DM.VOL*** and ***Ch*** in the expression [4.1] were replaced by ***EC.VOL****:*

$$dH_{eff}60s.VOL = f\,(SWC.VOL,\ \mathbf{EC.VOL,}\ D,\ DWF,\ PWF\mathbf{)} \qquad [4.3]$$

Density and porosity are strongly interrelated; however, they both were used since their effect on the particular type of the physical-chemical process of live fuel combustion is quite different. To indicate the importance of ***EC.VOL*** as the energy-generation component of the equation, the expression of flammability of live fuel [4.3] was re-written:

$$dH_{eff}60s.VOL = f\,\mathbf{(EC.VOL,}\ SWC.VOL,\ D,\ DWF,\ PWF) \qquad [4.4]$$

The flammability of live fuel therefore can be explained by 5 volumetric variables, where *EC.VOL* represents the reaction-fueling agent, *SWC.VOL* represents the reaction-suppressing agent, while *D, DWF,* and *PWF* represent the reaction rate- and characteristics-determining components. The expression of the flammability of live fuel [4.4] was further used as a base for the proposed approach on assessing and modelling of live fuel flammability that is considered in detail in the following sub-sections.

4.3.1.4 Energy content use: energy content minus reduction in energy release

The change in energy release to the frontal flame caused by the interaction with the live fuel element burning within the flame can be expressed as:

$$dH_{eff}60s.VOL = EC.VOL - E.LOSS_{O_2} - E.LOSS_{H_2O} \quad [4.5]$$

Where:

EC.VOL – total energy release of the live fuel element's flame with combustion of the element's dry matter content in the ideal conditions of full oxygen supply and without presence of water or its vapor

$E.LOSS_{O_2}$ - combined reduction in energy release for live fuel element's flame and for the frontal flame due to oxygen deficiency in the flames interaction zone

$E.LOSS_{H_2O}$ - combined reduction in energy release for live fuel element's flame and for the frontal flame due to effects of live fuel's water content in the flames interaction zone

Using the assumption that combined reduction in energy release for the live fuel's flame and the frontal flame in the flames interaction zone due to oxygen deficiency and due to effects of live fuel's water content is proportional to *EC.VOL, they can be written:*

$$E.LOSS_{O_2} = EC.VOL * Loss_{O_2} \quad [4.6]$$

$$E.LOSS_{H_2O} = EC.VOL * Loss_{H_2O}, \quad [4.7]$$

Where:

$Loss_{O_2}$ - per unit of *EC.VOL*, reduction in energy release for both frontal flame and live fuel element's flame due to oxygen deficiency in the flames interaction zone (relative reduction in energy release due to oxygen deficiency)

$Loss_{H_2O}$ - per unit of *EC.VOL*, reduction in energy release for both flames in the flames interaction zone due to effects of live fuel's water content (relative reduction in energy release due to effects of live fuel's water content)

Use of [4.6] and [4.7] in the expression [4.5] produces:

$$dH_{eff}60s.VOL = EC.VOL - EC.VOL * Loss_{O_2} - EC.VOL * Loss_{H_2O} \quad [4.8]$$

The expression [4.8] can be, therefore, written:

$$dH_{eff}60s.VOL = EC.VOL * (1 - Loss_{O_2} - Loss_{H_2O}) \quad [4.9]$$

Where:

$dH_{eff}60s.VOL$ - volumetric flammability of live fuel as a potential (in the conditions of maximal heating rates and oxygen supply corresponding to max possible fire weather condition) energy release contribution of the burning live fuel into the intensity (energy release) of the frontal flame measured as differential effective heat of combustion (kJ cm^{-3})

EC.VOL - volumetric energy content of live fuel calculated as measured dry matter content multiplied by calorimetric content (gross heat of combustion), (kJ cm^{-3})

$Loss_{O_2}$ – reduction in energy release (kJ cm^{-3}) due to oxygen deficiency in the flames interaction zone per unit of energy content *EC.VOL* (kJ cm^{-3}) → (relative reduction in energy release), ( )

$Loss_{H_2O}$ - reduction in energy release (kJ cm^{-3}) caused by high water content of live fuel per unit of energy content *EC.VOL* (kJ cm^{-3}) → (relative reduction in energy release), ( )

4.3.1.5 Model frame development

Flammability, as the resulting change in total energy release to the incoming frontal flame during the first 60 seconds of combustion, was expressed in [4.9] as part of fuel's energy content *(EC.VOL)* that was used for change in total energy release of frontal flame. The change in energy release to the incoming frontal flame decreases with more substantial relative (per unit of energy content) reduction in energy release due to oxygen deficiency *($Loss_{O_2}$)* and due to high water content of live fuel *($Loss_{H_2O}$).* Energy release contribution of the live fuel element burning within the frontal flame is determined, therefore, by three main components: (1) energy content *(EC.VOL),* (2) relative reduction in energy release due to oxygen deficiency *($Loss_{O_2}$),* and (3) relative reduction in energy release due to high water content of live fuel *($Loss_{H_2O}$),* (Fig. 4.11):

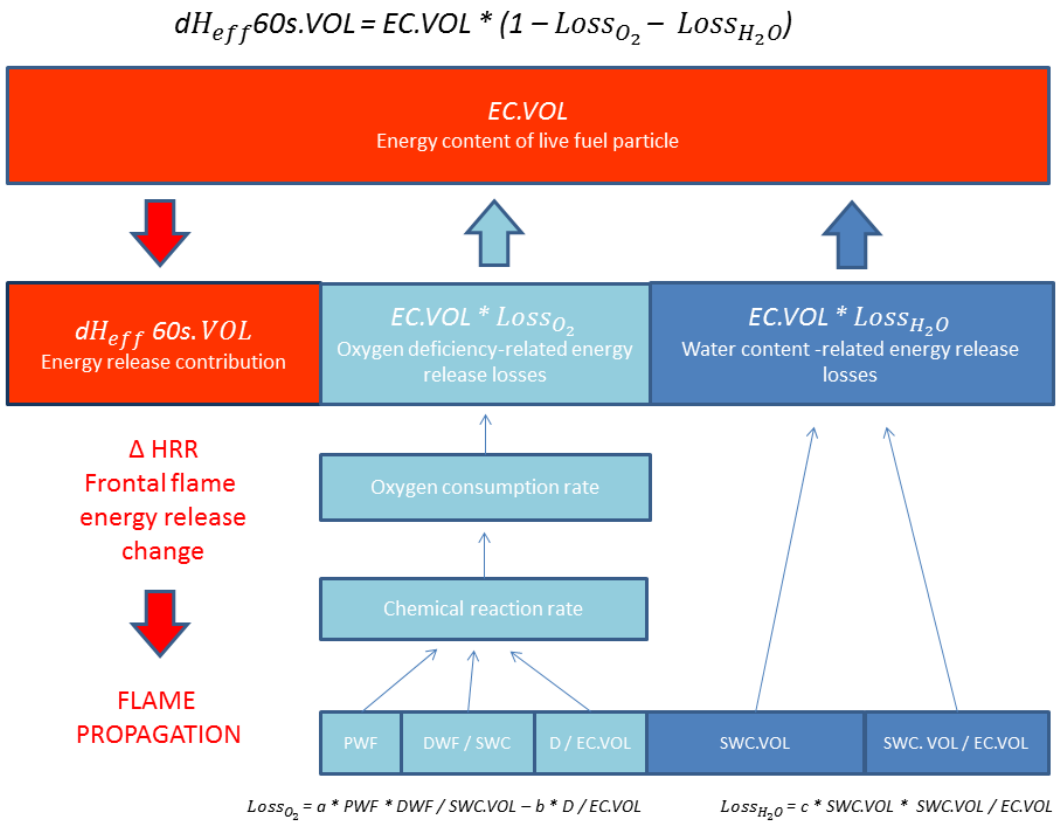

Figure 4.11 Factors affecting energy release contribution of the burning live fuel to intensity of the frontal flame. The figure graphically represents the situation when reduction in energy release for both flames is lower than energy content – flammability is positive *($dH_{eff}60s.VOL > 0$)*

1. ***Energy content (EC.VOL)*** of a tested fuel element is an important variable determining flammability in the expression [4.9] and was selected for use in the flammability model together with other four variables. It represents an *energy source component* of the combustion (red color in Fig. 4.11) and can be calculated using equation [2.14]. In the conditions of the frontal flame, this theoretical potential energy content of live fuel will be released only partially due to oxygen deficiency ($EC.VOL * Loss_{O_2}$) and water content-associated reduction in energy release ($EC.VOL * Loss_{H_2O}$). The energy release contribution of the burning live fuel to the intensity of the frontal flame (flammability, $dH_{eff}60s.VOL$) cannot be higher than the energy content of the live fuel. Flammability can be close to energy content for dry fuel in the ideal conditions of a pure oxygen environment (oxygen

bomb calorimetry). It will be positive if reduction in energy release mentioned above for both flames (live fuel's flame and frontal flame) is less than energy content, and negative if reduction in energy release is higher than the energy content of live fuel. The relative reduction in energy release in the equation [4.9] *($Loss_{O_2}$* and *$Loss_{H_2O}$)* was considered in relation to another 4 volumetric variables selected earlier for flammability modelling: shoot water content *(SWC.VOL),* fresh density *(D),* density water-free *(DWF)*, and porosity water-free *(PWF)*.

2. ***Relative reduction in energy release due to oxygen deficiency ($Loss_{O_2}$)*** in the interaction zone of the frontal flame and of the burning live fuel element flame represents energy sink component-1 in the equation [4.9] (light-blue color in Fig. 4.11). This reduction in energy release is directly related to the oxygen consumption rate for burning live fuel and hence to the chemical reaction rate *(RR_{ch})* of the live fuel element's flame. The higher the RR_{ch}, the lower is the concentration of oxygen in the flames interaction zone. RR_{ch} increases with higher porosity of the cell wall material (cell wall material alone for the cell space free of water) defined and measured as porosity water-free ***(PWF)***. The higher is porosity, the higher is the surface area to volume ratio (higher surface area to absorb the ignition flux and to evaporate pyrolizates), hence the pyrolysis rate, and, therefore, a higher chemical reaction rate. RR_{ch} will also be higher with a higher ratio of dry matter content to water content for cell wall material free of water. This ratio can be expressed as a ratio of density water-free to shoot water content: ***DWF / SWC.VOL***. The ratio represents the proportion of combustion source (fuel amount) and suppression source (water amount) in the unit of volume of cell wall substance. The combined effect of *PWF and DWF / SWC.VOL* on RR_{ch} and, hence, on $Loss_{O_2}$ can be written:

$$Loss_{O_2} = f(RR_{chem}) \rightarrow$$

$$Loss_{O_2} = f(PWF * DWF / SWC.VOL) \qquad [4.10]$$

The rate of chemical reaction of live fuel's flame and hence oxygen deficiency declines proportionally to the ratio of density to energy content *(D/EC.VOL).* The higher density the plant tissue is, the higher is its thermal conductivity. Ratio *D/ EC.VOL,* therefore, represents the ratio of thermal conductivity to energy content of plant material which reflects the rate of energy losses to the internal unburned part of the fuel due to thermal conductivity. A higher ratio of thermal conductivity to energy content causes a lower temperature gradient at the surface layer of the fuel, lower temperature at the fuel surface, hence lower rate of wood pyrolysis, and eventually a lower reaction rate at the gaseous phase. Considering this reduction effect of ***D/EC.VOL*** on chemical reaction rate in the equation [4.10], the rate of chemical reaction and the associated reduction in energy release due to oxygen deficiency can be expressed:

$Loss_{O_2} = f(RR_{chem})$ →

$Loss_{O_2} = = f(PWF * DWF / SWC.VOL - D / EC.VOL)$ →

$Loss_{O_2} = a * PWF * DWF / SWC.VOL - b * D / EC.VOL$ [4.11]

Where:

a ( ) and b (kJ/g) – empirical parameters

3. ***Relative reduction in energy release due to high water content of live fuel*** ***($LOSS_{H_2O}$)*** for both flames in the flames' interaction zone represent energy sink component-2 in the equation [4.9] (dark-blue color in Fig. 4.11). Reduction in energy release caused by the dilution of oxygen and flammable volatiles by water vapor is directly related to the water content of live fuel ***(SWC.VOL).*** With the

given concentration of water in live fuel, reduction in energy release caused by energy absorption for water evaporation and consequent decrease in chemical reaction temperature and rate will be higher for low-calorie fuels; rate of chemical reaction for high-calorie fuels will be less affected by the same concentration of water. Hence reduction in energy release caused by energy absorption for water evaporation and consequent decrease in chemical reaction temperature and rate is determined by the ratio of water content to energy content ***(SWC.VOL / EC.VOL).*** Therefore, the combined water content-associated reduction in energy release can be expressed:

$Loss_{H_2O}$ = *f (SWC.VOL * SWC.VOL / EC.VOL)* →

$Loss_{H_2O}$ = *f (*$SWC.VOL^2$ */ EC.VOL)* →

$Loss_{H_2O}$ = c * $SWC.VOL^2$ / *EC.VOL* [4.12]

Where:

c (kJ/g per g/cm^3) – an empirical parameter

Combining the expression [4.11] for $Loss_{O_2}$ with [4.12] for $Loss_{H_2O}$ in the initial (base) equation [4.9], the flammability of live fuel as energy release contribution to the frontal flame intensity can be written:

$dH_{eff}60s.VOL$ =

*EC.VOL**[1 - (a**PWF*DWF/ SWC.VOL* – b**D/ EC.VOL)* - c*$SWC.VOL^2$*/ EC.VOL*] [4.13]

4.3.1.6 Model parameters optimization

R-software was used for non-linear model parameters optimization (nls-function). Among many mathematical expressions for $dH_{eff}60s.VOL$ using combinations of 5 volumetric variables, the model frame [4.13] presented above gave the best statistical result. For all ages of shoots (new, 1-year, and 2+year old) plotted together, the developed model explained 87% of variation in live fuel flammability of for white spruce (Fig. 4.12):

$$dH_{eff}60s.VOL = EC.VOL*[1 - (0.6114 *PWF*DWF/ SWC.VOL – 6.1546 *D/ EC.VOL)-(29.6133 *SWC.VOL^2/ EC.VOL)] \quad [4.14]$$

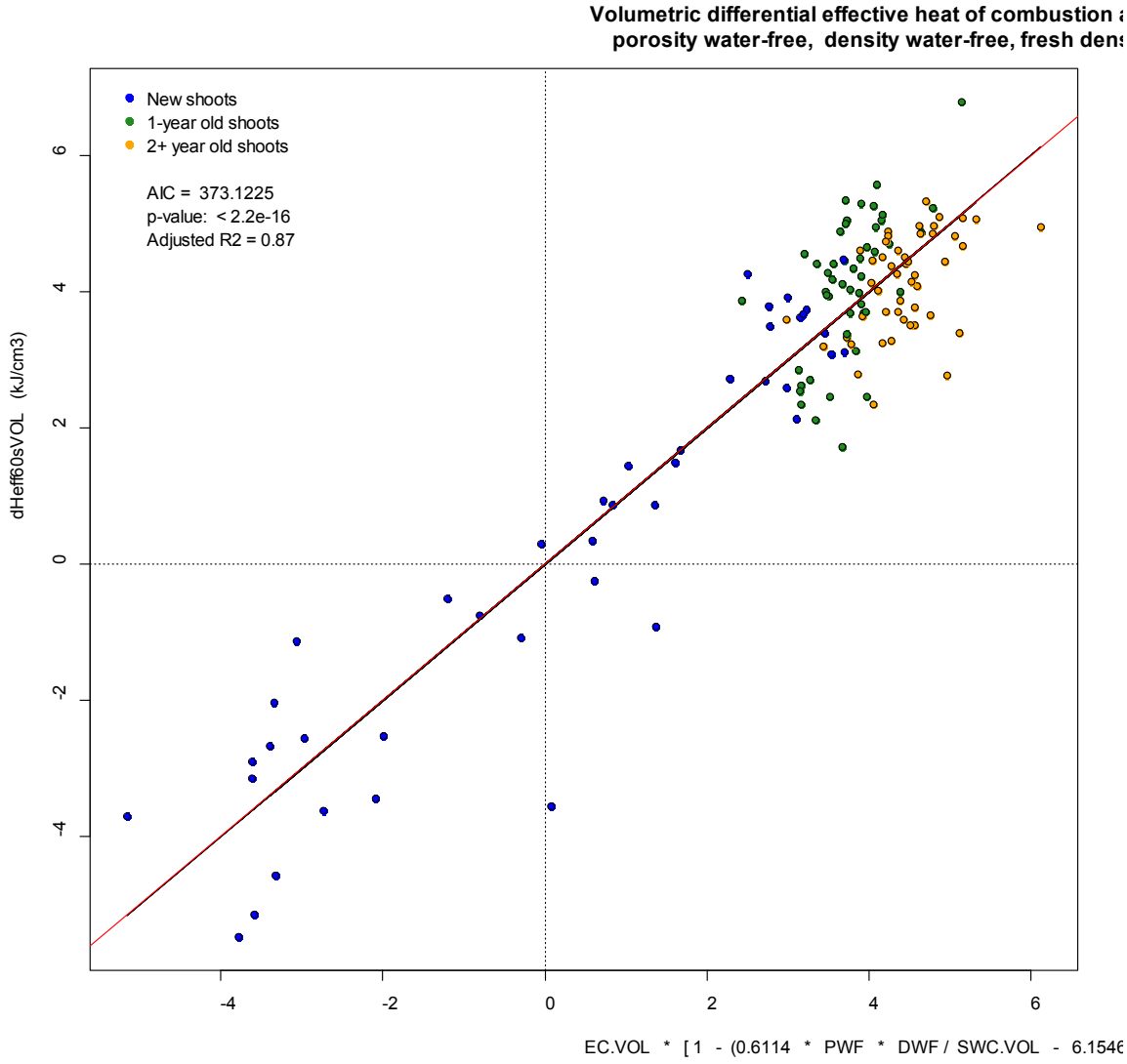

Figure 4.12 All ages of shoot live fuel flammability model for white spruce (new, 1-year, 2+year old shoots plotted together). Modelled flammability *($dH_{eff}60s.VOL$)* was plotted at X-axis, and measured $dH_{eff}60s.VOL$ was plotted at Y-axis. The solid red line is the hypothetical line where each point has equal X (predicted) and Y (observed) values. The solid black line (which is almost invisible because it coincides with the red line) indicates the actual regression line between the X values (predicted) and Y values (observed).

1

4.3.1.7 Model performance and physical meaning

The proposed volumetric multivariable model for all ages of shoots [4.14] presented above (Fig. 4.12) explained 87% variation in flammability (adjusted $R^2 = 0.87$). This allowed for only marginally better explaining the variance in flammability compared to the best gravimetric single-variable flammability model $dH_{eff}60s.VOL \sim DM.GRAV$ in Fig 4.7 that explained 84 % variation in flammability (adjusted $R^2 = 0.84$). This seemingly suggests that, due to simplicity, this gravimetric single-variable flammability model is preferable for practical applications. However, the main goal of the study was the development of the volumetric model since volumetric approach allows for remote sensing-based practical applications in spatial fire behaviour modelling. The combined use of several variables such as the existing volumetric variable fresh density *(D)* and newly introduced in this study volumetric variables *EC.VOL, SWC.VOL, DWF,* and *PWF* in the proposed volumetric multivariable model [4.14] in Fig. 4.12 allowed for the improvement in the explanation of the flammability (adjusted $R^2 = 0.87$) compared with the best volumetric single-variable flammability model (adjusted $R^2 = 0.79$, $dH_{eff}60s.VOL \sim DM.VOL$, in Fig. 4.7).

The structure of the model [4.14] allowed for the best representation of the main physical processes involved in live fuel combustion within the frontal flame and accounting for the main factors affecting an interaction of the burning live fuel element's flame and the incoming frontal flame. The energy release contribution of live fuel to the intensity of the frontal flame $(dH_{eff}60s.VOL)$ was considered as a sum of three major components: energy content *(EC.VOL),* reduction in energy release due to oxygen deficiency $(Loss_{O_2})$, and water content-related reduction in energy release $(Loss_{H_2O})$ (model frame equation [4.9], Fig. 4.11).

According to the equation of the fitted model [4.14], in particular, energy release contribution is directly proportional to the energy content of live fuel (*EC.VOL).* The energy release contribution to the frontal flame declines with more substantial reduction in energy release and can be negative. Reduction in energy release is directly proportional to *EC.VOL* and per unit of *EC.VOL* is determined by *SWC.VOL, PWF, DWF,* and *D.*

Reduction in energy release for both flames is caused by incomplete combustion due to oxygen deficiency and due to effects of the water content of live fuel. The rate of live fuel combustion and the associated reduction in energy release due to oxygen deficiency (0.6114 **PWF*DWF/ SWC.VOL* – 6.1546 **D/ EC.VOL)* in the equation [4.14] is proportional to the porosity of cell walls material free of water *(PWF,* represents surface area to volume ratio for the internal plant tissue structure water-free). The reduction in energy release is also proportional to the ratio of cell wall material density to shoot water content *(DWF/ SWC.VOL,* which represents the ratio of fuel amount (energy source) to water amount (suppression source) in the unit of volume of cell wall substance water-free). The rate of live fuel combustion and oxygen deficiency-related losses decreases with growth in the ratio of fresh density to energy content (*D/ EC.VOL*) that represents the proportion of thermal conductivity to the energy content of plant material. Water content-associated reduction in energy release is determined by shoot water content *(SWC.VOL,* reagents dilution by water vapor) and by the ratio of shoot water content to energy content (*SWC.VOL/ EC.VOL,* reduction caused by drop in reaction temperature with energy absorption for water evaporation) resulting in the expression *(*29.6133 $*SWC.VOL^2/$ *EC.VOL)* in the equation [4.14].

It needs to acknowledge that terms such as *PWF, DWF,* and *D* in the model frame [4.13] and fitted model [4.14] are highly intercorrelated, as was shown earlier (Section 3.4). However, due to their completely different effects on combustion processes, they all were used in the proposed multivariable flammability model [4.14] allowing to keep a conceptual framework of the proposed approach in quantifying the flammability. The development of simpler and more rigid models for all main forest species using the proposed approach is the important goal of future research.

4.3.1.8 Modelling flammability of different ages of shoots and tree branches

The statistical quality of the *all ages of shoot* model [4.14] (adjusted $R^2 = 0.87$ in Fig. 4.12) where different ages of shoots were plotted together (new, 1-year, 2+year old shoot fuel samples) was high. First, this suggests that the proposed model is able to predict the

flammability of live fuel regardless of age of shoots. Also, this suggests that performance of the live fuel flammability model was not affected significantly by the absence of other variables that were not used in the model, such as season time (phenophase), growth conditions, or drought level. The proposed model, therefore, is able to predict the flammability of live fuel regardless of age, phenophase, growth conditions, and the level of natural disturbances – if energy content, water content, density, and porosity of plant material are known.

However, for *all fuel samples types* model (*all ages of shoots* dataset and *mixed shoot* dataset), the explanation of variation in live fuel flammability was slightly lower (adjusted R^2 =0.84) (Fig. 4.13). This can be explained by a substantial seasonal variation in the properties and flammability of tree branches caused by variation in the proportions of plant material of different ages in the composition of the branch (Fig. 3.1) and by substantial differences in properties for old and new growth (Fig. 3.5, 3.9, 3.15, 3.17, 3.19, and 3.21). The model's coefficients were slightly different from [4.14]:

$$dH_{eff}60s.VOL = EC.VOL*[1 - (0.5241 *PWF*DWF/ SWC.VOL – 4.9357 *D/ EC.VOL)-(27.6228 *SWC.VOL^2/ EC.VOL)] \quad [4.15]$$

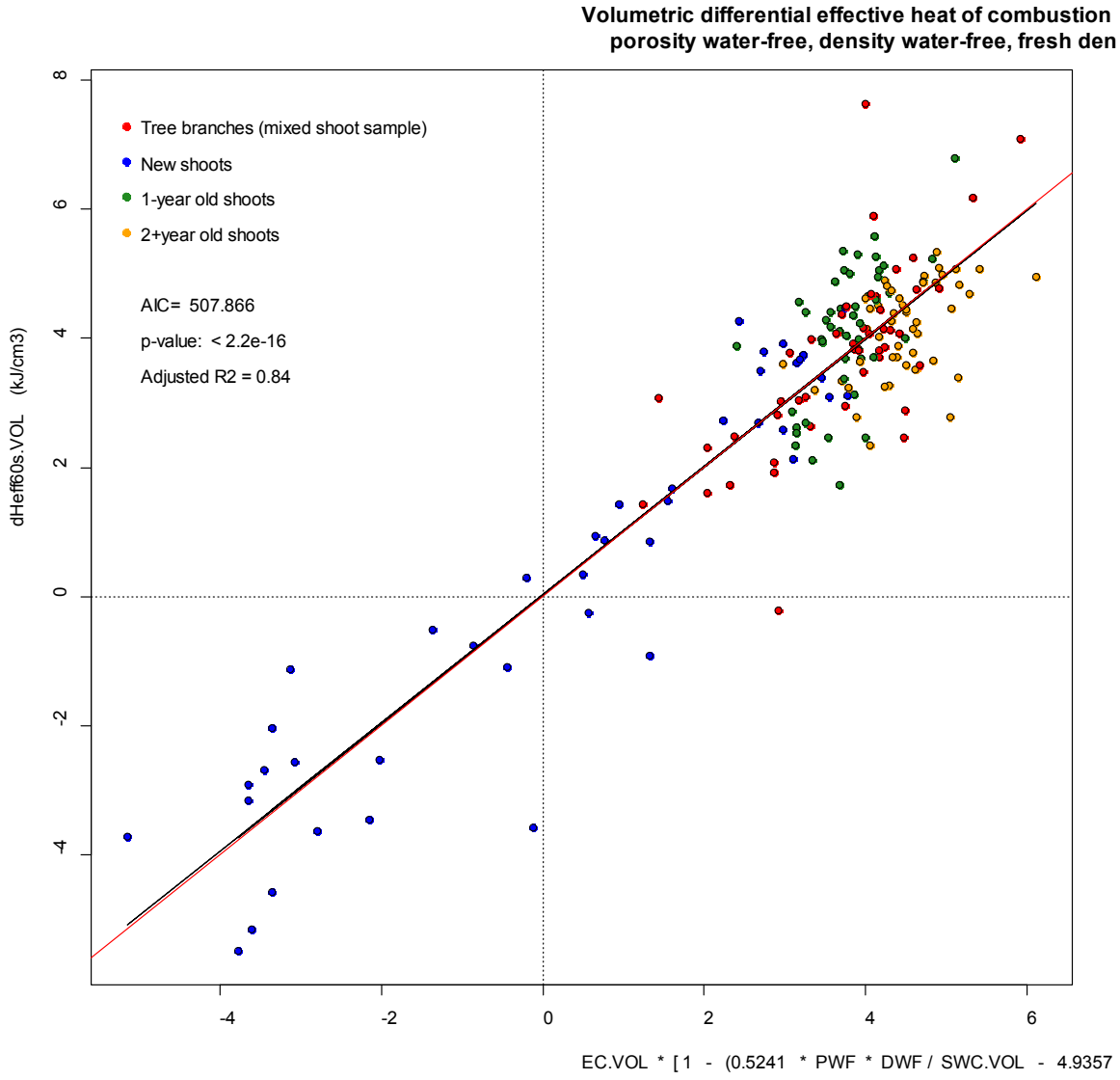

Figure 4.13 All fuel samples types live fuel flammability model for white spruce (new, 1-year, 2+year old shoots, and mixed shoot sample representing tree branch plotted together). Modelled flammability *($dH_{eff}60s.VOL$)* was plotted at X-axis, and measured flammability was plotted at Y-axis. The solid red line is the hypothetical line where each point has equal X (predicted) and Y (observed) values. The solid black line (which is almost invisible because it coincides with the red line) indicates the actual regression line between the X values (predicted) and Y values (observed).

The *all fuel samples types model* (comprising *all ages of shoots* dataset and *mixed shoot* dataset) presented above (equation [4.15]) was mainly developed to investigate if the flammability of tree branches (mixed shoot sample) can be predicted using the same model as for *all ages of shoot model.* According to the results (Fig. 4.13), points representing

flammability of a separate tree branch (mixed shoot sample) were centered on the 45-degrees relationship (regression) line suggesting that *all ages of shoot model* can be used to represent the flammability of the separate tree branch.

The model frame [4.13] did not perform well for 1-year and 2+year old shoots (adjusted R^2 of 0.33 and 0.20 respectively in Fig. 4.14). It performed marginally (adjusted $R^2 = 0.52$) for tree branches (mixed shoot sample). Despite being based on about 75% fewer observations than the *all ages of shoots* dataset (Fig. 4.12), the model performed surprisingly well for the *new shoots* dataset, showing the same high statistical quality (adjusted $R^2 = 0.87$ in Fig. 4.14).

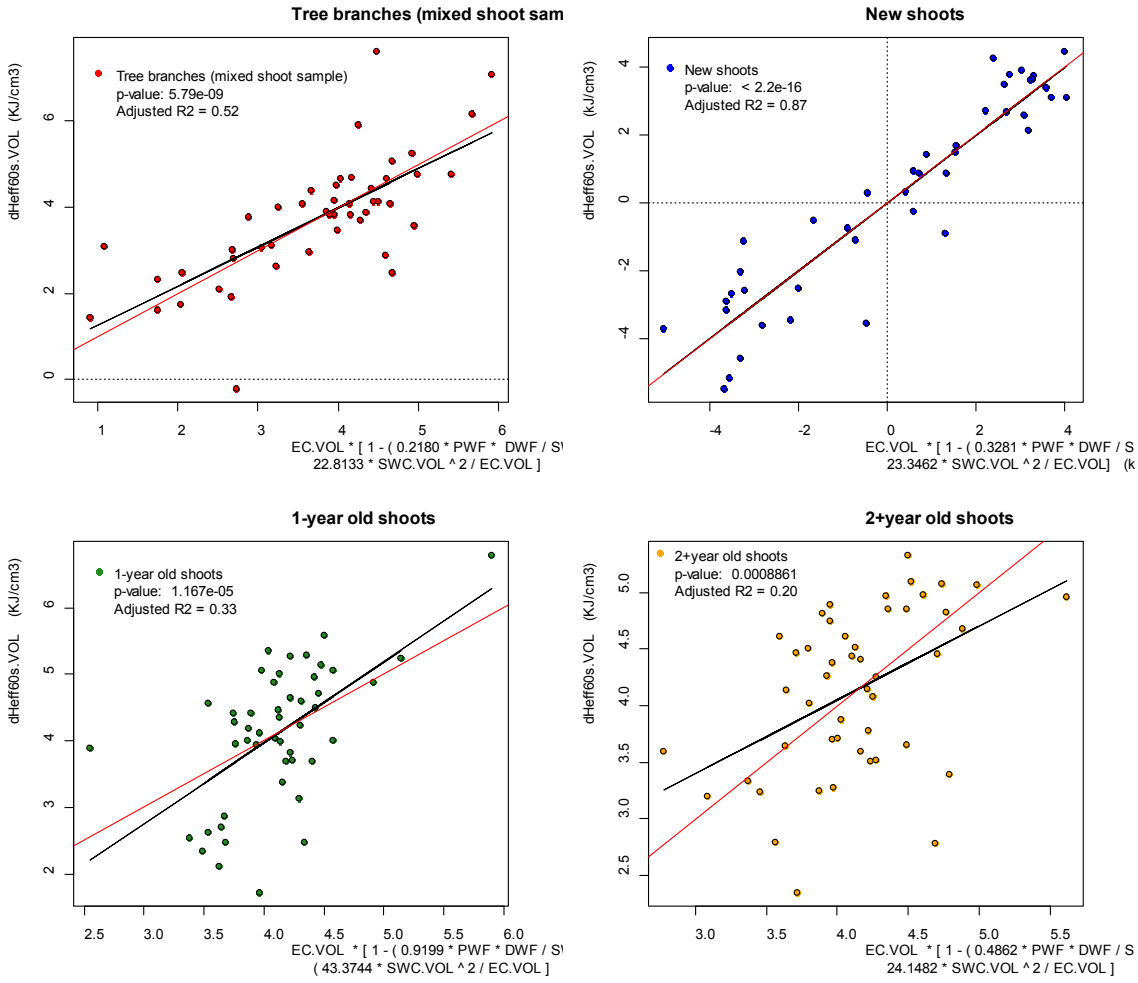

Figure 4.14 Live fuel flammability models for fuel samples types separately (tree branch, new shoots, 1-year, and 2+year old shoots of white spruce). Modelled flammability $dH_{eff}60s.VOL)$ was plotted at X-axis, and measured $dH_{eff}60s.VOL$ was plotted at Y-axis. The solid red line is the hypothetical line where each point has equal X (predicted) and Y (observed) values. The solid black line (which is almost invisible for new shoots because it coincides with the red line) indicates the actual regression line between the X values (predicted) and Y values (observed).

One of the important issues with using remote sensing data for spatial fire modelling is that data acquired after live-out (flushing) usually represent mainly new growth (new shoots) while fire consumes all ages of shoots. The exceptionally high statistical quality of the flammability model based on new shoots data set (Fig. 4.14) suggests that the flammability of white spruce can be successfully modeled using experimental and remote sensing data on the properties of the new shoots only. This can have an additional advantages considering that every particular tree branch meets fire by new shoots. It is quite possible that go-no-go (threshold) conditions for flame propagation and initiation of

crowning are determined mainly by the properties and flammability of new shoots. According to this, and considering performance of the flammability models discussed above, the all fuel sample types model (Fig. 4.13), the all ages of shoots model (Fig. 4.12), the tree branch (mixed shoot sample) model, and the new shoots model (Fig. 4.14) were evaluated. The modeled seasonal trends of live fuel flammability were compared against measured seasonal data on live fuel flammability *($dH_{eff}60s.VOL$)* for 2014 and with the seasonal pattern of live fuel flammability assumed by the FBP CFFDRS model.

4.4 SEASONAL CHANGES IN FLAMMABILITY OF LIVE FUEL

Phenology- and drought-related changes in flammability of live fuel are considered in the FBP CFFDRS very partially and according to the results of our study, nor quite correctly. For all conifers, the FBP CFFDRS model assumes only one maximum in flammability at early-mid June. It is caused by phenological changes in the properties of live plant tissue during the so-called "spring dip (the lowest seasonal values) in foliar moisture content (Fig. 4.15, Fig. 4.16). The spring dip corresponds to the maximum in flammability expressed as the crown spread factor (Van Wagner, 1974; Turner & Lawson, 1978) (Fig. 4.16). CSF is used in the FBP CFFDRS model for calculations of the crown spread index (CSI) (Van Wagner, 1974): CSF times the initial spread index (ISI).

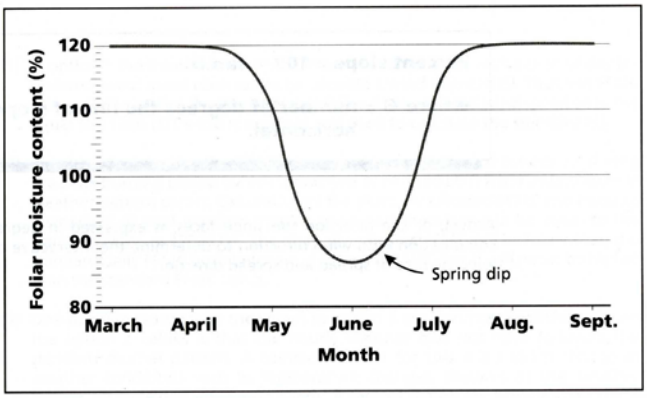

Figure 4.15 Seasonal trend in foliar moisture content (FMC) for conifers as estimated by the FBP CFFDERS Model (from Hirsch, 1996).

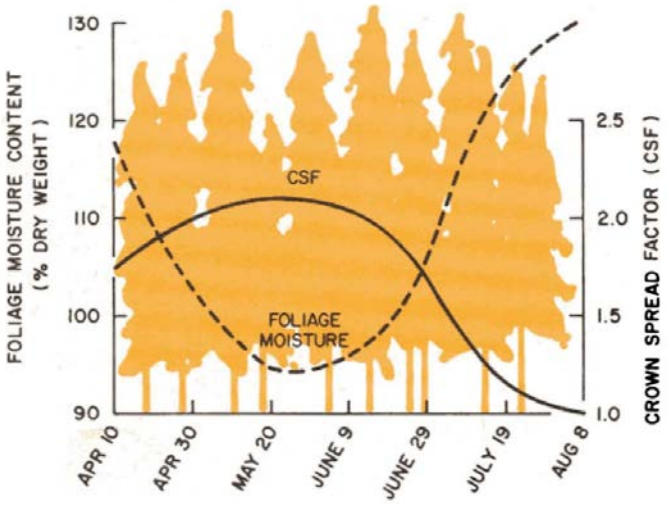

Figure 4.16 Phenology-related seasonal trend in foliar moisture content (FMC) and live fuel flammability expressed as the crown spread factor (CSF) for conifers as illustrated by (J. A. Turner & Lawson, 1978).

It is assumed that the flammability of live fuel is slightly lower in April and early May before the spring dip, that it is maximal at early-mid June, that it gradually decreases through June and July, and then sharply decreases during July to the lowest seasonal values in August to the end of the season (Fig. 4.16). The measured pattern of flammability for white spruce in 2014 (Fig. 4.17) was substantially different from the pattern expected by the FBP CFFDRS model. Both gravimetric and volumetric flammability ($dH_{eff}60s.GRAV$ and $dH_{eff}60s.VOL,$ respectively) revealed nearly identical seasonal patterns (Fig. 3.23 and Fig. 3.25). In general, the measured volumetric flammability for tree branches (mixed shoot sample) was higher in the beginning and the end of the season in 2014 compared to mid-season (Fig. 4.17). It decreased slightly from snow-melt to mid-summer and then increased towards the end of October. Three seasonal maximums in flammability that occurred on May 6, July 7, and August 12 were satisfactorily predicted by all four proposed multivariable volumetric flammability models based on the model-frame equation [4.13] (that is, all tissue types model, all ages of shoots model, new shoots model, and mixed shoot model). The new shoots model showed slightly better ability in prediction of seasonal maximums in flammability compared with other models. The lowest seasonal values of flammability were measured on June 17th and were precisely predicted by the proposed models (Fig. 4.17).

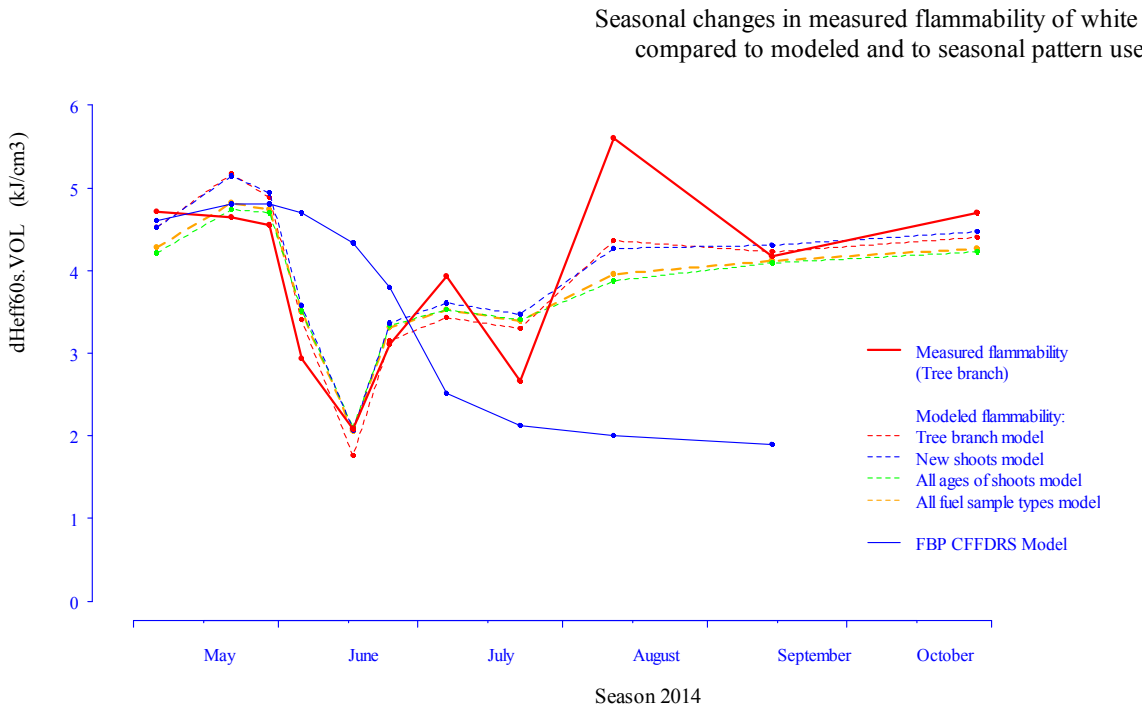

Figure 4.17 Measured pattern of seasonal changes in flammability of white spruce during 2014 compared to modeled patterns and that assumed by FBP CFFDRS System. The used by FBP CFFDRS seasonal trend of live fuel flammability expressed as CSF (Van Wagner, 1974) was scaled and plotted from Turner & Lawson, (1978).

Water content is one of the most important factors determining flammability of live fuel. The measured seasonal pattern of actual variation in the water content of live fuel (volumetric shoot water content, SWC.VOL) in 2014 was noticeably different compared with that assumed by the FBP CFFDRS model pattern of FMC variation. According to measured *SWC.VOL,* the lowest point of the first seasonal minimum in volumetric water content (spring dip) occurred on May 6 in 2014 or probably earlier (no data exists for this period) (Fig. 3.5). This corresponds with the timing of the first seasonal maximums in flammability on May 6 (Fig. 4.17). According to the FBP CFFDRS model, however, the first and the only seasonal minimum in the water content of live fuel (spring dip) and the corresponding spike in flammability were expected in 1.5 month later: between mid-May and mid-July with the lowest point in water content in mid-June (Hirsch, 1996) (Fig. 4.15). Moreover, by that time (mid-June), the actual measured volumetric water content

(SWC.VOL) showed the highest seasonal values (Fig. 3.5) and measured flammability *($dH_{eff}60s.VOL$)* showed, correspondingly, the lowest seasonal minimum in flammability (Fig. 4.17).

According to the FBP model, the lowest seasonal values of live fuel flammability were expected in July and later in the season (Fig. 4.16) due to recovery in water content of live fuel after spring dip (Fig 4.15). By contrast, according the results, there were two more spikes in flammability during that period: on July7 and August 12. The timing of the third measured seasonal maximum in flammability on August 12 (Fig. 4.17) (that was even more substantial than during spring dip) corresponded exactly to the lowest "late-summer dip" (minimum) in volumetric shoot water content *(SWC.VOL),* (Fig. 3.5). The lowest seasonal values of volumetric water content *(SWC.VOL* on August 12 (lesser than 0.33 g/cm^3) clearly indicated the reason for the mid-August spike in flammability – late summer drought in 2014.

The proposed volumetric approach also showed a better ability to represent the actual physiological changes in the live plant tissue properties that govern flammability compared to the gravimetric approach. According to the measured gravimetric shoot water content *(SWC.GRAW),* the maximum in spring dip occurred on May 30 (Fig. 3.3), which is almost one month later then when the spring maximum in flammability actually occurred. The traditional gravimetric measure of water content on the dry mass basis did not clearly show the lowest seasonal concentrations of water in live plant tissue on August 12 (Fig. 3.3), while they were clearly shown by the volumetric shoot water content (Fig. 3.5). Gravimetric water content does not represent the actual plant water status during drought since dry mass (dry matter content) varies substantially due to phenological development through the season (Fig. 3.7 and 3.9). The proposed volumetric approach and method for assessment and modelling of flammability of live fuel, therefore, showed better results in general compared with the existing techniques. With additional studies and further development, the proposed method has the potential to further improve the accuracy of the predictions of live fuel flammability and of wildland fire behaviour.

4.5 LIMITATIONS AND SOURCES OF UNCERTAINTY

The properties and flammability of live fuel vary depending on the species, age, phenophase, and physiological state of plants. The physiological state is determined by growth conditions: the level of natural disturbances, landscape characteristics, soil-water conditions, geographical location, weather and climate. The present study does not of course include all these factors. Only mid-age white spruce trees were studied without separate analysis for different stages of phenological development. The study is limited to the WUI of the Central Parkland Natural Subregion of Central Alberta and its weather, climate, and some of its soil conditions and water availability. The effects of growth conditions on flammability were not studied. Each data point of the time-series for 2014 was represented by the limited sample size of 3-6 observations for each variable measured. Seasonal data for the very beginning of the season, from May to mid-June, were not fully reliable for new shoots due to their sensitivity to dehydration and the prolonged storage time before testing. The inter-seasonal variation in properties and flammability is not represented.

Flammability was measured as a potential energy release contribution of the burning live fuel to the frontal flame energy release during 60 seconds of combustion (an average residence time of a flame-front). The residence time, however, can vary depending on the species composition and spatial characteristics of the plant canopy. While *dHRR* was measured for up to 240 seconds of combustion, calculations and analysis of the $dH_{eff}60s.GRAV$ *and* $dH_{eff}60s.VOL$ were performed only for the first 60 seconds of live fuel and frontal flame interaction. A methane flame of nominal intensity of only 500 kW m^{-2} was used and monitored; the response of the live fuel to different flame intensities needs additional investigation. The intensity of the ignition heat flux on the surface of the tested sample and flame temperature should also be monitored since these are important characteristics of the fire conditions of the interaction of the live fuel and the frontal flame. High concentrations of water wapor which may be present in the incoming frontal flame were not represented in the tests since methane flame was used. The density of

shoots in the sample holder and the distance between burner and sample holder can both have an effect on the resulting energy release of the combined flame. This effect should also be studied.

The characteristics of the ignition and consumption of the live fuel and the effects of the characteristics of live fuel (water, dry matter contents, chemical composition, density, and porosity) require further detailed examination. Another important volumetric predictor variable that was not used in the study, is surface area to volume ratio (S/V). The S/V can have a substantial effect on flammability of live fuel and should be included in future research.

4.6 FURTHER RESEARCH AND PRACTICAL APPLICATIONS

4.6.1 Test method

An essential element in improving the test method is better representation the live fuel and the conditions of the frontal flame. Additional studies are required to evaluate the potential intensity and residence time of the flame front for the different fuel types used in the FBP CFFDRS System. These data will allow assessment of the potential flammability for more specific fire conditions using corrected residence time and frontal flame intensities, which can be different from those for the methane flame used in the tests. To control the required fire conditions in tests corresponding to those in the real fire, the intensity of the ignition heat flux at the sample surface and flame temperature should be registered, rather than only the nominal energy release of the methane flame. Use of the methane flame premixed with water vapor and carbon dioxide will also provide more realistic conditions of combustion of live fuel. With more detailed data on the typical spatial structure of the fuel types (in particular the average distance between fuel elements in the real tree branch for the particular species), the distance between flame base (upper surface of the methane burner) and fuel sample should be adjusted as well.

4.6.2 Use in fire behaviour modelling

4.6.2.1 Seasonal models of flammability of live fuel

In the present study, the flammability of live fuel was evaluated using an energy release criterion. Another important characteristic of flammability is ignition delay time (time to ignition). It also requires detailed consideration and additional study in relation to water, dry matter contents, chemical composition, density, and porosity. The use of an additional predictor variable, such as surface area to volume ratio, can be useful in improving results both in energy release and in time to ignition studies. The model of flammability of live fuel for white spruce proposed in this study can be improved with additional research by detailed examination of the seasonal and inter-seasonal variation in flammability of live fuel for young and mature stands, according to the phase of phenological development as determined by the geographical location, weather, and climate. With additional studies, similar models can be developed for all main forest and grassland plant species.

While based on the internal characteristics of live plant tissue, these models can also be further used for development of flammability models based on characteristics compatible with remote sensing. These are spectral reflectance (visible and short-wave infrared diapason) as proxy for water and energy contents, density and porosity; surface temperature (thermal infrared diapason) as an indicator of water content and the level of natural disturbance (in particular drought); and characteristics of the response to the artificially emitted microwave (radar) and shortwave (LiDAR) electromagnetic radiation as indicators of water content and spatial structure of the plant canopy respectively. This will require extensive studies on the relation of the predictor variables used in the proposed model of live fuel flammability to the remote sensing variables mentioned above. When used together with data on the flammability of dead fuel, and data on the spatial structure and species composition of plant canopies, such remote sensing-based flammability models will be able to provide information on the spatial distribution of the potential energy release response of plant canopies to the potential (maximal expected) fire weather conditions. This quantitative measure of the *potential flammability of the vegetative*

canopy can be further used for the development of the numerical stand characteristics-based fuel classification.

4.6.2.2 Potential flammability of live fuel – use in fuel classification

Using the proposed method, the potential energy release of a plant canopy in the potential (maximal expected) fire weather conditions during the average flame-front residence time of 60 seconds can be estimated without evaluation or modeling of fuel consumption. When measured by the traditional oxygen consumption calorimetry method, energy release (H_{eff}) is expressed as proportion to mass loss (fuel consumed). To estimate or model the total energy release of the live fuel in a plant canopy, therefore, both (H_{eff}) and fuel consumption should be known. Their product gives the total energy release. The fuel consumption should be separately modeled using multiple variables such as characteristics of fuel flammability, spatial structure of fuel, topography, and fire weather conditions. There are two reasons why the proposed approach does not require evaluation of live fuel consumption for calculation of the potential energy release in the potential most severe fire weather conditions (potential flammability of the live fuel). First, in this study, measurements of the flammability of live fuel were performed in conditions that are close to these for the fire front under the most severe fire-weather. Second, as was discussed in the section 4.1.2, the assessment of flammability as a proportion to fresh mass or volume of fuel was possible due to practically complete fuel consumption in the tests. Evaluation of the potential heat content of live fuel (potential energy release contribution to the frontal flame) can be performed on a vegetative canopy scale, with use of the species-specific flammability models for live fuel discussed in the previous section 4.6.2. Since $dH_{eff}60s.GRAV$ *and* $dH_{eff}60s.VOL$ were measured as proportion to fresh mass and volume respectively, the potential heat content of the live fuel in the vegetative canopy can be calculated as a product of live fuel amount and $dH_{eff}60s.GRAV$ *or* $dH_{eff}60s.VOL$.

The same approach can be also applied for dead fuel. Species composition and the amount of live and dead fuel in the vegetative canopy that is consumed by frontal flame (live fuel is live plant material less than 1cm, dead fuel is dry plant material less 3 cm in diameter

(Albini, 1985) can be retrieved by means of forest inventory and remote sensing. This will allow calculation of the *PNHC* – the *Potential Net Heat Content of the vegetative canopy (forest stand)* – as the sum of the potential heat content of live and dead fuel. This number representing the potential heat content of the vegetative canopy *(PNHC)* can be used as a numerical measure of its flammability. When combined with new more detailed spatial structure classification (height, density, vertical and horizontal continuity and homogeneity), *PNHC,* therefore, can be used as a physics- and stand characteristics-based criteria of the flammability of the vegetative canopy for fuel classification within the new generation CFFDRS System (NG-CFFDRS).

4.6.2.3 Actual flammability of live fuel – use in dynamic fuel models

The proposed experimental methodology can be also used in the development of the physically-based dynamic fuel models for use in new surface fire spread, initiation of crowning, and crown fire spread models within the NG-CFFDRS System. This will require (1) quantitative characterization of the spatial structure of a vegetative canopy and (2) evaluation of flammability of live and dead fuel separately due to the substantial differences in their properties, factors, and seasonal changes (see section 1.3.1). Dead fuel flammability is well predicted and linked with the FBP System using dead fuel moisture content indices; however, dead fuel flammability should be also well described using the proposed method. Live fuel flammability is represented in the FBP System by FMC; however, as it was already discussed in the section 1.3.2, this representation is very limited. The results of the study showed that seasonal pattern of FMC and live fuel flammability assumed by FBP System is substantially different from that for shoot water content and flammability measured for white spruce in 2014 (section 4.4). The proposed energy release-based method allows for more realistic characterization of live fuel flammability and its seasonal changes. As was discussed in the previous section 4.6.3, differential effective heat of combustion can be used directly for the development of fuel classification since it is a measure of the potential energy release response of live fuel to the maximal severe fire weather conditions. However, for use in the fuel models it needs further corrections to actual fire weather conditions.

Under moderate or low fire weather conditions the energy release response might be lower due to lower intensity of the incoming frontal flame (lower intensity of the ignition heat transfer), to lower oxygen supply (less wind), and, especially, to lower fuel consumption (the proposed method evaluates energy release per unit of the initial mass of the fuel, so it is more sensitive to test conditions compared with mass loss-based approach). With low surface fire intensity, for instance, the energy release response of crown live fuel can be critically low, preventing the initiation of the crowning. The *actual flammability of live fuel* (actual change in energy release to the frontal flame), therefore, can be substantially lower than measured in this study where high intensities of the methane flame and the open-air oxygen supply conditions were used for testing. To provide new dynamic fuel models with values of actual flammability of live fuel, flammability should be measured under the test conditions that correspond to actual fire weather conditions and that are lower than potential maximal conditions. It is an exceptionally important task to provide data on the range of variation of actual flammability of live fuel with change in the fire weather conditions from the potential (= 1), already applied in the tests during this study, to minimal (= 0). This task is probably the main goal of the next step in further research on flammability of live fuel.

The species-specific empirical data on actual flammability of live fuel ($dH_{eff}60s.GRAV$ *or* $dH_{eff}60s.VOL$ corrected to actual fire weather conditions, as discussed above) will allow for two potential applications. First, data on actual flammability of live fuel for the particular date can be directly linked with the FBP System and used currently (using a proposed approach on data processing that can be relatively easily applied). This will allow using data on the actual flammability of live fuel in new dynamic fuel models. Second, with the additional research and the development of the new fuel classification, it will be possible to evaluate actual flammability on a vegetative canopy scale, as discussed in the following section.

4.6.2.4 Actual flammability of live fuel – use in fire behaviour modelling

The actual heat content of the live fuel in the vegetative canopy can be evaluated using the same approach as for evaluation of the potential heat content *(PNHC)* discussed in the section 4.6.3. It can be calculated as a product of live fuel amount and its actual flammability ($dH_{eff}60s.GRAV$ *or* $dH_{eff}60s.VOL$ corrected to actual fire weather conditions). The same approach can be also applied for dead fuel. This will allow calculation of the *ANHC – the Actual Net Heat Content of the vegetative canopy (forest stand)* – as the sum of the actual heat content of live and dead fuel. This number representing the actual heat content of the vegetative canopy *(ANHC)* can be used as a numerical measure of its flammability in the particular fire weather conditions that are different from the potential (maximal). The *ANHC* thus will be always less than *PNHC.* Combined with new more detailed spatial structure classification, *ANHC,* therefore, can be used as a physics- and stand characteristics-based criteria of the flammability of the vegetative canopy and as an fuel conditions input for flame propagation and fire behaviour modelling within the NG-CFFDRS System.

4.6.3 Other applications

The proposed method and equipment for rapid assessment of flammability of live fuel (Paskaluk, Ackerman, & Melnik, 2015) can be used for the planning of prescribed burns of high value and importance by providing more accurate real-time estimation of actual fuel conditions. It can also be used to examine fire-resistance of different species by comparing the seasonal variation in the time to ignition and the potential energy release ($dH_{eff}60s.GRAV$ *or* $dH_{eff}60s.VOL$*);* this will be essential for the planning of vegetative modification for community protection. The methodology would also be more efficient than the existing techniques for fire chemicals (gels and retardants) performance testing because it allows evaluation of chemical performance in response to an incoming flame front rather than simply assessing ignition delay time in response to a purely radiative heat load.

5 CONCLUSIONS

The extremely dangerous fire behaviour associated with drought and other natural disturbances is enhanced by the simultaneous increase in the flammability of live and dead fuel. The changes in the flammability of live fuel are only partially accounted for in the current fire-modelling systems. According to the analysis of live fuel consumption in the flame-front performed in this study, live fuel, however, is responsible for more than 54% of the total fuel consumption by the flame-front.

This study introduces a new experimental methodology for assessment of the flammability of live fuel using gravimetric and volumetric approaches as well as a new and more accurate time- and cost-efficient method for volume measurements. The flammability was measured using modified oxygen consumption calorimetry method by testing live fuel directly in the flame providing high intensity combined radiative and convective heat flux of the direction that coincides with the flame propagation through the fuel sample. Firstly, these new methodologies allowed for close representation of the plant material consumed by the flame-front (shoots rather than foliage), providing consistent ignition, and almost complete fuel consumption. Secondly, oxygen deficiency, high concentrations of water vapor and associated reduction in energy release in the common combustion zone of the flame of the burning live fuel and the incoming frontal flame were represented better than in existing techniques. Finally, the proposed approach allows for the evaluation of flammability on the frontal flame propagation scale as an energy source (generation) component of the energy balance of the frontal flame. Flammability of live fuel burning within the frontal flame was defined and measured as the change in energy release to the frontal flame resulting from interaction with live fuel during the first 60 seconds of combustion (average frontal flame residence time).

The contribution of the burning live fuel to the energy release of the frontal flame (change in energy release) expressed gravimetrically and volumetrically varied from high-positive to low-negative values. Negative values of flammability for new shoots in the beginning of the season confirmed the existence of a considerable negative effect of the burning live fuel on the energy release of the frontal flame due to incomplete combustion caused by the

high water content of live fuel and oxygen deficiency. The range of variation in the flammability measured gravimetrically and volumetrically was more than two times larger than is measured by the existing test methods suggesting that variation in live flammability is critically underestimated by the existing methods and current fire modelling systems. Similar to previous studies, the results showed minor differences in the flammability of old growth (1-year compared with 2-year and older shoots). For new shoots, the flammability was substantially lower compared with older shoots during the first half of the season; the seasonal variation in flammability was substantially higher for new shoots. These findings suggest the importance of properties and flammability of new shoots in the determining live fuel flammability.

The variation in live fuel flammability was studied in relation to water content, dry matter content, density, and porosity. The gravimetric dry matter content, energy content, and ratio of energy content to water content showed practically the same results in explaining flammability compared with gravimetric water content. In contrast, volumetric dry matter content, energy content, and ratio of energy content to water content were noticeably more effective in explaining flammability compared with volumetric water content. To minimize the number of variables for the multivariable regression analysis, dry matter content and multiple variables characterizing chemical composition were replaced by a newly-introduced variable – energy content – representing calorimetric content (gross heat of combustion) per unit of fresh mass (gravimetric) or per unit of volume (volumetric). The energy content showed the same results in explaining variation in flammability as water content for the gravimetric approach and noticeably higher results for the volumetric approach. This suggests the equal importance of dry matter content and energy content in modelling live fuel flammability compared with water content. Flammability was much more strongly affected by the characteristics of live plant tissue proposed in this study, such as density water-free and porosity water-free, rather than by the traditional fresh density. In general, the effectiveness of the volumetric single-variable regression models in explaining flammability was slightly lower compared with gravimetric.

The combined use of the volumetric variables in the proposed volumetric multivariable model allowed for marginally better (adjusted $R^2 = 0.87$) explanation of flammability

compared with the best gravimetric single-variable flammability model (gravimetric dry matter content, adjusted $R^2 = 0.84$). However, unlike the gravimetric, the volumetric approach is fully compatible with remote sensing techniques; so it was paid the most of the attention in this study. The proposed volumetric multivariable model allowed for better explanation of flammability (adjusted $R^2 = 0.87$) compared with the best volumetric single-variable flammability model (volumetric dry matter content, adjusted $R^2 = 0.79$). Also, more importantly, the structure of the proposed multivariable model better represents the main physical processes and factors involved in live fuel combustion within the frontal flame as well as it allows changing more variables and fitting the model within a conceptual framework.

Seasonal changes in the flammability for white spruce in 2014 were substantially different from those assumed by the FBP CFFDRS System with only one maximum in flammability at early-mid June that corresponds to the seasonal minimum in the FMC. The results showed that this maximum in flammability actually occurred one month earlier, on May 6 or probably earlier. Two additional spikes in flammability were registered on July 7 and on August 12, when, according to the FBP model, the lowest seasonal values of live fuel flammability were expected in July and later in the season. These three seasonal maximums in flammability were satisfactorily predicted by the proposed multivariable volumetric model of live fuel flammability.

The measured seasonal pattern of variation in the water content in 2014 was noticeably different compared with that by the FBP CFFDRS System assuming one seasonal minimum in water content during "spring dip" in early-mid June that causes corresponding peak in flammability discussed above. By that time (mid-June), the actual measured volumetric water content showed the highest seasonal values. Measured spring dip in water content actually occurred in 2014 on May 6, one month earlier than expected. According to the results, the most distinct seasonal minimum in water content occurred on August 12. The timing of this "late-summer dip" in volumetric shoot water content corresponded exactly to the third measured seasonal maximum in flammability on August 12, which was even more substantial than during spring dip due to late-summer drought.

Unlike the FBP CFFDRS System, the proposed multivariable flammability model was able to successfully predict seasonal pattern in flammability of live fuel in 2014.

The proposed volumetric approach and flammability assessment method and modelling, therefore, showed better results compared with the existing techniques. Due to the use of sufficiently high intensity heat flux resulting in nearly complete fuel consumption, the proposed method also allowed for evaluation of change in energy release to the frontal flame proportionally to fresh mass or volume of live fuel. By knowing the amount of fuel that will be consumed by a fire of maximal intensity, it is possible to evaluate the combined potential energy release contribution of the fuel to the flame-front by calculation of *PNHC*. As a measure of the potential flammability of the vegetative canopy, it can be further used for the development of fuel classification. As a measure of the actual flammability of the vegetative canopy, together with detailed data on its spatial structure, *ANHC* can be directly used as an input in fire behaviour modelling. The most significant outcome of the development and use of numerical live fuel flammability models in fuel and fire modelling is more realistic and accurate prediction of fire behaviour, a higher efficiency of fire management, and most importantly – a higher level of firefighter and civilian safety.

REFERENCES

Abbott, B. W., Jones, J. B., Schuur, E. A. G., Chapin III, F. S., Bowden, W. B., Bret-Harte, M. S., … Zimov, S. (2016). Biomass offsets little or none of permafrost carbon release from soils, streams, and wildfire: an expert assessment. *Environmental Research Letters*, *11*(3), 34014. http://doi.org/10.1088/1748-9326/11/3/034014

Alberta Sustainable Resource Development. (2001). *Chisholm Fire* (Final Documentation Report. Section 02). http://www1.agric.gov.ab.ca/$department/deptdocs.nsf/all/formain15906/$file/ChisholmFire-FinalDocumentationReport-Section02.pdf?OpenElement

Albini, F. A. (1985). A Model for Fire Spread in Wildland Fuels by Radiation. *Combustion Science and Technology*, *42*(5–6), 229–258. http://doi.org/10.1080/00102208508960381

Alexander, M. E., & Cruz, M. G. (2012). Assessing the effect of foliar moisture on the spread rate of crown fires. *International Journal of Wildland Fire, 22,* 869–870. http://dx.doi.org/10.1071/WF12008

Allen, C. D., Macalady, A. K., Chenchouni, H., Bachelet, D., McDowell, N., Vennetier, M., … Cobb, N. (2010). A global overview of drought and heat-induced tree mortality reveals emerging climate change risks for forests. *Forest Ecology and Management*, *259*(4), 660–684. http://doi.org/10.1016/j.foreco.2009.09.001

Amiro, B. D., Logan, K. A., Wotton, B. M., Flannigan, M. D., Todd, J. B., Stocks, B. J., & Martell, D. L. (2004). Fire weather index system components for large fires in the Canadian boreal forest. *International Journal of Wildland Fire, 13*(4) 391-400. https://cfs.nrcan.gc.ca/publications?id=25118

Anderson, H. E. (1969). *Heat transfer and fire spread*. Intermountain Forest and Range Experiment Station, Forest Service, US Department of Agriculture. http://www.fs.fed.us/rm/pubs_int/int_rp069.pdf

Anderson, H. E. (1970). Forest fuel ignitibility. *Fire Technology*, *6*(4), 312–319. http://doi.org/10.1007/BF02588932

Babrauskas, V. (1984). Development of the cone calorimeter—a bench-scale heat release rate apparatus based on oxygen consumption. *Fire and Materials*, *8*(2), 81–95.

Babrauskas, V. (2006). Effective heat of combustion for flaming combustion of conifers. *Canadian Journal of Forest Research*, *36*(3), 659–663.

Babrauskas, V., & Peacock, R. D. (1992). Heat release rate: the single most important variable in fire hazard. *Fire Safety Journal*, *18*(3), 255–272.

Beer, T. (1991). The interaction of wind and fire. *Boundary-Layer Meteorology*, *54*(3), 287–308.

Blanch, J.-S., Peñuelas, J., Sardans, J., & Llusià, J. (2009). Drought, warming and soil fertilization effects on leaf volatile terpene concentrations in Pinus halepensis and Quercus ilex. *Acta Physiologiae Plantarum*, *31*(1), 207–218. http://doi.org/10.1007/s11738-008-0221-z

Bradshaw, L. S., Deeming, J. E., Burgan, R. E., & Cohen, J. D. compilers. (1984). *The 1978 National Fire-Danger Rating System: technical documentation*. http://www.treesearch.fs.fed.us/pubs/29615

Byram, G. M. (1959). Combustion of forest fuels. In *Forest fire: control and use.* (pp. 61–89). New York: McGraw-Hill.

Call, P., & Albini, F. (1997). Aerial and surface fuel consumption in crown fires. *International Journal of Wildland Fire*, *7*(3), 259–264.

Cameron, P. A., Mitra, B., Fitzgerald, M., Scheinkestel, C. D., Stripp, A., Batey, C., … Cleland H. (2009). Black Saturday: the immediate impact of the February 2009 bushfires in Victoria, Australia. *Medical Journal of Australia*, *191*(1), 11–16.

Campbell, D. (1995). The Campbell Prediction System: A Wild Land Fire Prediction and Communication System. Self-Published.

Canadell, J., Jackson, R. B., Ehleringer, J. B., Mooney, H. A., Sala, O. E., & Schulze, E.D. (1996). Maximum rooting depth of vegetation types at the global scale. *Oecologia*, *108*(4), 583–595.

Chrosciewicz, Z. (1986a). Foliar heat content variations in four coniferous tree species of central Alberta. *Canadian Journal of Forest Research*, *16*(1), 152–157. http://doi.org/10.1139/x86-028

Chrosciewicz, Z. (1986b). Foliar moisture content variations in four coniferous tree species of central Alberta. *Canadian Journal of Forest Research*, *16*(1), 157–162.

Cruz, M. G., Sullivan, A. L., Gould, J. S., Sims, N. C., Bannister, A. J., Hollis, J. J., & Hurley, R. J. (2012). Anatomy of a catastrophic wildfire: The Black Saturday Kilmore East fire in Victoria, Australia. *Forest Ecology and Management*, *284*, 269–285. http://doi.org/10.1016/j.foreco.2012.02.035

Dale, V. H., Joyce, L. A., McNulty, S., Neilson, R. P., Ayres, M. P., Flannigan, M. D., … Wotton,B.M. (2001). Climate change and forest disturbances: climate change can affect forests by altering the frequency, intensity, duration, and timing of fire, drought, introduced species, insect and pathogen outbreaks, hurricanes, windstorms, ice storms, or landslides. *BioScience*, *51*(9), 723–734.

de Groot, W. J., Flannigan, M. D., & Cantin, A. S. (2013). Climate change impacts on future boreal fire regimes. *Forest Ecology and Management*, *294*, 35–44.

Development and structure of the Canadian Forest Fire Behavior Prediction System / Forestry Canada, Fire Danger Group. (1992). Ottawa : Forestry Canada, Science and Sustainable Development Directorate, 1992.

Dickinson, K. J. M., & Kirkpatrick, J. B. (1985). The flammability and energy content of some important plant species and fuel components in the forests of southeastern Tasmania. *Journal of Biogeography*, *12*(2). 121–134.

Downing, D. J., & Pettapiece, W. W. (2006). *Natural Regions and Subregions of Alberta* (No. T/852). Natural Regions Committee 2006. Government of Alberta. https://www.albertaparks.ca/media/2942026/nrsrcomplete_may_06.pdf

Ferguson, S. C., Dahale, A., Shotorban, B., Mahalingam, S., & Weise, D. R. (2013). The role of moisture on combustion of pyrolysis gases in wildland fires. *Combustion Science and Technology*, *185*(3), 435–453.

Finney, M. A., Cohen, J. D., Grenfell, I. C., & Yedinak, K. M. (2010). An examination of fire spread thresholds in discontinuous fuel beds. *International Journal of Wildland Fire*, *19*(2), 163–170.

Finney, M. A., Cohen, J. D., McAllister, S. S., & Jolly, W. M. (2012). On the need for a theory of wildland fire spread. *International Journal of Wildland Fire*. http://www.publish.csiro.au/?paper=WF11117

Flat Top Complex Wildfire Review Committee. (2012). *Flat Top Complex* (Final Report). http://wildfire.alberta.ca/wildfire-prevention-enforcement/wildfire-reviews/documents/FlatTopComplex-WildfireReviewCommittee-A-May18-2012.pdf

Frankman, D., Webb, B. W., Butler, B. W., Jimenez, D., Forthofer, J. M., Sopko, P., … Ottmar, R. D. (2013). Measurements of convective and radiative heating in wildland fires. *International Journal of Wildland Fire*, *22*(2), 157–167.

Gillett, N. P., Weaver, A. J., Zwiers, F. W., & Flannigan, M. D. (2004). Detecting the effect of climate change on Canadian forest fires. *Geophysical Research Letters*, *31*(18), L18211.

Groisman, P. Y., Sherstyukov, B. G., Razuvaev, V. N., Knight, R. W., Enloe, J. G., Stroumentova, N. S., … Karl, T. R. (2007). Potential forest fire danger over Northern Eurasia: Changes during the 20th century. *Global and Planetary Change*, *56*(3–4), 371–386. http://doi.org/10.1016/j.gloplacha.2006.07.029

Hirsch, K. G. (1996). *Canadian forest fire behavior prediction (FBP) system: user's guide* (Vol. 7). http://www.cfs.nrcan.gc.ca.login.ezproxy.library.ualberta.ca/publications/?id=11792

Jessup, R., & Green, C. (1934). Heat of combustion of standard sample benzoic acid. *Journal of Research of the Rational Bureau of Standards*, *13*(October), 469–494.

Jolly, M., & Butler, B. W. (2013). *Linking Photosynthesis and Combustion Characteristics in Live Fuels: The Role of Soluble Carbohydrates in Fuel Preheating* (Final Report No. 10-1-8–6). Missoula: USA Forest Service. https://www.firescience.gov/projects/10-1-08-6/project/10-1-08-6_final_report.pdf

Jolly, W. M., Hintz, J., Kropp, R. C., & Conrad, E. T. (2014). Physiological drivers of the live foliar moisture content "spring dip"in Pinus resinosa and Pinus banksiana and their relationship to foliar flammability. In *Advances in forest fire* research. Coimbra. http://www.lakestatesfiresci.net/docs/Jolly_et_al_Spring_Dip_Physiology_15Jul2014.pdf

Jolly, W. M., Parsons, R. A., Hadlow, A. M., Cohn, G. M., McAllister, S. S., Popp, J. B., … Negron, J. F. (2012). Relationships between moisture, chemistry, and ignition of Pinus contorta needles during the early stages of mountain pine beetle attack. *Forest Ecology and Management*, *269*, 52–59. http://doi.org/10.1016/j.foreco.2011.12.022

Kasischke, E. S., & Turetsky, M. R. (2006). Recent changes in the fire regime across the North American boreal region—spatial and temporal patterns of burning across Canada and Alaska. *Geophysical Research Letters*, *33*(9), L09703.

Keyes, C. R. (2006). Foliar moisture contents of North American conifers. In: Andrews, Patricia L.; Butler, Bret W., comps. 2006. Fuels Management—How to Measure Success: Conference Proceedings. 28-30 March 2006; Portland, OR. Proceedings RMRS-P-41. Fort Collins, http://www.fs.fed.us/rm/pubs/rmrs_p041/rmrs_p041_395_399.pdf

Leroy, V., Cancellieri, D., & Leoni, E. (2006). Thermal degradation of ligno-cellulosic fuels: DSC and TGA studies. *Thermochimica Acta*, *451*(1), 131–138.

Lewis, D. C., & Burgy, R. H. (1964). The Relationship between oak tree roots and groundwater in fractured rock as determined by tritium tracing. *Journal of Geophysical Research*, *69*(12), 2579–2588. http://doi.org/10.1029/JZ069i012p02579

Lieffers, V. J., & Rothwell, R. L. (1987). Rooting of peatland black spruce and tamarack in relation to depth of water table. *Canadian Journal of Botany*, *65*(5), 817–821. http://doi.org/10.1139/b87-111

Little, C. H. A. (1970). Seasonal changes in carbohydrate and moisture content in needles of balsam fir (Abies balsamea). *Canadian Journal of Botany*, *48*(11), 2021–2028. http://doi.org/10.1139/b70-295

Madrigal, J., Guijarro, M., Hernando, C., Diez, C., & Marino, E. (2011). Effective heat of combustion for flaming combustion of Mediterranean forest fuels. *Fire Technology*, *47*(2), 461–474.

Martin, A. (1994). Assessing the flammability of domestic and wildland vegetation. *Proceedings of the International Conference on Fire and Forest Meteorology*, *12*, 130–137.

Melnik, O. M., Paskaluk, S. A., Flannigan, M. D., & Ackerman, M. Y. (2015). A proposed experimental methodology for assessing the effects of water and dry matter content on live fuel flammability. In *Proceedings of the 13th International Wildland Fire Safety Summit and 4th Human Dimensions of Wildland Fire Conference*. Boise, Idaho, USA: International Association of Wildland Fire, Missoula, Montana, USA. http://www.iawfonline.org/Safety_Summit_2015_Proceedings-updated%205.23.2016.pdf

Merrill, D. F., Alexander, M. E. (1987). *Glossary of forest fire management terms*. Ottawa: Canadian Committee on Forest Fire Management, National Research Council of Canada. https://cfs.nrcan.gc.ca/publications?id=35337

NFDRS. (2011). Appendix E. NFDRS Technical Reference. https://www.google.ca/search?q=Appendix+E.+NFDRS+Technical+Reference%2C+Update+2011&rlz=1C1AVNC_enCA594CA594&oq=Appendix+E.+NFDRS+Technical+Reference%2C+Update+2011&aqs=chrome..69i57j69i60.1578j0j7&sourceid=chrome&es_sm=93&ie=UTF-8

NIFC. (2014). Wildland Fire Fatalities by Year. https://www.nifc.gov/safety/safety_documents/Fatalities-by-Year.pdf

Norum, R. A., & Miller, M. (1984). Measuring fuel moisture content in Alaska: standard methods and procedures. http://www.treesearch.fs.fed.us/pubs/7574

Ormeño, E., Céspedes, B., Sánchez, I. A., Velasco-García, A., Moreno, J. M., Fernandez, C., & Baldy, V. (2009). The relationship between terpenes and flammability of leaf litter. *Forest Ecology and Management*, *257*(2), 471–482. http://doi.org/10.1016/j.foreco.2008.09.019

Paskaluk, S., Ackerman, M., & Melnik, O. (2015). A modified method to evaluate flammability of forest fuels using oxygen consumption calorimetry. *Proceedings of Combustion Institute – Canadian Section*, (Spring Technical Meeting University of Saskatchewan).

Philpot, C. W. (1971). *The seasonal trends in moisture content, ether extractives, and energy of ponderosa pine and Douglas-fir needles /*. Ogden, Utah. http://hdl.handle.net/2027/umn.31951d02988143a

Pickett, B. M., Isackson, C., Wunder, R., Fletcher, T. H., Butler, B. W., & Weise, D. R. (2009). Flame interactions and burning characteristics of two live leaf samples. *International Journal of Wildland Fire*, *18*(7), 865–874.

Podur, J., & Wotton, M. (2010). Will climate change overwhelm fire management capacity? *Ecological Modelling*, *221*(9), 1301–1309.

Ramanathan, V., & Carmichael, G. (2008). Global and regional climate changes due to black carbon. *Nature Geoscience*, *1*(4), 221–227. http://doi.org/10.1038/ngeo156

Rivera, J. de D., Davies, G. M., & Jahn, W. (2012). Flammability and the Heat of Combustion of Natural Fuels: A Review. *Combustion Science and Technology*, *184*(2), 224–242. http://doi.org/10.1080/00102202.2011.630332

Royer, P. D., Cobb, N. S., Clifford, M. J., Huang, C.-Y., Breshears, D. D., Adams, H. D., & Villegas, J. C. (2011). Extreme climatic event-triggered overstorey vegetation loss increases understorey solar input regionally: primary and secondary ecological implications. *Journal of Ecology*, *99*(3), 714–723. http://doi.org/10.1111/j.1365-2745.2011.01804.x

Sharples, J. J., McRae, R. H. D., Weber, R. O., & Gill, A. M. (2009). A simple index for assessing fire danger rating. *Environmental Modelling & Software*, *24*(6), 764–774. http://doi.org/10.1016/j.envsoft.2008.11.004

Siau, J. F. (1995). Wood: Influence of moisture on physical properties. *Dept. of Wood Science and Forest Products, Virginia Polytechnic Institute and State University.*

Simmonds, P. G., Manning, A. J., Derwent, R. G., Ciais, P., Ramonet, M., Kazan, V., & Ryall, D. (2005). A burning question. Can recent growth rate anomalies in the greenhouse gases be attributed to large-scale biomass burning events? *Atmospheric Environment*, *39*(14), 2513–2517. http://doi.org/10.1016/j.atmosenv.2005.02.018

Smith, S. G. (2005). *Effects of moisture on combustion characteristics of live California chaparral and Utah foliage*. Brigham Young University. http://www.mariloureiro.net/ciencia/ignicao_vegt/EFFECTSofMOISTURE.pdf

Stocks, B. J. (1987). Fire behavior in immature jack pine. *Canadian Journal of Forest Research*, *17*(1), 80–86. http://doi.org/10.1139/x87-014

Stocks, B. J., Alexander, M. E., Wotton, B. M., Stefner, C. N., Flannigan, M. D., Taylor, S. W., … Lanoville, R. A. (2004). Crown fire behaviour in a northern jack pine – black spruce forest. *Canadian Journal of Forest Research*, *34*(8), 1548–1560. http://doi.org/10.1139/x04-054

Turner, J. A., & Lawson, B. D. (1978). Weather in the Canadian forest fire danger rating system. A user guide to national standards and practices, *177*. https://cfs.nrcan.gc.ca/publications?id=1843

Turner, M. G. (2010). Disturbance and landscape dynamics in a changing world1. *Ecology*, *91*(10), 2833–2849. http://doi.org/10.1890/10-0097.1

van Altena, C., van Logtestijn, R. S. P., Cornwell, W. K., & Cornelissen, J. H. C. (2012). Species Composition and Fire: Non-Additive Mixture Effects on Ground Fuel Flammability. *Frontiers in Plant Science*, *3*. http://doi.org/10.3389/fpls.2012.00063

Van Wagdendonk, J. W., Sydoriak, W. M., & Benedict, J. M. (1998). Heat content variation of Sierra Nevada conifers. *International Journal of Wildland Fire*, *8*(3), 147–158.

Van Wagner, C. E. (1963). Flammability of Christmas Trees. http://lac-repo-live7.is.ed.ac.uk/handle/1842/5718

Van Wagner, C. E. (1974). A spread index for crown fires in spring / by C. E. Van Wagner. In *Petawawa Forest Experiment Station. Information report PS-X ; 55*. Chalk River, Ont. : Petawawa Forest Experiment Station, 1974.

Van Wagner, C. E. (1977). Conditions for the start and spread of crown fire. *Canadian Journal of Forest Research*, *7*(1), 23–34.

Van Wagner, C. E. (1987). *Development and structure of the Canadian Forest Fire Weather Index System* (Vol. 35). https://cfs.nrcan.gc.ca/publications?id=19927

Viegas, D. X. (1993). Fire behaviour and fire-line safety. *Ann. Medit. Burns Club*, *6*(179–85), 1998.

Viegas, D. X., Simeoni, A., Xanthopoulos, G., Rossa, C., Ribeiro, L. M., Pita, L. P. (2009). Recent forest fire related accidents in Europe. *European Commission Joint Research Centre Institute for Environment and Sustainability, Luxembourg*. http://www.infopuntveiligheid.nl/Infopuntdocumenten/2009%20JRC%20Recent%20forest%20fire%20related%20accidents%20in%20Europe.pdf

Weise, D. R., White, R. H., Beall, F. C., & Etlinger, M. (2005). Use of the cone calorimeter to detect seasonal differences in selected combustion characteristics of ornamental vegetation. *International Journal of Wildland Fire*, *14*(3). http://doi.org/10.1071/WF04035

White, R. H., & Zipperer, W. C. (2010). Testing and classification of individual plants for fire behaviour: plant selection for the wildland–urban interface. *International Journal of Wildland Fire*, *19*(2), 213–227.

Wilson, C. C. (1977). Fatal and near-fatal forest fires: the common denominators. *International Fire Chief*, *43*(9), 9–10.

Wotton, B. M., Gould, J. S., McCaw, W. L., Cheney, N. P., & Taylor, S. W. (2012). Flame temperature and residence time of fires in dry eucalypt forest. *International Journal of Wildland Fire*, *21*(3), 270–281.

Wotton, B. M., Nock, C. A., & Flannigan, M. D. (2010). Forest fire occurrence and climate change in Canada. *International Journal of Wildland Fire*, *19*(3), 253–271.

APPENDICES

APPENDIX 1. HISTORY OF WILDFIRES WITH MULTIPLE FATALITIES

There were several devastating fires with multiple losses occurred from 1870 to 2010 (Table A.1):

1871 – 1200 losses (Peshtigo, Wisconsin, USA)

1899 – 400 losses (Cape York, Old, Australia)

1916 – 233 losses (Matheson, Ontario, Canada)

1918 – 453 losses (Cloquet, Minnesota, USA)

1949 – 230 losses (Landes region, France)

1987 – 213 losses (Greater Hinggan, China)

1997 – 240 losses (Sumatra, Kalimantan, Indonesia)

2009 – 173 losses (Black Saturday Victorian Bushfires, Australia)

Table A.1 Wildfire-related losses by country and year

Country	Time period	Loss of lives			Average	Fire(s)	Loss of lives one location	Source
		Fire fighters	Civilians	Total				
USA	1871					Peshtigo, Wisconsin, USA	1200	(Cameron et al., 2009)
	1918					Cloquet, Minnesota, USA	453	
	1894					Hinckley, Minnesota, USA	418	
	1881					Thumb region, Michigan, USA	282	
	1910-2014	1086			10			NIFC, 2014
	1910	84				Idaho Coeur d'Alene	78	
	1988	29						
	1994	35				Colorado Glenwood Springs	14	
	2003	30					8	
	2013	34				Arizona Yarnell	19	
Canada	1825					Miramichi, New Brunswick, Canada	160	(Cameron et al., 2009)
	1916					Matheson,	233	

						Ontario, Canada		
Portugal	1982-2007 2003 2005			110 21 22	4			(Viegas et al., 2009)
Spain	1982-2005			186	8			
France	1949					Landes region, France	230	(Cameron et al., 2009)
France	1982-2007			20	1			(Viegas et al., 2009)
Croatia	1980-2007			28	1			
Greece	1980-2007 2007			177 78	7			
Australia	1899 2009 1983 1974 1967					Cyclone Mahina, Cape York, Qld Victorian bushfires Ash Wednesday bushfires, Vic and SA Cyclone Tracy, Darwin, NT Tasmanian bushfires	>400 173 75 64 62	(Cameron et al., 2009)
Indonesia	1997					Sumatra, Kalimantan, Indonesia	240	
China	1987					Greater Hinggan, China	213	

APPENDIX 2. PROPORTION OF LIVE FUEL CONSUMTION

Total fire consumption includes both frontal and post-front consumption. Fire intensity and the resulting fire behaviour in the given fire weather and topographic conditions are determined by the amount of fuel consumed by the fire front. As of now, there is no an experimental data on the consumption of the live fuel by the fire front. To estimate quantities of the live and dead fuel consumed by the fire front separately from the quantities of fuel consumed after passing the fire front, data on the Sharpsand Creek experimental fires (Stocks, 1987) were used. According to the approach used in the study on fuel consumption modelling (Call & Albini, 1997) and to the data of the international crown fire behaviour experiment (Stocks et al., 2004), it was assumed that live fuel greater than 1.0 cm in diameter and dead fuel greater than 3.0 cm in diameter would probably burn after the passing a fire front. Data on the preburn fuel loadings and fuel consumed (Stocks, 1987) that were used in the analysis are presented in the Table A.2.

Table A.2 Preburn fuel loadings and fuel consumed

Fire #	Preburn fuel loadings (kg m^{-2})						Fuel consumed (kg m^{-2})			
	Under-story (live)	Surface fuel		Crown fuel loads			Under story (live)	Surface fuel		Crown fuel total
		<1cm	1-3 cm	Live trees		Dead trees		<1 cm	1-3 cm	
				Foliage (live)	<0.99 cm (dead)	<0.99 cm				
2	0.088	0.072	0.047	0.939	0.512	0.142	0.088	0.048	0.032	0.89
3	0.088	0.100	0.089	0.622	0.339	0.073	0.088	0.054	0.057	1.16
4	0.088	0.070	0.158	0.718	0.414	0.313	0.088	0.053	0.061	0.99
5	0.088	0.101	0.113	0.782	0.466	0.183	0.088	0.084	0.073	1.27
6	0.088	0.078	0.125	0.836	0.430	0.133	0.088	0.052	0.079	1.06
11a	0.088	0.040	0.084	0.888	0.437	0.131	0.088	0.032	0.056	1.40
11b	0.088	0.040	0.084	0.888	0.437	0.131	0.088	0.032	0.056	1.40
12	0.088	0.081	0.167	0.646	0.389	0.176	0.088	0.057	0.127	1.04
13	0.088	0.062	0.230	0.977	0.572	0.182	0.088	0.062	0.158	1.03
14	0.088	0.111	0.270	0.682	0.398	0.151	0.088	0.081	0.197	1.11

Data in the column “Crown fuel total” in “Fuel consumed” (Table A.2) were collected without separation on live and dead fuel. To evaluate amount of live fuel consumed by the fire front in the crown (in “Fuel consumed”), it was assumed that the proportion of live fuel consumption to the total crown fuel consumption in the crown was equal to the proportion of the preburn quantity of live fuel to total preburn crown fuel loads. In the “Preburn fuel loadings (kg m^{-2})”, the proportion of live fuel consumption can be calculated as the ratio of values in the column “Foliage” in “live trees” to the sum of the values in the column “<0.99 cm (dead)” in “live trees” and column “<0.99 cm” in ”Dead trees”. For the fire number 2, for instance, proportion of preburn loadings in the crown for live fuel (foliage) to dead roundwood less than 0.99 cm in diameter on live and dead trees was equal 0.939 to (0.512+0.142) (Table A.2) resulting in the proportion 58.95% to 41.06%. Using this proportion, fuel consumption in the column “Crown” was calculated

separately for needles (column "Foliage") as 0.89 x 58.95% = **0.525** (kg /m^2) and for dead roundwood <0.99 cm (column "<0.99 cm dead") as 0.89 x 41.06% = **0.365** (kg /m^2) (Table A-3):

Table A.3 Fuel consumption separately for live and dead fuel

Fire #	Fuel consumed (kg m^{-2})						
	Understory (live)	Surface		Crown			TOTAL
		<0.99 cm	1.0-2.99 cm	Foliage (live)	<0.99cm (dead)	Total	
2	0.088	0.048	0.032	0.525	0.365	0.89	1.058
3	0.088	0.054	0.057	0.698	0.462	1.16	1.359
4	0.088	0.053	0.061	0.492	0.498	0.99	1.192
5	0.088	0.084	0.073	0.694	0.576	1.27	1.515
6	0.088	0.052	0.079	0.633	0.427	1.06	1.279
11a	0.088	0.032	0.056	0.854	0.546	1.40	1.576
11b	0.088	0.032	0.056	0.854	0.546	1.40	1.576
12	0.088	0.057	0.127	0.555	0.485	1.04	1.312
13	0.088	0.062	0.158	0.581	0.449	1.03	1.338
14	0.088	0.081	0.197	0.615	0.495	1.11	1.476

Proportion of live fuel consumption to total frontal fire consumption was calculated (Table A.4) and compared to DC (Fig. A.1), BUI (Fig. A.2), FWI (Fig. A.3) indices, and frontal fire intensity (Fig. A.4). Proportion of the live fuel consumed to the total frontal fire consumption varied from 47.6% to 59.8% with average 53.9%.

Table A.4 Live fuel consumption compared to the frontal fire intensity, FWI, DC, and BUI indices

Fire #	Calculated % of live fuel consumption	DC	BUI	FWI	Frontal fire intensity
2	57.9	73	27	12	4717
3	57.8	73	27	15	9900
4	48.7	82	30	14	7728
5	51.6	108	44	20	10785
6	56.4	117	48	19	9171
11a	59.8	222	58	28	24274
11b	59.8	222	58	37	40903
12	49.0	245	67	22	17136
13	50.0	245	67	23	15790
14	47.6	272	70	25	25990

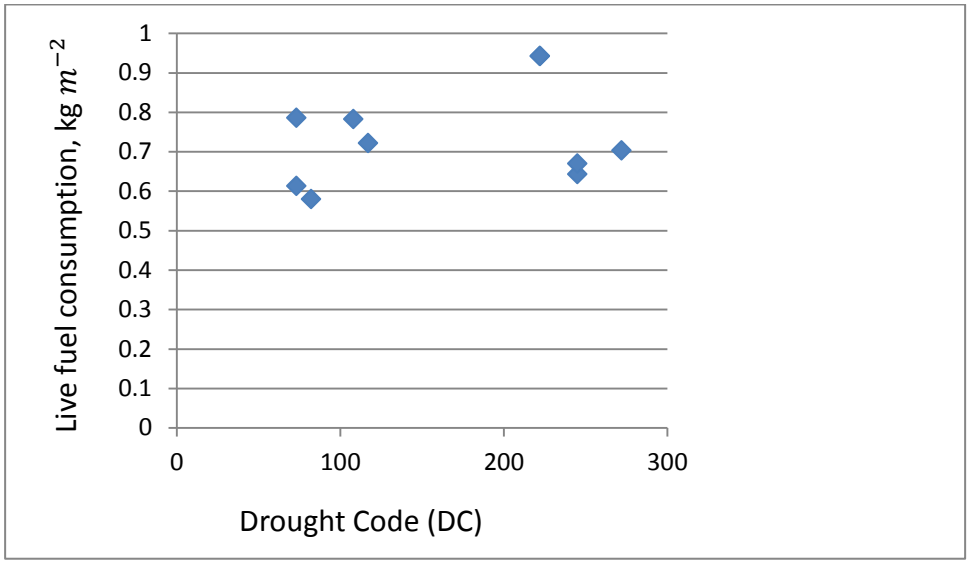

Figure A.1 Consumption of live fuel by fire front in relation to Drought Code (DC)

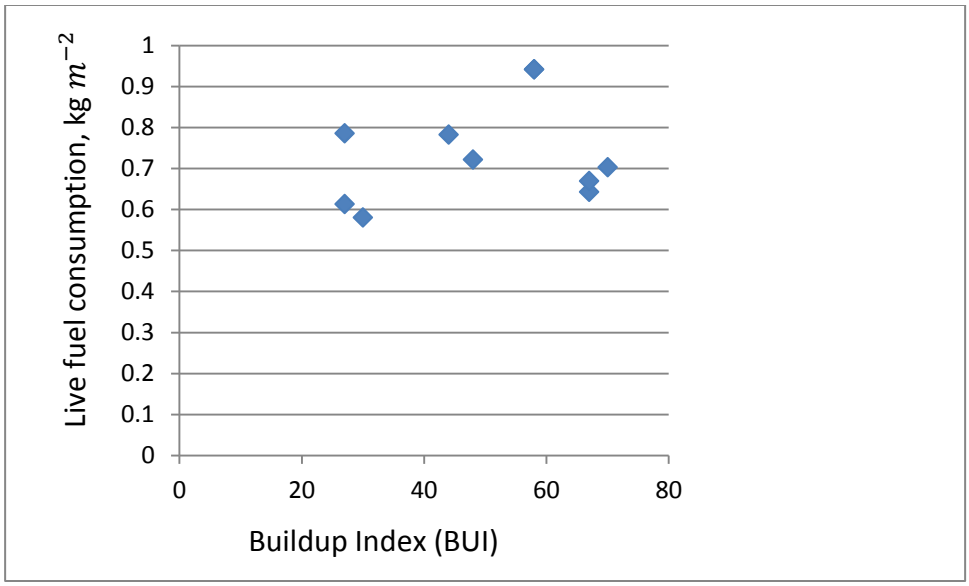

Figure A.2 Consumption of live fuel by the fire front in relation to Buildup Index (BUI)

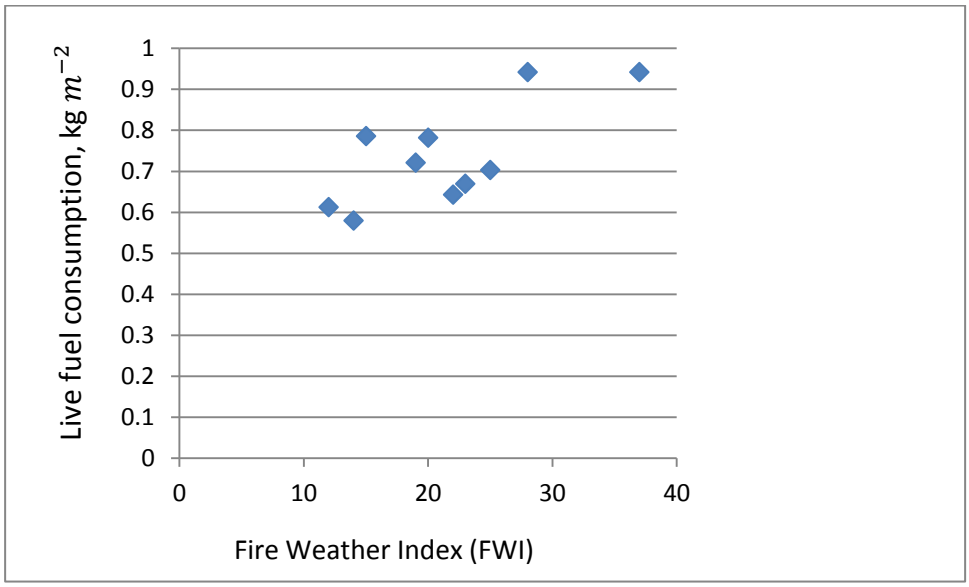

Figure A.3 Consumption of live fuel by the fire front in relation to Fire Weather Index (FWI)

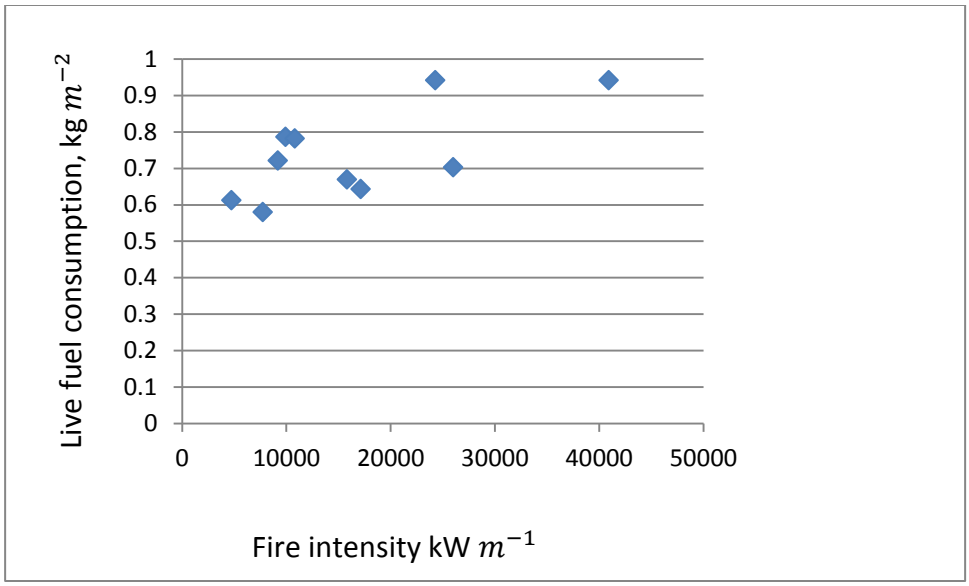

Figure A.4 Consumption of live fuel by the fire front in relation to fire intensity

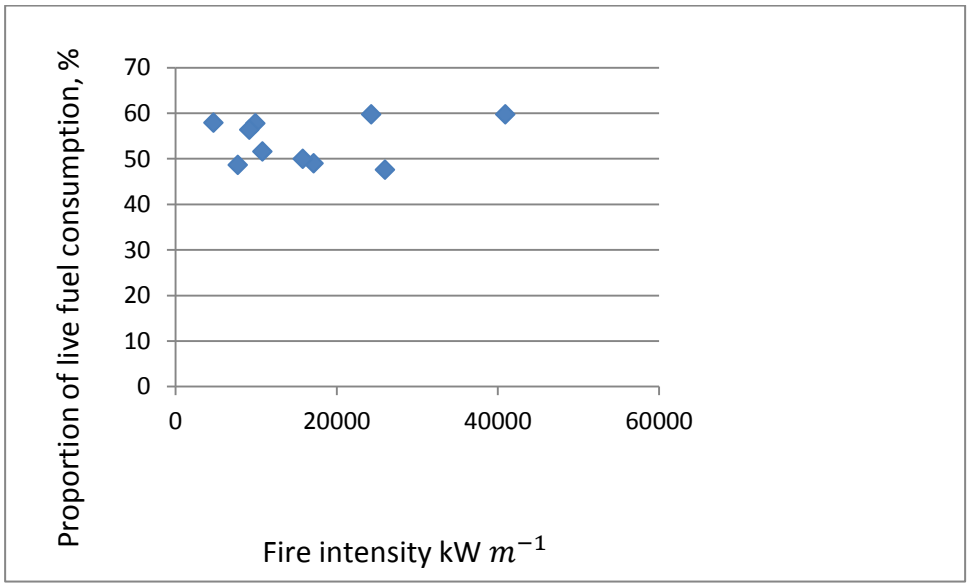

Figure A.5 Proportion of live fuel consumption to the total frontal fire consumption, % in relation to fire intensity

APPENDIX 3. OXYGEN BOMB CALORIMETER CALIBRATION DATA

Table A.5 Oxygen bomb calorimeter calibration data compared to heat of combustion of standard sample benzoic acid (Jessup & Green, 1934)

Number	Date	Test type	Test ID	Benzoic Acid heat of combustion, MJ/kg
1	20 March 2015	Cone	C52-Benzoic_Acid_Test-306	26.80
2	18 March 2015	Cone	C61-Benzoic_Acid_Test-276	27.04
3	13 March 2015	Cone	C83-Benzoic_Acid_Test-221	25.87
4	17 March 2015	Cone	C105-Benzoic_Acid_Test-258	26.59
5	12 March 2015	Cone	C158-Benzoic_Acid_Test-200	25.04
6	19 March 2015	Cone	C179-Benzoic_Acid_Test-294	25.69
7	09 March 2015	Cone	C187-Benzoic_Acid_Test-179	26.08
8	16 March 2015	Cone	C195-Benzoic_Acid_Test-242	25.02
			Heat of combustion of standard sample benzoic acid (Jessup & Green, 1934)	26.419